Characterization of Intrinsic and Extrinsic Factors that Regulate Human Telomerase Repeat Addition

by

Yinnan Chen

A Dissertation Presented in Partial Fulfillment
of the Requirements for the Degree
Doctor of Philosophy

Approved on March 2018 by the
Graduate Supervisory Committee:

Julian J-L Chen, Chair
Anne Jones
James Allen

ARIZONA STATE UNIVERSITY

May 2018

ABSTRACT

The linear chromosomes ends in eukaryotes are protected by telomeres, a nucleoprotein structure that contains telomeric DNA with repetitive sequence and associated proteins. Telomerase is an RNA-dependent DNA polymerase that adds telomeric DNA repeats to the 3'-ends of chromosomes to offset the loss of terminal DNA repeats during DNA replication. It consists of two core components: a telomerase reverse transcriptase (TERT) and a telomerase RNA (TR). Telomerase uses a short sequence in its integral RNA component as template to add multiple DNA repeats in a processive manner. However, it remains unclear how the telomerase utilizes the short RNA template accurately and efficiently during DNA repeat synthesis. As previously reported human telomerase nucleotide synthesis arrests upon reaching the end of its RNA template by a unique template-embedded pause signal. In this study, I demonstrate pause signal remains active following template regeneration and inhibits the intrinsic processivity and rate of telomerase repeat addition. Furthermore, I have found that the human telomerase catalytic cycle comprises a crucial and slow incorporation of the first nucleotide after template translocation. This slow nucleotide incorporation step drastically limits repeat addition processivity and rate, which is alleviated with elevated concentrations of dGTP. Additionally, molecular mechanism of the disease mutants on telomerase specific motif T, K570N, have been explored. Finally, I studied how telomerase selective inhibitor BIBR 1532 reduce telomerase repeat addition processivity by function assay. Together, these results shed new light on telomerase catalytic cycle and the importance of telomerase for biomedicine.

DEDICATION

This thesis dedicated to my parents who loved me unconditionally, to my wife who is always supportive of whatever I do, and our unborn child. Without their support, encouragement, and love I would not be where I am today.

ACKNOWLEDGMENTS

I would like to give my deepest gratitude towards everyone who has helped me through my graduate life.

Dr. Julian J.L. Chen, my Ph.D. advisor, has helped teach me more about science and correct me patiently when I made mistakes. He always pushed me to be a better than I am and what he told me will accompany with me pursing my scientific career.

To my graduate committee members, Dr. Anne Jones, Dr. James Allen, Dr. Giovanna Ghirlanda, and Dr. John Chaput. Their advice and guidance has been a great help over my course as a graduate student.

To my fellow members of Dr. Chen's research laboratory; Josh Podlevsky, Xiaodong Qi, Andrew Brown, Lina Franco, Dustin Rand, Dhenugen Logeswaran, Zhenqiu Huang, Lena Li and Bowen Liu. Their help, and friendship have been invaluable during my time as a graduate student. It has been a real pleasure working alongside each one of them.

TABLE OF CONTENTS

CHAPTER Page

APPENDIX Page

LIST OF FIGURES

Figure Page

CHAPTER 1

INTRODUCTION

1.1 History of telomerase research

Linear chromosomes in eukaryotic organisms require capping structures to maintain chromosomal termini during successive DNA replication (McClintock, 1941; Muller, 1938). These unique DNA sequences along with capping protein structures were termed ‘telomeres’ (McClintock, 1941). After 40 years, Elizabeth Blackburn reported the first telomeric sequece from the ciliate *Tetrahymena thermophila* (Blackburn & Gall, 1978). Telomere nucleoprotein complexes are composed of a vast array of short, highly repetitive DNA sequences (repetitive T_2G_4 in *Tetrahymena*). The guanosine rich strand was named ‘G-strand’ due to its high guanosine content compared to the complementary ‘C-strand’ for the high frequency of cytosine. Similar to *T. thermophila*, human telomeres are also composed of short, repetitive DNA sequences ‘TTAGGG’ (Moyzis et al, 1988). The sequence of telomeric DNA is conserved among vertebrate species, including humans as well as numerous marine invertebrates, fungi, plants, and protozoans (Meyne et al, 1989; Podlevsky et al, 2008). This indicates ‘TTAGGG’ as the common ancestral telomeric DNA sequence throughout major eukaryote lineages.

Following the discovery that the material of inheritance is DNA replicates semi-conservatively, the ‘end-replication problem’ was recognized (Lingner et al, 1995; Olovnikov, 1973; Watson, 1972). This problem arises due to the inability of conventional DNA polymerases to completely replicate linear chromosomal ends. DNA polymerases synthesize daughter DNA strand in a 5’-to-3’ direction and require a free 3’-hydroxyl group for the nucleotide addition. The RNA primers that provided

the free 3'-hydroxyl group for DNA synthesis will be degraded. At the very end of the chromosome, RNA primer cannot be filled with DNA and the daughter lagging strand will be shorter than the parental strand as the result. It has been found linear chromosome ends in eukaryotes have 3'single stranded DNA overhangs (Makarov et al, 1997). The exonucleases Apollo and Exo1 act upon and resect blunt-ended DNA produced by leading strand synthesis (Sfeir et al, 2005). The resection decreases the length of parental DNA in the leading strand and the daughter strand in the lagging strand (Huffman et al, 2000). Due to the end-replication problem, progressive loss of chromosome termini occurs and upon reaching critical lengths, which leads to genomic instability ensues followed by cellular senescence and apoptosis (de Lange, 2009). (Figure 1.1)

The biochemical activity to maintain telomeres from progressive loss of telomeric DNA was found to be from a specialized ribonucleoprotein complex named telomerase (Greider & Blackburn, 1985; Greider & Blackburn, 1987). Telomerase can synthesize short DNA repeats to the ends of chromosomes to offset the loss of telomere length following each round of DNA replication (Shippen-Lentz & Blackburn, 1990). (Figure 1.2) Unlike traditional reverse transcriptases, the telomerase enzyme is a ribonucleoprotein (RNP) consisting of two essential components for activity: the telomerase reverse transcriptase (TERT) protein and the integral telomerase RNA (TR) (Greider & Blackburn, 1987; Greider & Blackburn, 1989). The TERT protein is the catalytic subunit while the TR harbors a small region that provides the template for repeat addition. The TERT and TR form the minimal catalytic core of telomerase with accessory proteins for proper biogenesis,

localization, and regulation of telomerase (Egan & Collins, 2010; Fu & Collins, 2003; Kiss et al, 2010; Venteicher & Artandi, 2009).

Telomere length homeostasis is crucial for cell survival while mis-regulation leads to disorders and diseases in humans and other species. The expression of telomerase in human cells is tightly regulated. In most somatic cells, telomerase activity is undetectable while stem and germ-line cells show significant activity (Hiyama & Hiyama, 2007). Telomerase acts like a molecular clock for somatic cells, which limits their replicative capability. As a result, somatic cells will enter a stage of senescence and eventually death following a defined number of replications (Hayflick & Moorhead, 1961). Models such as protein counting and replication fork have been established to elucidate the telomere length regulation by telomerase (Greider, 2016; Marcand et al, 1997; Wellinger & Zakian, 2012). Mutations in telomerase or its accessory proteins that reduce telomerase activity can cause short telomere syndromes and a range of associated age-related disease (Armanios, 2009; Podlevsky & Chen, 2012; Sarek et al, 2015). On the contrary, with upgraded telomerase activity, cancer cells are able to maintain or even elongate telomeres and escape senescence allowing immortal growth. Nearly 90% of human cancers shown an up-regulation of telomerase, which make it a promising target for cancer therapy (Arndt & MacKenzie, 2016; Chen & Zhang, 2016; Kim et al, 1994). The importance of telomerase is evidenced by the Nobel Prize in Physiology or Medicine awarded to Elizabeth Blackburn, Carol Greider and Jack Szostak for their pioneering work in the discovery of how chromosomes are protected by telomeres and telomerase.

1.2 Telomerase reverse transcriptase

The TERT protein is the catalytic subunit of the telomerase enzyme, which is used for the synthesis of telomeric DNA using the hTR template. The TERT protein is composed of four highly conserved domains: the telomerase essential N-terminal (TEN) domain, the telomerase RNA binding domain (TRBD), the reverse transcriptase (RT) domain, and the C-terminal extension (CTE). (Figure 1.3A) The TEN and TRBD domains are TERT specific while RT and CTE domains share similar motifs with other DNA polymerases and reverse transcriptases (Lingner et al, 1997). The TRBD–RT–CTE domains of TERT form a ring like structure with a centralized active site to hold the RNA/DNA duplex during extension (Gillis et al, 2008). (Figure 1.3B)

The TEN domain of TERT binds TR and single-stranded telomeric DNA. The TEN domain contains a DNA 'anchor' site specifically binding single-stranded telomeric DNA, which is essential for processive telomeric DNA repeat synthesis. (Finger & Bryan, 2008; Jacobs et al, 2006; Lue & Li, 2007; Romi et al, 2007; Sealey et al, 2010). This binding can prevent complete release of the DNA substrate from the active site of enzyme and increases repeat addition processivity (Wyatt et al, 2010). It has been found that a conserved leucine residue outside of the DNA anchor site is reported to increase telomeric repeat addition processivity, whereas no homologous residues yet discovered in the TEN domains of human or yeast. Apart from the DNA anchor site and that leucine residue, the TEN domain contains a low-affinity RNA-binding site for the TR pseudoknot region. (Lai et al, 2001; Moriarty et al, 2004; Podlevsky & Chen, 2012). However, the mechanism of the interaction of TERT-pseudoknot unclear. Thought the TEN domain contains processivity-increasing

elements and a low-affinity RNA binding site, it is not indispensable for telomerase activity (Eckert & Collins, 2012). Insect species, such as *Tribolium castaneum*, has been reported without the TEN domain entirely in the telomerase (Gillis et al, 2008; Mitchell et al, 2010).

TRBD is a prevalently conserved domain of TERT, which contributes to the majority interaction between TERT and TR (Bley et al, 2011; Huang et al, 2014; Jansson et al, 2015; Moriarty et al, 2004). The TRBD consists three universally conserved motifs: CP, QFP, and T. These three motifs form a major RNA binding pocket with a highly helical structure in both *T. thermophila* and *T. castaneum* crystal structures (Gillis et al, 2008; Rouda & Skordalakes, 2007). The TERT specific motif T contains a highly conserved "FYXTE" sequence forming a hairpin structure. Motif T has been reported to interact with the RNA backbone of the RNA/DNA duplex and involved in repeat addition processivity (Drosopoulos & Prasad, 2010; Mitchell et al, 2010). There are also other TR binding elements such as vertebrate-specific region (VSR) and ciliate counterpart (CP2) present in TRBD (Harley, 2002; Moriarty et al, 2002).

The RT and CTE domains of TERT protein share motifs with other conventional reverse transcriptases, contain a right hand with finger, palm and thumb subdomains (Gillis et al, 2008; Mitchell et al, 2010; Nakamura et al, 1997). The RT domain consists of a structural and functional homolog of the “fingers”, “palm” domains and other seven conserved motifs: 1, 2 and A, B, C, D, and E (Figure 1.3). The finger domain (motifs 1 and 2) is responsible for binding incoming nucleotides as well as positioning the RNA template and the palm domain (motifs A, B, C, D, and E). It is constituting the catalytic site for polymerization (Bosoy & Lue, 2001). Within

the palm domain of the TERT protein, there are three invariant aspartic acids consistently conserved among all DNA polymerases (Lingner et al, 1997). These aspartic acids coordinate the positioning of two magnesium atoms. Mutation in any one of these three conserved aspartic acids will result in inactive telomerase *in vitro* and telomere shortening *in vivo* (Bryan et al, 2000; Counter et al, 1997; Harrington et al, 1997; Nakayama et al, 1998; Weinrich et al, 1997; Wyatt et al, 2010). Additionally, TERT contains an invariantly conserved lysine residue in motif D, which is believed to activate the pyrophosphate leaving group generated from the nucleotide addition. The mutation of this lysine in TERT compromises telomerase activity severely (Bryan et al, 2000; Miller et al, 2000; Sekaran et al, 2010). It has been reported that motif E functions in positioning the single strand DNA in the TERT palm domain (Peng et al, 2001; Wyatt et al, 2007). This is further supported by the TERT crystal structure in *Tribolium castaneum*, in which a coiled loop is close to the end of the DNA primer (Mitchell et al, 2010).

While the RT domain of TERT shares conserved motifs with conventional RTs, it also has several telomerase unique motifs to perform telomerase-specific functions. Mutagenesis studies of insertion in fingers domain (IFD), a large insertion found in the finger domain, have identified its important role in telomerase repeat addition processivity and telomere maintenance (Lue et al, 2003). According to the structural data, this domain, instead of direct contact with the DNA or RNA appears to be crucial for protein arrangement (Gillis et al, 2008; Mitchell et al, 2010). Motif 3, another telomerase-specific motif named due to its location following motif 2, is directly involved in repeat addition processivity (Xie et al, 2010). Specific residues within this motif have been shown to influence repeat addition rate independent of

altering repeat addition processivity of telomeric repeat synthesis. Motif 3 contains a helix-coil-helix structure close to the RNA/DNA duplex bound to the active site (Gillis et al, 2008; Mitchell et al, 2010).

The C-terminus of the TERT protein, called the C-terminal extension (CTE), contains little sequence homology to conventional RTs. The overall structure and function of CTE, however, is similar to the 'thumb' domain of retroviral RTs, such as HIV1 RT (Gillis et al, 2008; Mitchell et al, 2010; Nakamura et al, 1997). Structurally, it is close to the ring structure based on the *Tribolium castaneum* TERT, and it has been proposed that the CTE might interact with TR, when bound to the TRBD (Bley et al, 2011). Functionally, the CTE has been reported to have influence on telomeric DNA binding, telomerase activity and processivity (Hossain et al, 2002).

1.3 Telomerase RNA

In contrast to conventional RTs, telomerase contains an integral RNA component indispensable for enzymatic activity. Unlike the TERT protein, which is conserved, the TR is significantly divergent among different species. Despite the variation, there are two universally conserved motifs of TR: the template pseudoknot domain and distal stem-loop moiety or three-way junction (Blackburn & Collins, 2010; Brown et al, 2007; Chen & Greider, 2004; Chen et al, 2002; Chen et al, 2000; Lin et al, 2004). (Figure 1.4) These two TR elements are necessary for reconstituting telomerase activity *in vitro* when added *in trans* with the TERT (Mitchell & Collins, 2000; Tesmer et al, 1999).

The hTR pseudoknot domain contains a triple helix structure consist with Hoogsteen base-pairings to a Watson-Crick base-paired helix in human (Theimer et al, 2005). Several other species have also been shown or predicted to have a similar

triple helix pseudoknot in their respective TRs (Qiao & Cech, 2008; Shefer et al, 2007). Biochemical and structural studies have shown that the pseudoknot with a conserved triple helix is essential for proper telomerase activity (Chen & Greider, 2005; Ly et al, 2003; Qiao & Cech, 2008; Shefer et al, 2007; Theimer et al, 2005). However, the exact function of the structure remains unclear. The pseudoknot is distant from the template sequence in the primary sequence, but they are close to each other in the secondary structure. Therefore, the pseudoknot has been postulated to function in template positioning or retention near the active site. NMR structures have revealed that there is a sharp kink between the triple helix and the template, which could be responsible for the positioning of the template (Zhang et al, 2011; Zhang et al, 2010). In the template region of the TR, the 5' end is used as the template for synthesis of telomeric DNA repeats and a non-templating region at the 3' end is a realignment region for annealing of the extended DNA at beginning of each repeat synthesis. Mutations in the TR template demonstrate that the sequence plays a key role in regulating telomerase activity and telomere length. Meanwhile, it contains a unique pausing signal for self-regulation of human telomerase (Brown et al, 2014; Drosopoulos et al, 2005. The upstream region of the TR template is known as the Template boundary element (TBE) and it defines the 5’ boundary of the template. The TBE consists of the P1b helix and the single stranded RNA between the 5' end of the template in vertebrates (Chen & Greider, 2003). (Figure 1.4) Structurally, TBE bound to TRBD establishes the template boundary. Being localized at the correct distance from the active site, TBE prohibit copying of non-template nucleotides in *Tetrahymena*. (Jansson et al, 2015) Mutations that alter the length or disrupt P1b have been shown to affect the telomere repeat sequence (Chen & Greider, 2003; Theimer &

Feigon, 2006). The upstream region of the template/pseudoknot domain in hTR exists a guanosine-rich region, which may form a G-quadruplex structure. The G-quadruplex structure in association with the HEXH box RNA helicase RHAU has been reported to increase TR accumulation within cells (Lattmann et al, 2011; Sexton & Collins, 2011).

Another conserved region of telomerase RNA crucial for proper enzymatic activity is a stem-loop moiety located downstream of the pseudoknot region. This element has been termed as conserved region 4/5 (CR4/5) in vertebrates, three-way-junction (TWJ) in yeasts as well as helix IV in ciliates (Blackburn & Collins, 2010; Brown et al, 2007; Chen et al, 2000; Chen et al, 2002; Qi et al, 2013). In vertebrates, the CR4/5 domain contains a three-way junction three conserved stems P5, P6, and P6.1 (Blackburn & Collins, 2010; Brown et al, 2007; Chen et al, 2002; Chen et al, 2000). (Figure 1.4) This structure is indispensable for telomerase activity both *in vivo* and *in vitro* in major eukaryotic clades. Disruptions or mutations of two conserved residues in P6.1 can abolish telomerase activity (Bley et al, 2011; Chen et al, 2002). Cross-linking studies mapped the CR4/5 binding site onto TRBD and the binding surface was elucidated by an RNA-protein co-crystal structure (Bley et al, 2011; Huang et al, 2014). In yeast, a three-way junction structure similar to the CR4/5 domain of vertebrates has also been shown to be necessary for telomerase activity (Brown et al, 2007; Zappulla et al, 2005). Moreover, in the fission yeast *Schizosaccharomyces pombe* and filamentous fungi *Neurospora crassa*, a structure that is similar to CR4/5 in fungal termed P6/6.1 has been reported. The P6/6.1 of the filamentous fungal TR, like CR4/5 in vertebrate, is necessary for telomerase activity (Qi et al, 2013). Ciliate TRs has a conserved Helix IV instead of a three-way junction

structure, which is functionally analogous to helix P6.1 of the vertebrate CR4/5. Helix IV interacts with TERT and is required for telomerase function (Blackburn & Collins, 2010).

Other than the conserved pseudoknot domain and stem-loop moiety, the hTR contains another major structurally conserved domain known as the H/ACA domain. This H/ACA domain contains two stem-loops separated by box H and ACA moieties (Jády et al, 2004; Mitchell et al, 1999). (Figure 1.4) This domain is homologous to small nucleolar (sno-) and small cajal body-specific (sca-) RNAs. Two copies of the dyskerin complex binds to the H/ACA domain of hTR (Egan & Collins, 2010). The dyskerin complex contains four proteins: dyskerin, NOP10, NHP2, and GAR1 and is essential for the proper RNA maturation and RNP biogenesis (Cheng & Roberts, 2001; Girard et al, 1993; Hamma et al, 2005; Hockemeyer & Collins, 2015; Maiorano et al, 1999; Pogacić et al, 2000).

A number of human telomerase-mediated diseases are due to TR mutations, such as Aplastic Anemia, Idiopathic Pulmonary Fibrosis and Dyskeratosis Congenita (Alder et al, 2008; Alder et al, 2011; Armanios et al, 2007; Dokal, 2003; Du et al, 2009; Fogarty et al, 2003; Marrone et al, 2004; Tsakiri et al, 2007; Vulliamy, 2002; Vulliamy et al, 2006; Yamaguchi et al, 2003). These disorders occur due to the haplo-insufficiency of a single functional TR allele, which leads to insufficient TR accumulation, reduced telomerase levels and telomere shortening (Armanios et al, 2005). Disease mutations in template-pseudoknot, CR4/5, and H/ACA domains of hTR can disrupt RNA base-pairing, RNA secondary structure that is essential for enzymatic activity or RNA processing and accumulation (Podlevsky et al, 2008). Telomerase activity reduction or impaired RNA accumulation levels have been

reported for some disease mutations (Alder et al, 2008; Alder et al, 2011; Armanios et al, 2007; Cristofari et al, 2007; Fu & Collins, 2003; Ly et al, 2005; Theimer et al, 2003; Theimer et al, 2007).

1.4 Telomerase Mechanism

Contrary to conventional RTs which use a long RNA template and bind pre-annealed DNA/RNA duplex to synthesize DNA, telomerase uses single stranded DNA as its substrate and contains an internal short template in the TR to add multiple repeats of DNA sequence in a processive manner. Like many polymerases, telomerase catalyzes the addition of incoming nucleotides to the 3' hydroxyl group of substrate primer, forming a product–template duplex. The mechanism of polymerization is same as other RTs employing a metal-dependent chemistry of nucleotide addition (Steitz, 1999). Incoming nucleotides are bound by the binding pocket between the fingers and the palm domain of the TERT protein and three conserved aspartic acid residues in the palm domain of TERT coordinate two Mg^{2+} ions in the active site (Gillis et al, 2008). The DNA/RNA duplex is placed in the active site and interacts with many regions of TERT including motif T, motif 3, the fingers domain and the CTE (Gillis et al, 2008; Mitchell et al, 2010; Wu et al, 2017; Xie et al, 2010). Once polymerization begins, the DNA/RNA duplex will be moved through the cavity of TERT's ring like structure to position the 3' end of newly synthesized DNA into the active site. It has been shown the length of the extended DNA/RNA duplex is maintained at a length of five to seven base pairs by concomitantly unpairing base pairs at the 5' end of the DNA for additional base pairs made at the 3' end (Förstemann & Lingner, 2005; Qi et al, 2012). Structurally, the central cavity of the

protein is only sufficient to harbor a duplex of seven to eight base pairs in *T. castaneum* (Gillis et al, 2008).

A highly unique property of telomerase compared to other polymerases is "repeat addition", which is the repetitive synthesis of a long telomeric DNA without complete dissociation of the telomerase enzyme by using the short template in TR (Greider, 1991). While the exact process remains unclear, several working models for telomerase catalytic cycle have been proposed. A repeat addition cycle may contain several major steps: nucleotide addition, duplex disassociation, strand unpairing, template realignment, and duplex binding.

Accurate template use requires DNA synthesis to stop at the 5' end of the template. Once telomerase reaches the 5' end of its boundary, the duplex should dissociate from the active site to regenerate the template. The 5' end of the template is determined by the spacing from an adjacent RNA–protein and/or an RNA–RNA interaction (Podlevsky & Chen, 2016). Interestingly, in human telomerase the pause signal embedded in the sequence of template–product duplex makes the dominant contribution to prevent template read through (Brown et al, 2014). Then telomerase dissociates from the extended substrate regenerating the internal template. To achieve this, the two strands of the duplex need to be separated, followed by realignment at the beginning of the template for a next round of repeat addition. Template unpairing and repositioning require significant conformational changes compared to nucleotide addition (Wu et al, 2017). To explain the thermodynamic driver of duplex melting, there are several models have been proposed. For instance, DNA/RNA duplex could release together and reposition outside the active site (Qi et al, 2012); the TR template flanking elements serve to position the template for nucleotide addition while the

DNA remain bound to the active site (Berman et al, 2011); or product DNA forms a hairpin structure while still bound to telomerase (Yang & Lee, 2015).

Biochemical data support that the active site of telomerase becomes accessible and unoccupied to a short external DNA/RNA duplex during repeat synthesis (Qi et al, 2012). This indicates full dissociation of the DNA/RNA duplex from the active site during template translocation. Using a comparison between the crystal structures of TERT in *T. castaneum* with and without a duplex bound to the active site, it could be predicted that the duplex melting in the active site would not be feasible. It requires a drastic conformation altering to disrupt not only the hydrogen bonds of the duplex, but also the protein-nucleic acid contacts which hold the duplex in the active site. It has been reported in several species that the sequence of the primer determines the binding affinity to the telomerase instead of base pairing between the DNA primer and RNA template (Finger & Bryan, 2008; Hammond & Cech, 1998; Wallweber et al, 2003). This indicates that protein nucleic acid interactions play an essential role in stabilizing the DNA/RNA duplex.

Another working model proposes that during repeat synthesis progression, the template 5' loop could reel into the active site while the 3' end of the template could be extruded from it. A 3' loop formed by complete repeat synthesis could make an RNA–RNA or RNA–protein interaction (Wu et al, 2017). Protein remodeling is required to dissociate the product–template duplex, thus promoting template translocation and default positioning of template. The single-stranded DNA retention surface (SRS) retains some interactions between DNA and TERT protein that were formed during repeat synthesis. The DNA unpaired from the TR template remains bound to TERT at SRS (Wu et al, 2017). Single-stranded DNA could thread passively

across the TERT surface and bring the template's 3' end closer to the 3' end of the DNA for base pairing. A single-molecule FRET study that monitors telomere DNA structure and dynamics during the telomerase catalytic cycle indicates that template translocation is a rapid process. There could be a second slow conformational change repositioning the DNA/RNA hybrid into the telomerase active site that drives the extrusion of the 5' end of the DNA primer out from the enzyme complex (Parks & Stone, 2014).

During template translocation, the telomeric DNA remains bound to the TEN domain of TERT even while upon dissociation from the central cavity near the active site (Finger & Bryan, 2008; Jacobs et al, 2006; Wyatt et al, 2007; Zaug et al, 2008). This interaction tethers the telomeric DNA to the TERT protein to increase the translocation efficiency because the DNA must dissociate from the active site for repeat synthesis. Additionally, at the TEN domain anchor site two telomerase accessory proteins, POT1 and TPP1, have been shown to play a significant role in decreasing the probability of DNA dissociation by direct interactions with both the single stranded DNA and TERT protein (Latrick & Cech, 2010; Wang et al, 2007). While the DNA is still bound to the TERT, the 3' end of the substrate can find the free RNA template and anneal to the template realignment region. Proper positioning of DNA and realignment region to prevent reannealing to the 5' end of templating region is driven by steric forces of the TR scaffold, which stretch and compress in the template flanking regions (Berman et al, 2011). Or duplex formation could be a cause or consequence of reversing the structural change that released the template 5' end from the active site (Wu et al, 2017). The length of complementary sequence in the

realignment region could be responsible for the efficiency for longer sequences producing more processive enzymes (Chen & Greider, 2003).

After forming the DNA/RNA duplex, it is then free to bind to the active site for next round of repeat addition. The newly formed duplex is very short because of the length of the alignment region (five nucleotides in humans), it could be unstable at 37°C. To stabilize the binding of the duplex, the protein-nucleic acid interaction would be crucial for efficient template translocation. It has been proven both duplex substrates and short eight nucleotide primers, which lack upstream nucleic acid to from additional protein interactions to hold TERT during translocation, showed an obvious correlation between the binding affinity of the substrates and the repeat addition processivity of various TERT mutants (Qi et al, 2012; Xie et al, 2010). This indicates that the duplex binding affinity of TERT is important for repeat addition processivity. Repeat addition processivity can be stimulated by higher concentration of dGTP by enhancing the rate of addition as in human or the translocation efficiency for telomerase from Chinese hamster ovary (CHO) (Maine et al, 1999; Sun et al, 1999). It has also been shown this dGTP dependent processivity could be due to a secondary allosetric binding site for the deoxyguanosine moiety in *T. thermophila* (Hardy et al, 2001).

1.5 Project

The telomerase reaction is a highly orchestrated but poorly understood catalytic cycle to regenerate the short RNA template for synthesis of multiple telomeric DNA repeats. There are many independent subunits of telomerase that must coorperate to perform its function completely. Even though it has been studied for many years, there are many unanswered questions and numerous phenomena that

have not been explained. This study aims to identify and explore the mechanism of intrinsic and extrinsic factors that affect the telomerase catalytic function, including hTR template sequence, specific motif of hTERT, nucleotide concentration as well as telomerase inhibitor.

In chapter 2, characteristics of the template embedded pausing signal are identified in human telomerase. After investigating the pausing signal, we explored telomerase activity with a series of distinct lengths of DNA/RNA duplex in the template free telomerase system. The 5' DNA overhang can alleviate the pausing signal but not the 3' RNA overhang. No effect on pausing signal by the RNA 5' end flanking sequence indicates its existence is before and after template translocation. Further, the competition assay with circular permutated duplexes showed sequence dependent pausing is attributed to catalytic deficiency.

In chapter 3, the mechanism of dGTP dependent stimulation of telomerase activity is explored. Employing template free system, the apparent K_M of nucleotide addition for each position on the hTR template is measured. The K_M of the first nucleotide after pausing signal is significantly higher, and it requires higher concentrations of the respective nucleotide for incorporation. To address why dGTP stimulates accumulation of longer DNA products, we applied bound-release and pulse-chase assays to quantify the repeat addition processivity and repeat addition rate of telomerase. We observed that higher concentration of dGTP cause the increase both repeat addition processivity and rate which can be explained that it is the first nucleotide added after translocation. Furthermore, the dGTP failed to stimulate the repeat addition processivity after disrupting the pausing signal. Additionally, we also

explored the usage of deoxynucleoside diphosphates for telomerase as well as other RTs and DNA polymerases.

In chapter 4, the postulated mechanism of how the disease-causing K570 residue mutation in TERT affects telomerase activity will be described. To determine its defects in processivity, alanine screening was done to determine the role of K570 residue in telomerase processivity. Moreover, we explore the essentiality of charge and position of this residue by additional mutagenesis experiments. Next, the apparent K_M value for K570A mutant is determined to test the deficiency of nucleotide incorporation. Additionally, the mutant shows binding defects with its DNA substrate as well as DNA/RNA duplex in template free system.

In chapter 5, the mechanism of telomerase inhibitor BIBR 1532 is investigated. We tested the inhibition of human telomerase activity with titration of BIBR 1532, following exploration of its function in TERT expression, RNP reconstitution and enzymatic reaction. Without influencing TERT expression or RNP reconstitution, BIBR 1532 shows no effect in nucleotide addition or on the apparent K_M value. Taken together, all above studies provided a novel understanding of human telomerase function and further refining the working model of the telomerase catalytic cycle.

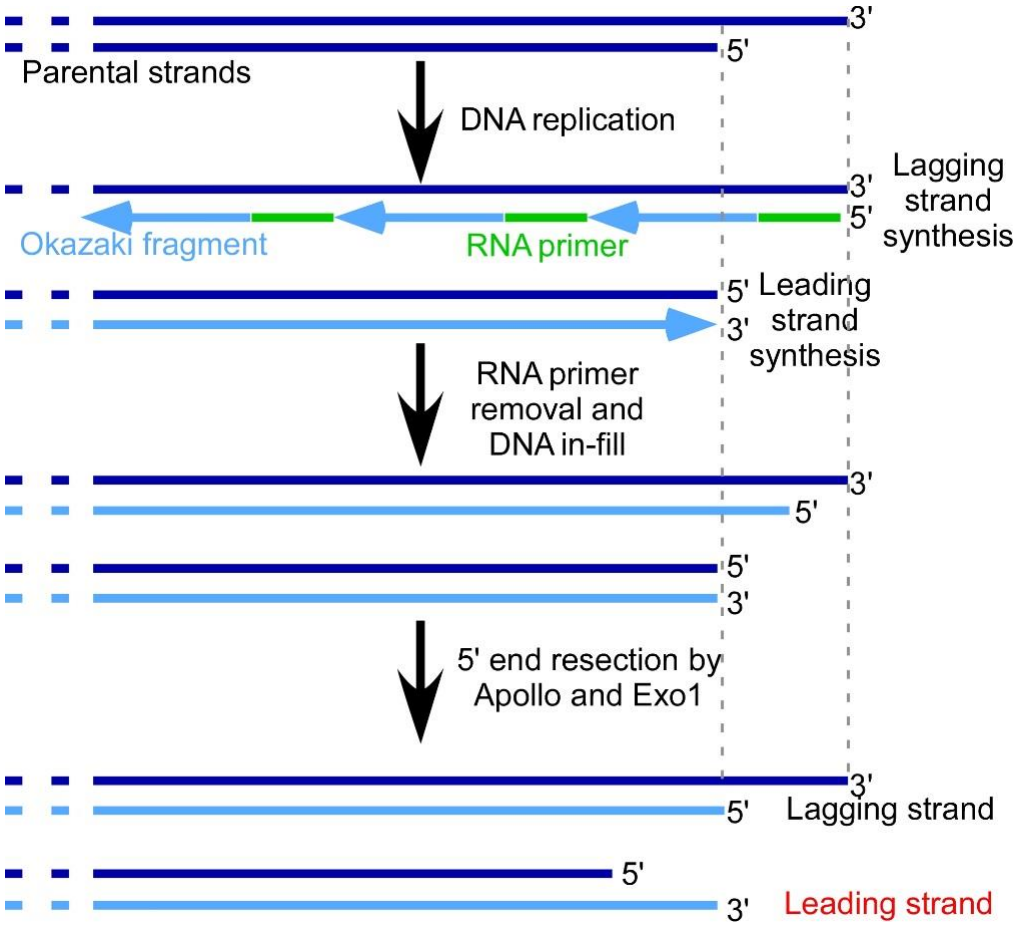

Figure 1.1. The end-replication problem is the critical loss of chromosomal ends with each replication cycle. Conventional DNA polymerases are unable to fully replicate the ends of linear chromosomes leading to shorter DNA products (light blue) than the parental DNA strands (dark blue). The end-most lagging strand RNA primer (green) cannot be replaced with DNA resulting in a slightly shorter DNA strand (light blue). Leading strand synthesis generates a blunt-end, which is then processed by the exonucleases Apollo and Exo1 to generate a far shorter DNA product (dark blue).

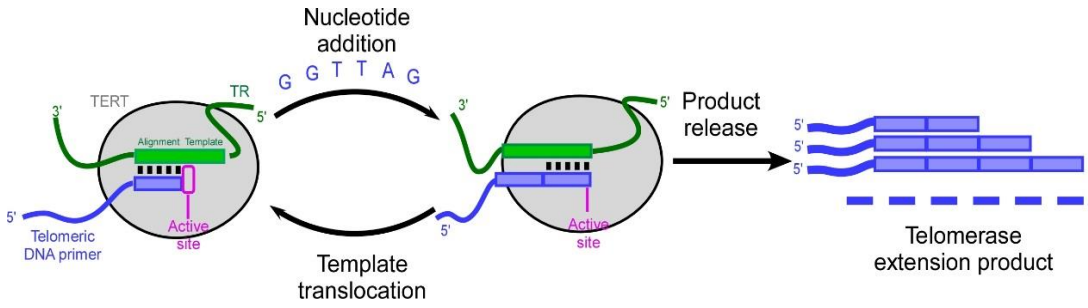

Figure 1.2. The telomerase catalytic cycle. Telomerase acts as a conventional reverse transcriptase by extending single-stranded telomeric DNA primer (*blue*) or onto the ends of telomeric DNA utilizing an intrinsic RNA template (*green*). Different from conventional polymerases, after reaching the end of the template, telomerase can regenerate the template by template translocation for an additional round of nucleotide addition. This leads to the generation of longer telomeric DNA products. After each round of DNA synthesis, unsuccessful template translocation can terminate additional repeat addition leading to product release.

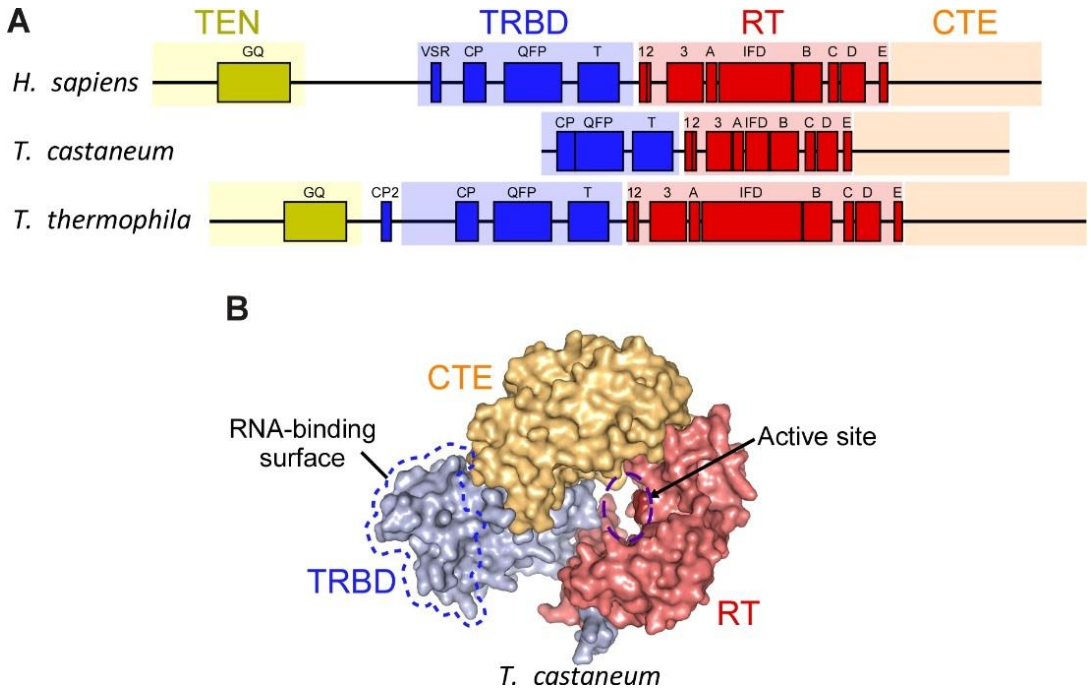

Figure 1.3. Structure of the catalytic TERT protein subunit. (**A**) TERT consists of four structural domains: telomerase essential N-terminal (TEN, *yellow*) domain, telomerase RNA-binding domain (TRBD, *blue*), reverse transcriptase (RT, *red*), and the C-terminal extension (CTE, *orange*). The TEN and TRBD are telomerase-specific, essential for template translocation. Important motifs within each domain are colored similarly. (**B**) The *Tribolium castaneum* TERT crystal structure demonstrates that TRBD, RT, and CTE domains form a ring like structure, unseen in other polymerases. TRBD contains the crucial TR binding site (dashed line) within TERT. The TERT active site (*purple*), motif 3 (*dark red*) and motif IFD (*red-orange*) in the RT domain are denoted.

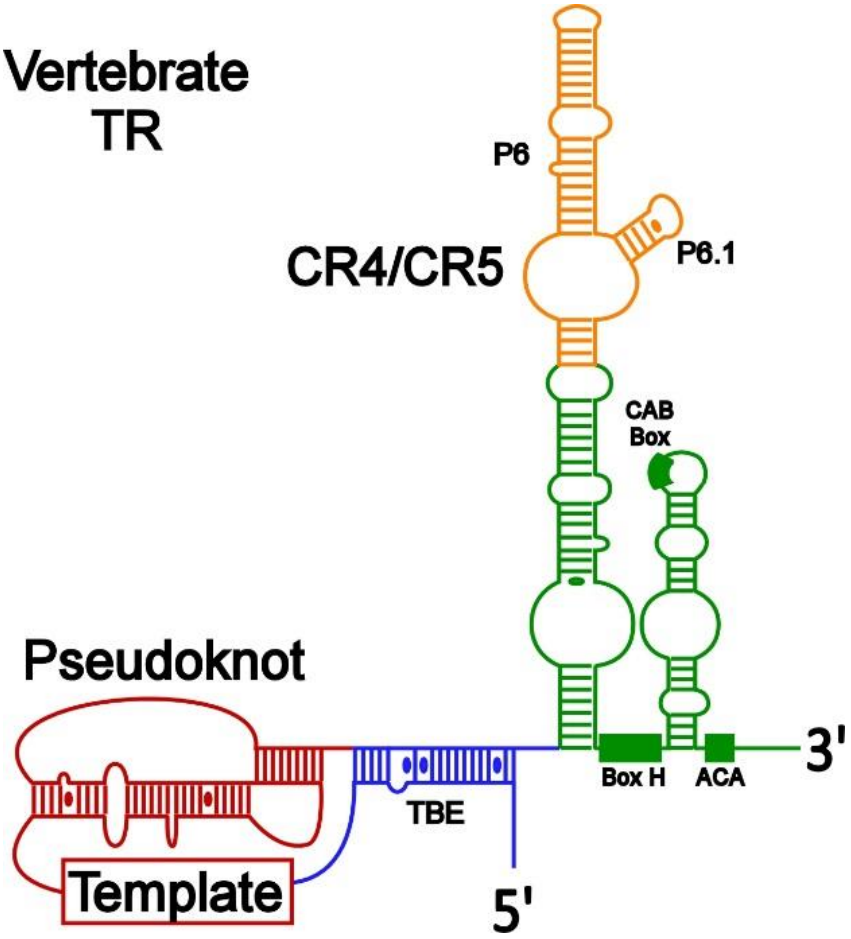

Figure 1.4. Secondary structure of vertebrate TR. Two major structural elements are common to all known TRs: a template proximal pseudoknot (*red*) and template-distal three-helical junction CR4/5 in vertebrates (orange). Additionally, there is a template boundary element (TBE, *blue*) which defines the boundary of the TR template. Vertebrate TRs contain a CR4/5 domain (*red*) essential for activity and a distal H/ACA domain with a CAB box (*green*) for TR biogenesis and localization. Vertebrate TRs contain a CR4/5 domain (*orange*) composed of P6 and P6.1. The 3'-proximal H/ACA domain with a CAB box in the apical loop (*green*) is crucial for TR biogenesis and telomerase localization.

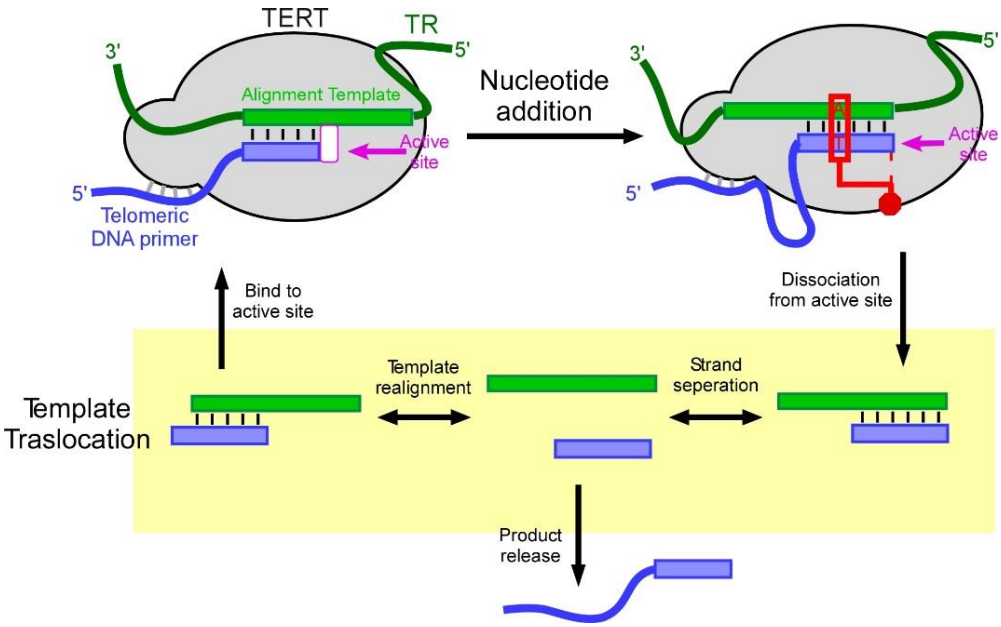

Figure 1.5. A working model for the telomerase catalytic cycle. Schematic of human telomerase bound to a telomeric DNA primer (*blue*). The TR alignment region (*green*) is base-paired with the 3'-end of the telomeric DNA primer (*blue*) to form 5 base pairs adjacent to the active site (*purple arrow*). TERT (*gray*) catalyzes the addition of six deoxyribonucleotides to the 3' end of the DNA primer by reverse transcribing the TR template sequence. After nucleotide addition, a new repeat is generated which retains only 5-6 base pairs. After reaching the end of the template, the nucleotide addition is arrested by the pausing signal (*red*) along with the restriction imposed by the physical boundary. The duplex dissociates from the active site. Outside the active site, the DNA/RNA duplex undergoes template translocation (*yellow box*) involving strand separation and template realignment to reform 5 base pairs. Further nucleotide addition can proceed with the regenerated template. Unsuccessful realignment of the DNA primer to the RNA template eventually results in complete dissociation of the DNA product from the enzyme. Strand separation and template realignment are postulated as reversible, with multiple binding/separation steps possible.

CHAPTER 2

IDENTIFICATION OF THE PROPERTIES OF TEMPLATE-EMBEDDED PAUSE SIGNAL

Reproductions with permission in part from:

Brown, A. F., Qi, X., Podlevsky, J. D., Chen, Y., Mingyi, X., & Chen, J. J.-L. (2014). A Self-Regulating Template in Human Telomerase. Proc. Natl Acad. Sci. USA, 111, 11311-11316.

2.1 Abstract

Telomerase is a special reverse transcriptase (RT) containing an intrinsic telomerase RNA (TR) component. It synthesizes single strand telomeric DNA repeats reiteratively by copying a precisely defined, short template sequence from the integral TR. The mechanism of how the telomerase accurately and efficiently uses this short template region during processive DNA repeat synthesis is unclear. The human TR template, in addition to specifying the DNA repeat sequence, is embedded with a single-nucleotide signal enabling the pause of DNA repeat synthesis. This pause site coincides precisely with the physical template boundary, and it precludes the incorporation of non-telomeric nucleotides from the hTR template flanking region. To characterize the sequence-defined pausing mechanism, we employed template-free telomerase system and found the pausing signal following template translocation also has a similar influence on the incoming nucleotide incorporation. Additionally, the pausing signal is attributed to the inefficient catalysis for the duplex instead of binding affinity defect. The processive addition of DNA repeats by native telomerase could be explained by the comprehensive interaction of the telomerase core enzyme with telomeric DNA substrate. The 5’ end overhang of DNA, designed to imitate the

intermediate products of a native telomerase reaction, is able to alleviate the pausing signal. In this study, the identified properties of pausing signal provide essential clues to understand the accurate synthesis of the GGTTAG repeats as well as the catalytically regulatory function of telomerase.

2.2 Introduction

The ends of human chromosomes are composed of precise repetitions of a 6-nucleotide sequence synthesized by the specialized reverse transcriptase (RT) --- telomerase (Meyne et al, 1989; Moyzis et al, 1988). The telomerase core enzyme is composed of the catalytic telomerase reverse transcriptase (TERT) and the integral telomerase RNA (TR). Human TR (hTR) is a 451-nt RNA containing a very short 11-nt template which encodes for the telomeric DNA repeat "GGTTAG". The shelterin complex is bound to the highly repetitive tract of DNA a sequence-specific manner to protect natural chromosome termini from end-to-end fusions and other DNA damage responses (Palm & de Lange, 2008; Sfeir & de Lange, 2012). High fidelity synthesis of telomeric DNA repeats by telomerase is critical for maintaining telomere function and chromosome stability. The TR template itself is highly conserved, even though TR sequences are highly divergent across species (Chen et al, 2000; Xie et al, 2008). In vertebrates, the template sequence is conserved as a specific register with the 5' boundary defined physically by a long-ranged based-paired region known as helix P1 (Chen & Greider, 2003). It has been proven the importance of the specific TR template sequence for the telomerase enzymatic function, whereby alterations in the template or realignment sequence affect the rate and processivity of telomeric DNA repeat synthesis (Drosopoulos et al, 2005; Förstemann et al, 2003; Gilley & Blackburn, 1996; Gilley et al, 1995; Qi et al, 2012). Additionally, telomerase has been

shown to exhibit differential activity toward telomeric DNA primers with permuted sequences (Maine et al, 1999; Wallweber et al, 2003).

During telomere repeat synthesis, telomerase catalyzes nucleotide incorporation to the DNA primer with the RNA template which forms a duplex in the active site (Qi et al, 2012). After each nucleotide addition, it would become a different RNA/DNA duplex sequence inside the binding pocket of the catalytic TERT subunit. Human telomerase lacking the template region from hTR (TF telomerase) has been tested with pre-annealed six permuted RNA/DNA duplexes as substrates for the activity (Figure 2.1). TF telomerase exhibited distinct extension patterns and diverse activities with each permuted duplex. Further studies demonstrated that the first rA:dT base pair formed in the duplex inducing a pausing signal in the telomeric DNA synthesis following the incorporation of three additional base pairs. A single-nucleotide signal embedded in hTR to pause nucleotide addition at an exact position to safeguarding the 5' boundary of the template region. In this study, I investigated the properties of the pausing signal in the role of telomerase DNA synthesis and catalytic cycle. By employing a telomerase-free telomerase system and specific assay conditions the sequence-defined pausing signal is essential for not only the accurate synthesis the GGTTAG repeats but also regulating the catalytic function of telomerase.

2.3 Material and Methods

Oligonucleotides and RNA/DNA hybrid substrates

All DNA and RNA oligonucleotides were purchased from Integrated DNA Technologies (IDT). The specific sequences of oligonucleotides used in each experiment are shown in the text or figures. The RNA/DNA duplexes were prepared

by adding the RNA and DNA oligos at a final concentration of 200 μM in 1x annealing buffer (100mM Tris–HCl pH 7.5, 500mM NaCl and 50mM EDTA). Duplex formation was facilitated by incubation at 65°C for 5 min, followed by slowly cooling to room temperature.

Reconstitution of telomerase

Reconstitution of human telomerase *in vitro* was carried out in RRL as previously described (Xie et al, 2010). Briefly, hTERT was expressed from pN-FLAG-hTERT using the TnT® T7 Quick coupled transcription/translation kit (Promega) according to the manufacturer's instruction. The hTR fragments, TF-PK (nt 64–184) and CR4/5 (nt 239–328), were transcribed *in vitro*, gel purified and added at a final concentration of 1 μM to assemble with hTERT in RRL. For quantification, hTERT was synthesized in the presence of ^{35}S-Methionine (>1000 Ci/mmol, 10.2 mCi/ml, Perkin-Elmer) and analyzed by SDS–PAGE.

Telomerase activity assay

For analyzing TF telomerase, 1 μl *in vitro* reconstituted TF telomerase was assayed in a 10 μl reaction containing 1x duplex reaction buffer (50 mM Tris- HCl, pH8.0, 50 mM KCl, 3 mM $MgCl_2$, 2 mM DTT and 1 mM spermidine), 40 μM pre-annealed RNA/DNA duplex, specified dNTPs and 0.165 μM of the denoted α-^{32}P-dNTP. The reaction was incubated at 20°C for 60 min followed by 55 °C for 5 min with the addition of 10 μg of RNase A and terminated by phenol/chloroform extraction, followed by ethanol precipitation. The DNA products were resolved on a 15% polyacrylamide/8 M urea denaturing gel, dried, exposed to a phosphorstorage screen and imaged on a Bio-Rad FX-Pro phosphorimager. The AMV RT duplex assay was identical to the TF telomerase duplex assays with the exception of substituting TF

telomerase with 0.5 unit of AMV RT enzyme (Promega) and the products were analyzed directly by denaturing polyacrylamide gel electrophoresis. The size markers for the template free duplex assay were prepared in a 10 μl reaction containing 1x reaction buffer (100 mM sodium cacodylate, pH 6.8, 1 mM $CoCl_2$ and 0.1 mM DTT), 10 μM oligonucleotide as indicated, 10 units of terminal deoxynucleotidyl transferase (TdT, Affymetrix) and 0.165 μM α-^{32}P-dGTP (3000 Ci/mmol, 10 mCi/ml, Perkin-Elmer). The reaction was incubated at 30°C for 5 seconds and terminated by the addition of 10 μl 2x formamide loading buffer (10 mM Tris-HCl, pH 8.0, 80% formamide, 2 mM EDTA, 0.08% bromophenol blue and 0.08% xylene cyanol).

Duplex Competitive Inhibition Assay.

One microliter of *in vitro* reconstituted template-free telomerase was assayed in a 10 μL reaction containing 1x duplex reaction buffer, 40 μM non-telomeric duplex as substrate, 5 μM or 20 μM nonreactive telomeric duplex as competitor, 2 μM dGTP, and 0.165 μM [α-^{32}P]dGTP (3,000 Ci/mmol, 10 mCi/mL; Perkin-Elmer). The reaction was incubated at 20 °C for 60 min followed by 55 °C for 5 min with the addition of 10 μg of RNase A and terminated by phenol/chloroform extraction followed by ethanol precipitation. The DNA products were resolved on a 15% (wt/vol) polyacrylamide/8 M urea denaturing gel, dried, exposed to a phosphorstorage screen, and imaged on an FX-Pro phosphorimager (Bio-Rad).

2.4 Results

The pause site was retained before or following template translocation.

When the DNA substrate extended to the end of the template, the pausing signal together with TBE prevents the usage of the flanking region of the template. According to the telomerase working model, template translocation is required for

regenerating the short hTR template. After template translocation, the telomeric DNA substrate and hTR alignment region will form the duplex with the same sequence. To explore the sequence-dependent pausing signal after translocation, I tested the function of the 5' end of RNA template flanking sequence. I employed two RNA sequences, UGUU and CCAA with an overhang at 5' end, which represents the hTR template 5' regions flanking the RNA/DNA duplex prior to or following template translocation (Figure 2.2). Regardless of the flanking sequence, both duplexes stopped after incorporation of three nucleotides on a template dependent manner which is under the control of the pausing signal. It indicates the pause site was retained with each of these two duplexes and independent from 5' end of the RNA template.

A DNA overhang alleviates nucleotide addition pausing.

In the native telomerase, interactions between the DNA primer, TR template, and TERT anchor sites collectively contribute to nucleotide addition processivity (Berman et al, 2011; Qi et al, 2012). Therefore, the D4 and D6 duplexes appended with either DNA or RNA overhangs to imitate the intermediate products of a native telomerase reaction were tested for nucleotide addition activity. (Figure 2.3). While D4 containing an effective pausing signal represents a post-pause signal extended duplex, D6, without pausing site, is the negative control. The results demonstrate it is the DNA 5' overhang instead of RNA 3' overhang allowing partial bypass of the sequence-defined pause site for the D4 duplex (Figure 2.3). The P6 duplex, lacking the pause signal, also exhibited a higher nucleotide addition processivity in comparison to the DNA 5' overhang (Figure 2.3). In the presence of [α-^{32}P] dGTP, the DNA primers from all duplex substrates were extended to the end of each RNA template regardless of the duplex sequence in avian myeloblastosis virus (AMV) RT.

Additionally, various lengths of DNA overhangs or base-pair region of D4 substrates have been assayed. It displayed a similar partial bypass of the pause signal with a different length of DNA 5' overhang, and longer DNA 5' end overhang slightly increases nucleotide addition. And the shorter DNA/RNA duplex, 6 or 7 bp duplex, showed relative higher activity which consistent with the previous results that the proximal anchor site is could actively maintain a constant 5-6 bp DNA/RNA hybrid by breaking a single base pair in the duplex when a new base pair is formed (Qi et al, 2012). But the length of the duplex did not affect pause signal (Figure 2.4) The protein-DNA interactions between TERT anchor sites and the DNA 5' overhang presumably facilitated duplex translocation and thus increased nucleotide addition processivity. TERT binding with the DNA primer, and not the RNA strand, appears to promote nucleotide addition processivity and lessen the sequence-defined pausing.

P5 inactivity results from catalysis deficiency.

In addition to the distinct extension patterns, the six permuted RNA/DNA duplexes also exhibited markedly different activities with TF-telomerase (Figure 2.5A). Among the six duplexes, D5 displayed little activity even in the presence of a DNA 5' overhang. This is consistent with a previous report that Chinese hamster telomerase failed to react with a DNA primer ending in the exact register as D5, GGTTAG (Maine et al, 1999). The inactivity of the D5 duplex with TF telomerase presumably results from the inability of telomerase to either bind the D5 duplex or catalyze nucleotide addition onto this substrate. To discern the relative binding affinity of D5 to the telomerase active site, we performed a competitive inhibition assay with the six permuted telomeric duplexes as inhibitors competition against a non-telomeric duplex substrate for binding to the telomerase active site (Figure 2.5B).

The RNA template for these telomeric duplex inhibitors was blocked with an rG residue, preventing incorporation of dGTP and therefore could not be extended when bound to the telomerase active site. Thus, the inhibition of telomerase activity with the non-telomeric substrate correlates with a telomerase binding affinity for the duplex inhibitors. At 5 or 20 μM, the D4, D5 and D6 duplex inhibitors had similar levels of inhibition with the non-telomeric substrate, indicating comparable binding affinities to the active site (Figure 2.5B). Thus, P5 inactivity would appear to result from inefficient catalysis, such as improper positioning of DNA 3'-OH within the catalytic site.

2.5 Discussion

Telomeric DNA repeats were synthesized by telomerase iteratively copying the intended template sequence from an integral RNA component. The template region from the larger TR must be precisely defined to prevent incorporation nucleotides from the template flanking region. The sequence-defined pausing mechanism identified in human telomerase provides new insights into the template boundary definition mechanism for vertebrate telomerase. In our current working model of the telomerase catalytic cycle, the single-residue sequence-defined pause signal functions together with the structure defined template boundary. Following the processive addition of six nucleotides to the DNA primer, the first rA:dT base pair in the duplex signals a pause in DNA synthesis at the end of the template region. This pausing permits DNA/RNA duplex dissociation from the active site.

In a processive telomerase reaction, DNA/RNA duplexes formed immediately prior to and following template translocation have the sequence register GGTTAG, which is identical to the D5 duplex. In the context of TF telomerase, the D5 duplex is

inactive, despite the presence of a DNA 5' overhang (Figure 2.5A). The sequence of the single stranded RNA region flanking the duplex fails to alter sequence-defined pausing with TF telomerase (Figure 2.2). It indicates after template translocation the pausing signal still has an influential effect on the incoming nucleotide incorporation. We proposed that the incorporation of the first nucleotide after template translocation onto the D5 duplex is the rate limiting step for processive telomeric DNA repeat synthesis which is under the control of the pausing signal. This is also supported by the recently published single molecular FRET data that showed the realignment of DNA/RNA duplex is fast process, while the conformational rearrangement for next round nucleotide addition is slower during template translocation (Parks & Stone, 2014).

In the processive human telomerase reaction, DNA/RNA duplexes formed immediately before or following template translocation have the sequence register GGTTAG, identical to the D5 duplex. However, the processive addition of DNA repeats by native telomerase requires extension of the D5 duplex formed post-template translocation. When comparing TF and template-containing telomerase, the principal difference is the tethering of the RNA template to the core enzyme. In the native telomerase, the DNA primer could interact with TR template as well as TERT anchor sites corporately for nucleotide addition processivity (Berman et al, 2011; Qi et al, 2012). The 5' end overhang of DNA, which imitate the intermediate products of a native telomerase reaction, can alleviate the pausing signal. It demonstrates the processive addition of DNA repeats by native telomerase, the D5 duplex formed after template translocation as well as the native telomerase is active for all six template circular permutations of primers. Meanwhile, the inefficient nucleotide addition onto

the D5 duplex post-template translocation is responsible for the low repeat addition rate and processivity of human telomerase core enzyme. In the context of native telomerase, the detail mechanism of extending the D5 duplex following template translocation remains unknown.

These findings are supportive of the conservation of the vertebrate TR template for synthesizing the specific GGTTAG sequence register and the acutely deleterious effects of template mutations that impair the sequence-defined pausing mechanism (Chen et al, 2000; Drosopoulos et al, 2005; Stohr et al, 2010). The fidelity of telomeric repeat synthesis by telomerase is crucial for telomere function and genome stability in the germ line, stem cells and cancer cell. The sequence-defined pausing is a novel attribute of human telomerase to self-define the template region from adjacent sequences. This study sheds light on the mechanism of the repetitive synthesis of telomeric DNA substrate, and therefore informative for exploring the check point of the telomerase template translocation.

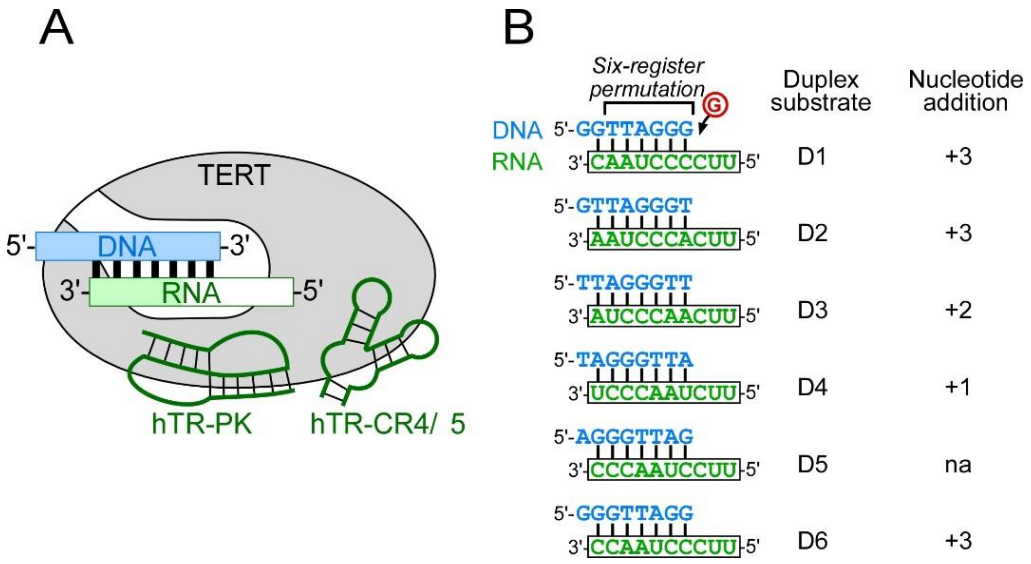

Figure 2.1. A single nucleotide in the RNA/DNA duplex signals a pause in nucleotide addition with template-free telomerase. (A) *In vitro* assembly of template-free (TF), telomerase was reconstituted by assembling *in vitro* expressed human TERT protein with the two essential hTR fragments, CR4/5 and the pseudoknot (PK) that had the template region excised. The pre-annealed DNA primer and RNA template are the substrates used for the TF telomerase activity assay. (B *left*) Sequences of circular permuted telomeric RNA/DNA duplexes D1-D6. (B *right*) Summarize the results of an activity assay of *in vitro* reconstituted TF telomerase with D1-D6 duplex.

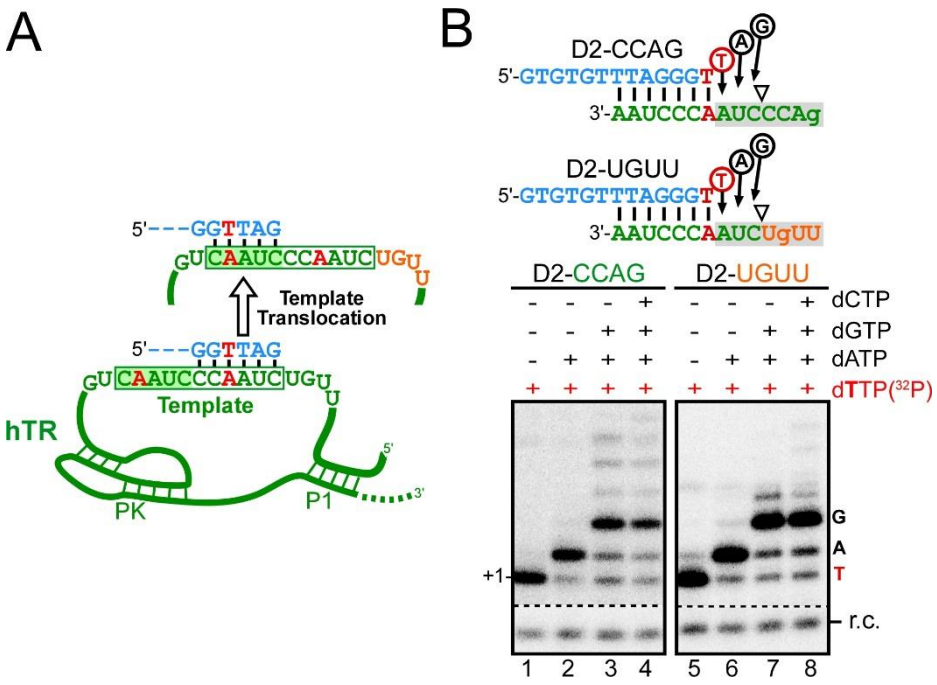

Figure 2.2. Sequence-defined pausing is retained for duplexes with different RNA 5′ flanking sequences. (A) Schematic comparing duplexes of TR template and DNA primer before and post-template translocation. (B) The sequences of the duplex D2 substrates, D2-CCAg and D2-UGUU, are shown (top). The sequence-defined pause site is denoted (white triangles). Activity assay of the D2 duplexes with *in vitro* reconstituted TF telomerase is shown (bottom). Substrates were extended by the enzyme with [α-^{32}P]dTTP in the presence (+) or absence (−) of 0.5mM dATP, dGTP, or dCTP as denoted above the gel. A ^{32}P end-labeled 7-mer oligonucleotide was included as a recovery control (r.c.).

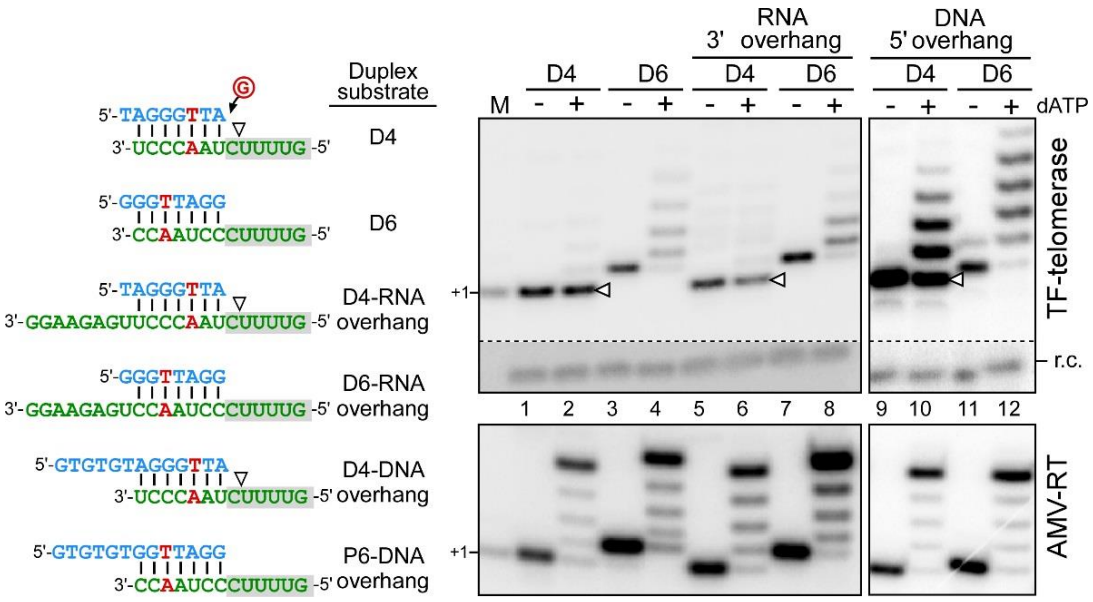

Figure 2.3. Functional assays of DNA/RNA duplex variants for sequence-defined pausing and binding affinity to TF telomerase. Activity assay of duplex substrates with various overhangs. Sequences of duplexes P4 and P6 appended either a 3' RNA or 5' DNA overhang. The sequence-defined pausing site is denoted (white triangles). Activity assay of duplex substrates with various overhangs (*left*). *In vitro* reconstituted TF telomerase (right upper panel) or AMV RT (right lower panel) was assayed with RNA/DNA duplexes and α -^{32}P-dGTP in the presence (+) or absence (-) of 0.5 mM dATP as denoted above the gel. A ^{32}P end-labeled 7-mer oligonucleotide is used as a recovery control (r.c.). The DNA primer TAGGGTTA extended by one α -^{32}P-dGTP with TdT was included as a size marker (M).

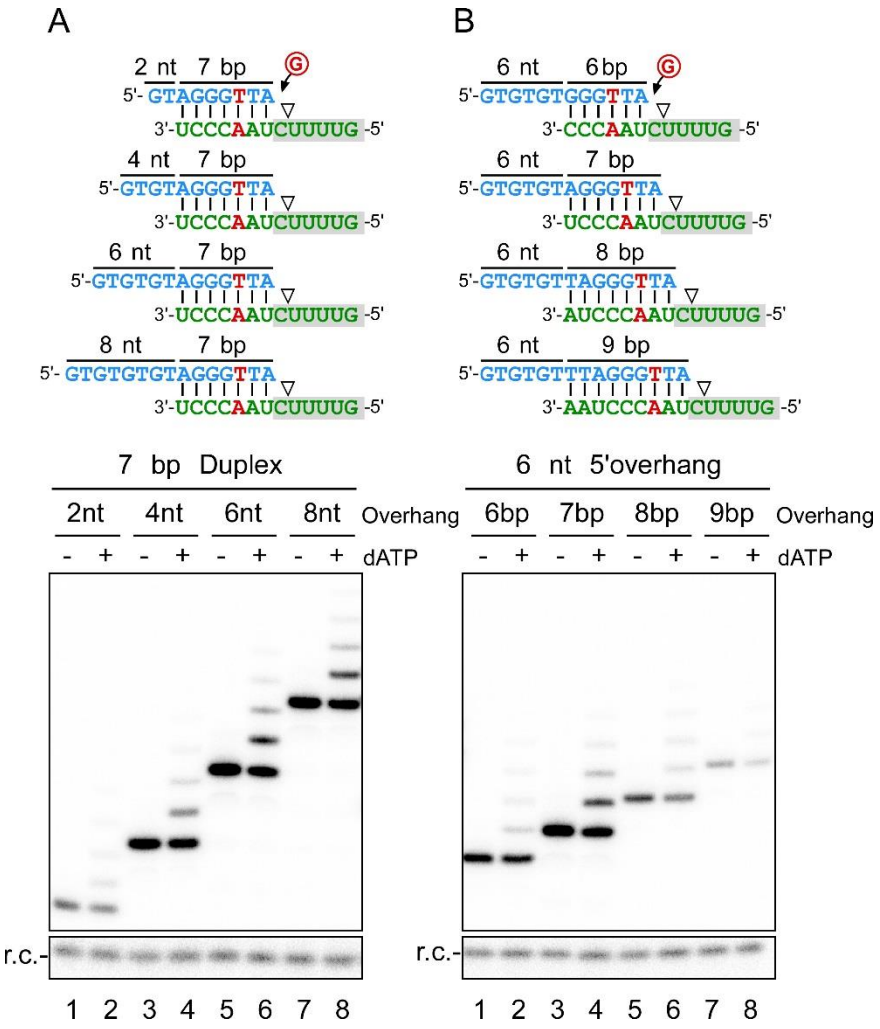

Figure 2.4. Effect of DNA 5' overhang length on nucleotide addition processivity and the sequence-defined pause site. (A and B, Upper) Sequences of duplexes with variable DNA 5' overhang length and variable duplex length. (A and B, Lower) Activity assay of *in vitro* reconstituted TF telomerase with various duplex substrates. Substrates were extended by the enzyme with [α-^{32}P]dGTP in the presence (+) or absence (−) of 0.5 mM dATP as denoted above the gel. A ^{32}P end- labeled 7-mer oligonucleotide was included as a recovery control (r.c.).

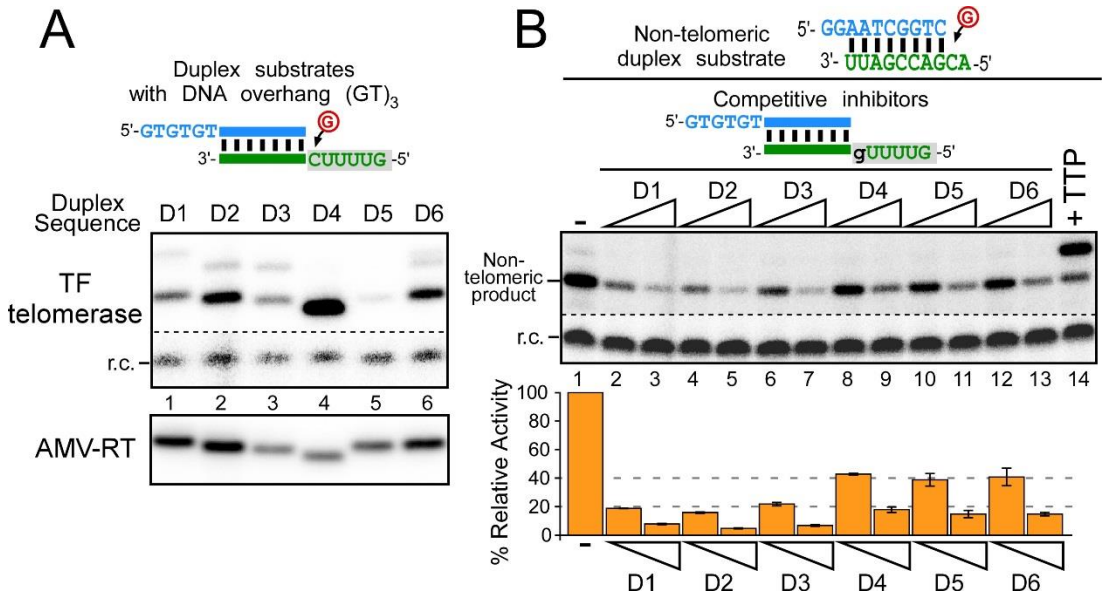

Figure 2.5. TF telomerase is inactive with the P5 duplex that contains a DNA 5' overhang. (A) Activity assay of *in vitro* reconstituted TF telomerase (top panel) and AMV RT (bottom panel) with duplex substrate variants (D1-D6) appended with DNA 5' overhangs. Substrates were extended by the enzyme with α-^{32}P-dGTP. A ^{32}P end-labeled 7-mer oligonucleotide was used as a recovery control (r.c.). (B) Competitive inhibition assay of telomeric duplex competitors against a non-telomeric duplex substrate. *In vitro* reconstituted TF telomerase (upper panels) and AMV RT (lower panels) were assayed with 40 μM non-telomeric substrate and 5 or 20 μM telomeric competitors (D1-D6 with a 5' DNA overhang) with α-^{32}PdGTP. The substrate is extended by two nucleotides with the addition of 0.2 mM dTTP (+TTP). A ^{32}P end-labeled 7-mer oligonucleotide was used as a recovery control (r.c.). Quantitation of the relative activity in the presence of competitor is displayed below the gel.

CHAPTER 3

A SINGLE NUCLEOTIDE INCORPORATION STEP LIMITS HUMAN TELOMERASE REPEAT-ADDITION ACTIVITY

Reproductions with permission in part from:

Chen, Y., J.D. Podlevsky, D. Logeswaran and J.J.-L. Chen (2018).

A single nucleotide incorporation step limits human telomerase repeat addition activity. EMBO J. 37:e97953, DOI 10.15252/emboj.201797953.

3.1 Abstract

Human telomerase synthesizes telomeric DNA repeats $(GGTTAG)_n$ onto chromosome ends using a short template from its integral telomerase RNA (hTR). However, telomerase is markedly slow for processive DNA synthesis among DNA polymerases. We report here that the unique template-embedded pause-signal restricts the first nucleotide incorporation for each repeat synthesized, imparting a significantly greater K_M. This slow nucleotide incorporation step drastically limits repeat addition processivity and rate under physiological conditions, which is alleviated with augmented concentrations of dGTP or dGDP, and not with dGMP nor other nucleotides. The activity stimulation by dGDP is due to nucleoside diphosphates functioning as substrates for telomerase. Converting the first nucleotide of the repeat synthesized from dG to dA through the telomerase template mutation, hTR-51U, correspondingly shifts telomerase repeat addition activity stimulation to dATP-dependent. In accordance, telomerase without the pause-signal synthesizes DNA repeats with extremely high efficiency under low dGTP concentrations and lacks

dGTP stimulation. Thus, the first nucleotide incorporation step of the telomerase catalytic cycle is a potential target for therapeutic enhancement of telomerase activity.

3.2 Introduction

The ends of linear eukaryotic chromosomes are capped by telomeres, an array of short DNA repeats bound by specific telomeric proteins (Arnoult & Karlseder, 2015). Telomere length is crucial for chromosome integrity and maintained by the unique cellular reverse transcriptase, telomerase, that adds telomeric DNA repeats (GGTTAG)n processively onto chromosome ends (Wu et al, 2017). Human telomerase utilizes a short 11-nt template from the long non-coding 451-nt telomerase RNA (TR) for DNA repeat synthesis catalyzed by the telomerase reverse transcriptase (TERT) subunit (Hockemeyer & Collins, 2015; Podlevsky & Chen, 2012). The 5' boundary of the TR template prevents non-template usage to ensure telomeric DNA synthesis fidelity and is physically safeguarded in different species by divergent structural elements: a distal RNA helix and single-stranded nucleotide span in vertebrates (Chen & Greider, 2003), TERT-binding TR elements in ciliates (Jansson et al, 2015; Jiang et al, 2015), or a template-adjacent RNA helix in fungi (Qi et al, 2013; Seto et al, 2003; Tzfati et al, 2000). The human TR (hTR) template 5' boundary is further protected by the template-embedded pause signal, the first dT:rA base-pair in the DNA product/RNA template hybrid, that restricts DNA synthesis beyond the 5' boundary (Brown et al, 2014). Upon completing synthesis of a DNA repeat and reaching the 5' template boundary, telomerase regenerates the RNA template for subsequent repeat synthesis (Wu et al, 2017). There have been identified telomerase mutations which impair specifically repeat addition processivity and not catalytic activity, yet result in stem cell defects that manifest as a spectrum of short telomere

syndromes (Alder et al, 2011; Gramatges et al, 2013; Robart & Collins, 2010; Zaug et al, 2013).

Telomerase repeat addition processivity relies on a highly complex and unique catalytic reaction cycle that comprises two distinct phases: (i) synthesis of a single telomeric repeat with six consecutive nucleotide incorporation steps and (ii) regeneration of the template for additional telomeric repeat synthesis (Podlevsky & Chen, 2012). Telomerase catalyzes the nucleotide incorporation reaction with an active site that comprises a triad of invariant aspartic acids universally conserved in DNA polymerases (Lingner et al, 1997). The template regeneration phase is unique to telomerase and is accomplished by a 'template translocation' mechanism whereby the template dissociates from and then realigns with the newly extended DNA product (Autexier & Lue, 2006). Recent findings indicate that template translocation is a rapid process (Parks and Stone 2014), although the precise mechanism remains enigmatic. Telomerase-synthesized DNA products are predominantly released from the enzyme between two consecutive cycles of repeat synthesis, which generates the characteristic 6-nt ladder banding pattern of the products (Greider, 1991). However, the specific steps that promote product release and limit processive repeat synthesis during telomerase catalytic cycle remain elusive.

Several intrinsic enzymatic determinants or reaction conditions that affect specifically repeat addition processivity have been identified. These reaction conditions include high dGTP concentration that stimulate telomerase repeat addition activity through an unknown mechanism (Hammond & Cech, 1997; Hardy et al, 2001; Maine et al, 1999; Sun et al, 1999; Wu et al, 2017). Herein, we report that human telomerase exhibits lower kinetics specifically for the incorporation of the first

nucleotide, a dG residue, of each telomeric repeat synthesized. This lower incorporation kinetic is mediated by the template-embedded pause signal that arrests nucleotide synthesis at the end of the template and remains active following template translocation, therefore impairing processive repeat synthesis. Elevated dGTP concentrations increase the incorporation efficiency of the first nucleotide for each repeat synthesis and consequently stimulates both processivity and rate of telomerase repeat addition. These results reveal a critical step in the telomerase catalytic cycle that underlies the dGTP stimulation of human telomerase repeat addition.

3.3 Materials and methods

In vitro reconstitution of TF human telomerase.

Human TERT protein was expressed in rabbit reticulocyte lysate (RRL) from the pNFLAG-hTERT plasmid DNA using the TnT T7 Quick Coupled transcription/translation kit (Promega) following manufacturer's instructions (Xie et al, 2010). The hTR pseudoknot (residues 64–184) and CR4/5 (residues 239–328) fragments were *in vitro* transcribed, gel purified, and assembled together with the TERT protein in RRL for 30 min at 30°C at a final concentration of 1.0 μM (Brown et al, 2014; Qi et al, 2012).

In vivo reconstitution of wild-type human telomerase.

HEK 293FT cells were grown in DMEM medium (Corning) supplemented with 10% FBS (Atlanta Biological), 1X Penicillin-Streptomycin-Amphotericin B mix (Lonza) and 5% CO_2 at 37°C to 80–90% confluency. Cells in a 6-well plate were transfected with 0.4 μg of pcDNA-NFLAG-hTERT, 1.6 μg of pBS-U1-hTR wildtype or template mutants and 6 μL of Fugene HD transfection reagent (Promega) following manufacturer's instruction. Cells were harvested 48 hours post transfection,

homogenized in HEPES lysis buffer (20 mM HEPES-KOH, pH 7.9, 400 mM NaCl, 0.2 mM EGTA, 2 mM $MgCl_2$, 10% glycerol, 5 mM β-mercaptoethanol and 1X complete protease inhibitor cocktail (Roche), 1 mM PMSF), incubated on ice for 30 min and the lysate clarified by centrifugation. Two hundred microliters of cell lysate were combined with 30 μL Anti-FLAG® M2 Beads (Sigma) pre-washed with 1X TBS buffer (50 mM Tris-HCl, pH 7.4 and 150 mM NaCl) and incubated at 4°C with gentle rotation for 1 hour. The beads were washed three times with 100 μL of 1X TBS buffer and once with 50 μL 1X telomerase reaction buffer (50 mM Tris-HCl, pH 7.5, 3 mM $MgCl_2$, 50 mM KCl, 2 mM DTT and 1 mM spermidine), followed by activity assay.

K_M measurement using TF telomerase.

One microliter of RRL reconstituted TF telomerase enzyme was assayed in a 10 μL reaction containing 1X telomerase reaction buffer, 40 μM pre-annealed DNA/RNA duplex, specified dNTPs and 0.165 μM of the denoted α-^{32}P-dNTP. For measuring the K_M values, the activity assays were performed with nucleotide concentrations varying from 0 to 200 μM, or up to 1 mM for high K_M measurement. Reactions were incubated at 30°C for 60 min and terminated by phenol/chloroform extraction, followed by ethanol precipitation. The DNA products were resolved on a 15% (wt/vol) polyacrylamide/8 M urea denaturing gel, dried, exposed to a phosphorstorage screen and imaged on a Bio-Rad FX-Pro phosphorimager. The intensities of specific products were normalized to the total product intensity and plotted against the nucleotide concentrations with the Michaelis-Menten equation, Y=Vmax*X/(Km+X), used to fit the nonlinear curve to determine the K_M (Prism 5, Graphpad Software).

Activity assay for dNDP and dNMP incorporation.

One microliter of RRL reconstituted telomerase enzyme, 1 unit of AMV RT (Promega), 0.5 units of Taq DNA pol III (NEB), 1 unit of T4 DNA pol (Fermentas), or 0.5 units of Klenow fragment of DNA pol I (Invitrogen) were assayed in 10 μL reactions containing 1X telomerase reaction buffer, 40 μM of denoted pre-annealed DNA/RNA or DNA/DNA hybrid substrates, 100 μM dGTP, dGDP, or dGMP, and 0.165 μM α-^{32}P-dATP. The assay with TGIRT III group II intron RT (InGex) contained 50 units of enzyme, 1X reaction buffer (20 mM Tris-HCl, pH 7.5, 5 mM $MgCl_2$, 0.45 M NaCl, 5 mM DTT) and 10 μM dGTP, dGDP, or dGMP, and 0.165 μM α-^{32}P-dATP. Reactions were incubated at 30°C for 60 min and terminated by phenol/chloroform extraction, followed by ethanol precipitation. The size marker was prepared in a 10 μL reaction containing 1X reaction buffer (100 mM sodium cacodylate, pH 6.8, 1 mM $CoCl_2$, and 0.1 mM DTT), 10 μM oligonucleotide as indicated, 10 units of terminal deoxynucleotidyl transferase (TdT, Affymetrix), and 0.165 μM α-^{32}P-dATP (3,000 Ci/mmol, 10 mCi/mL; Perkin-Elmer). The reaction was incubated at 30°C for 5 seconds and terminated by addition of 10 μL 2× formamide loading buffer [10 mM Tris·HCl, pH 8.0, 80% (vol/vol) formamide, 2 mM EDTA, 0.08% bromophenol blue, and 0.08% xylene cyanol]. The DNA products were resolved on a 15% (wt/vol) polyacrylamide/8 M urea denaturing gel, dried, exposed to a phosphorstorage screen and imaged on a Bio-Rad FX-Pro phosphorimager.

Telomerase direct primer-extension assay.

Twenty microliters of immuno-purified *in vivo* reconstituted telomerase enzyme on beads was assayed in a 10 μL reaction containing 1X telomerase reaction buffer, 1 μM DNA primer, specified dNTPs and 0.165 μM of the denoted α-^{32}P-

dNTP. Reactions were incubated at 30°C for 60 min and terminated by phenol/chloroform extraction, followed by ethanol precipitation. The DNA products were resolved on a 10% (wt/vol) polyacrylamide/8 M urea denaturing gel, dried, exposed to a phosphorstorage screen and imaged on a Bio-Rad FX-Pro phosphorimager. Repeat addition efficiency was estimated as the ratio of the high M.W. DNA products (>6 repeats added) over the low M.W. DNA products (1-6 repeats added). The cutoff at 6 repeats was arbitrarily chosen to divide the gel into approximately two even sections. The relative High/Low ratios of reactions with varying nucleotide concentrations were determined through normalization to the ratio from the low nucleotide concentration reaction.

Telomerase product release assay for repeat addition processivity determination.

Twenty microliters of immuno-purified *in vivo* reconstituted telomerase enzyme on beads was assayed in a 10 μL reaction containing 1X telomerase reaction buffer, 1 μM DNA primer, a range of dNTPs and 0.165 μM of the denoted α-^{32}P-dNTP. Reactions were incubated at 30°C for 60 min and the DNA products in the supernatant was separated from the DNA products bound to the telomerase enzyme immobilized on the beads. Following ethanol precipitation, the DNA products were resolved on a 10% (wt/vol) polyacrylamide/8 M urea denaturing gel, dried, exposed to a phosphorstorage screen and imaged on a Bio-Rad FX-Pro phosphorimager. Repeat addition processivity was calculated using the equation: $Processivity = \frac{-ln2}{2.303k}$ (Latrick & Cech, 2010). The slope, *k*, was determined by plotting the intensity of each major band, normalized to the intensity of the first band, over the repeat number.

Pulse-chase time course assay.

Twenty microliters of immuno-purified *in vivo* reconstituted telomerase enzyme on beads was initially pulsed with 0.165 μM α-^{32}P-dTTP for 5 min and then chased with 100 μM dTTP and denoted concentrations of dATP and dGTP. Aliquots of the reactions were terminated by phenol/chloroform extraction at denoted time points, followed by ethanol precipitation. The DNA products were resolved on a 10 (wt/vol) polyacrylamide/8 M urea denaturing gel, dried, exposed to a phosphorstorage screen and imaged on a Bio-Rad FX-Pro phosphorimager. To determine the rate of repeat addition, the longest DNA products with the highest intensity above initial pulse product bands were used to deduce a 'modal band' to calculate the extension rate as previously described (Drosopoulos et al, 2005).

3.4 Results

Human telomerase template-embedded pause signal mediates high K_M for nucleotide incorporation.s

Telomerase synthesizes DNA at an exceedingly lower rate than most DNA polymerases (Hwang et al, 2014), which is presumably due to the unique telomerase catalytic cycle for processive short DNA repeat synthesis. During each of the reiterated cycles, telomerase catalyzes the incorporation of six consecutive deoxynucleotides, dG1, dG2, dT3, dT4, dA5 and dG6, onto the 3' hydroxyl of the DNA primer (Figure 3.1A), followed by template translocation to regenerate the template for the next cycle of repeat synthesis. With template translocation having been reported to be a rapid process (Parks & Stone, 2014), we investigated whether any of the six nucleotide incorporations limit overall telomerase repeat addition activity, especially as specific TR template residue mutations have been shown to affect telomerase enzymatic function (Brown et al, 2014; Drosopoulos et al, 2005;

Gilley & Blackburn, 1996; Gilley et al, 1995). The kinetics of the individual nucleotide incorporation steps have not been previously assessed due to technical complications associated with analyzing processive telomerase enzymes. To overcome this technical difficulty, we employed template-free (TF) human telomerase (Qi et al, 2012) that catalyzes a non-processive DNA synthesis reaction using RNA templates supplied in trans, which permits a simplified and defined primer-extension assay for determining the nucleotide incorporation efficiency at each individual position across the hTR template. Human TF telomerase was reconstituted by assembling *in vitro* expressed human TERT protein in rabbit reticulocyte lysate with the two essential hTR fragments, CR4/5 and a template-free pseudoknot fragment lacking the template sequence (Figures 3.1B and 3.2). This TF telomerase was assayed for nucleotide incorporation with a series of DNA/RNA duplex substrates comprising a DNA primer and an RNA oligo serving as the template (Figure 3.3). The preassembled DNA/RNA hybrid substrates were specifically designed with permuted telomeric sequences and a short RNA template for measuring the K_M of nucleotide incorporation specifically for dG1, dT3, dA5 and dG6, corresponding to positions 1, 3, 5 and 6 in the hTR template (Figures 3.1A and 3.3). The K_M measurements used extremely low concentrations of TF telomerase enzyme and excess nucleotide substrates ranging from 2 to 200 μM. With either 2 or 200 μM nucleotide substrate, the product formation over the incubation time remained linear indicating that the initial velocity of the reaction was measured (Figure 3.4). Remarkably, the K_M for incorporating dG1 was approximately 120 μM, exceptionally higher than the K_M for incorporating dT3, dA5 and dG6 that ranged from 3 to 31 μM (Figure 3.1C). To further investigate whether this was a result of nucleotide identity or the incorporation

position within the template sequence, we altered the identity of the nucleotide incorporated at positions 1, 5 and 6 to dA1, dT1, dG5 and dT6 (Figure 3.3). Altering the identity of the nucleotide incorporated at these positions did not substantially change the high K_M for nucleotide incorporation at position 1, nor the low K_M at other positions measured (Figure 3.1C). Interestingly, the dG-to-dT transversion at positions 1 and 6 noticeably increased K_M from 120 to 400 μM and from 5 to 14 μM, respectively (Figure 3.1C). This is consistent with results reported for Tetrahymena telomerase, where the K_M for incorporating dT was slightly higher than for dG (Collins & Greider, 1995; Lee & Blackburn, 1993). Overall, these results suggest that the high K_M of the first nucleotide incorporation is position-specific relative to the template sequence and independent of the identity of the nucleotide incorporated.

The incorporation of the first nucleotide, dG1, perfectly coincides with the DNA synthesis pause site governed by the pause signal embedded in the hTR template sequence (Figure 3.1C). The template-embedded pause signal dT:rA base-pair forms with the incorporation of dT3 and mediates DNA synthesis arrest after the incorporation of the three subsequent nucleotides, dT4, dA5 and dG6 (Brown et al, 2014). We hypothesized that the pause signal arresting DNA synthesis through an elevated K_M for nucleotide incorporation at the pause site would be mitigated with increased dGTP concentrations. To test this hypothesis, we designed a DNA/RNA hybrid substrate with a dT:rA pause signal embedded within and a single-stranded RNA template that allows for the incorporation of four nucleotides, corresponding to dA5, dG6, dG1, and a non-telomeric dC2 (Figure 3.1D). The pause signal would arrest DNA synthesis at the pause site following the incorporation of ^{32}P-dA5 and dG6. In the presence of only ^{32}P-dATP, a single ^{32}P-dA5 residue was incorporated to

the DNA primer, generating a single band (Figure 3.1D, lane 1). The inclusion of 5 μM dGTP in the reaction permitted the incorporation of dG6, while the subsequent dG1 incorporation was inhibited by the pause signal (Figure 3.1D, lane 2). Increasing the dGTP concentration to 20 or 50 μM increasingly overcame this DNA synthesis arrest and resulted in the dG1 incorporation, generating a pronounced third band (Figure 3.1D, lanes 3 and 4). These nucleotide incorporations were template-dependent as the fourth band corresponding to a dC2 incorporation was generated only in the presence of dCTP (Figure 3.1D, lane 5). These results reveal that elevated dGTP concentrations effectively overcome the DNA synthesis arrest at the pause site which is governed by the pause-signal and mediated through the high K_M of the dG1 incorporation.

To further explore the connection between the pause signal and the high K_M for dG1 nucleotide incorporation, we eliminated the pause signal from the DNA/RNA hybrid substrate by mutating the base-pair dT:rA to dA:rU and then measured K_M for the dG1 nucleotide incorporation (Figures 3.1E and 3.5). This transversion mutation has previously been shown to effectively inactivate the pause signal and permit DNA synthesis beyond the pause site (Brown et al, 2014). As expected, the removal of the pause signal significantly reduced the K_M for dG1 incorporation from 120 to 22 μM (Figures 3.1E and 3.5). In contrast, the loss of the pause signal in the DNA/RNA duplex did not affect the K_M for incorporating dG6 (Figures 3.1C and 3.1E). We thus conclude that the template-embedded pause signal has an inhibitory effect specifically on the dG1 nucleotide incorporation, mediated through a high K_M exclusively for this nucleotide incorporation.

dGTP stimulates telomerase repeat addition processivity and rate.

It has been previously proposed that the template-embedded pause signal may have dual functions (Brown et al, 2014): arresting DNA synthesis at the end of the template and inhibiting the first nucleotide incorporation after template translocation (Figure 3.6A). Processive repeat addition by telomerase necessitates reiterated cycles of nucleotide addition. The inhibitory effect of the pause signal on the first nucleotide dG^1 incorporation would impair initiating synthesis of each repeat, negatively affecting processive telomerase repeat addition. As high dGTP concentrations can effectively overcome the pause signal mediated inhibition of dG^1 incorporation (Figure 3.1D), we hypothesized that high dGTP concentrations would facilitate progression into subsequent catalytic cycles and in turn promote telomerase repeat addition activity, generating more high molecular weight (M.W.) DNA products. In fact, dGTP-dependent stimulation of repeat addition activity has been previously reported for human and ciliate telomerases (Hammond & Cech, 1997; Hardy et al, 2001; Maine et al, 1999; Sun et al, 1999). However, the underlying mechanism for dGTP-stimulation of telomerase repeat addition remained unclear. To ascertain that this previously reported nucleotide stimulation of human telomerase is specific to dGTP, and not dATP or dTTP, we reconstituted wild-type human telomerase with full-length, template-bearing hTR in human HEK293 cells and assayed the immuno-purified telomerase enzyme for repeat addition activity with a telomeric DNA primer $(TTAGGG)_3$ (Figure 3.6B-C). To determine the effects of dGTP and dATP concentrations on telomerase repeat addition, we performed the conventional telomerase primer-extension assay in the presence of ^{32}P-dTTP with increasing concentrations (10, 50 and 200 μM) of dGTP or dATP individually (Figure 3.6B). Elevated dGTP concentrations at 50 or 200 μM significantly increased the relative

ratio of high over low M.W. products by approximately 1.5-fold (Figure 3.6B, lanes 1, 4 and 5), while varying the concentration of dATP had no significant effect on repeat addition (Figure 3.6B, lanes 1-3). To examine the effects of dTTP, a similar assay was performed in the presence of ^{32}P-dATP. Similarly, increased dGTP concentrations increased repeat addition efficiency by approximately 1.5-fold (Figure 3.6C, lanes 1, 4 and 5), while elevated dTTP did not significantly increase repeat addition efficiency, but seemed to slightly increase the length of the highest M.W. products (Figure 3.6C, lanes 1-3). The slight increase of the highest M.W. products with elevated dTTP is consistent with a previous report (Drosopoulos & Prasad, 2010). Additionally, increasing nucleotide concentrations from 10 to 100 μM did not appear to alter single repeat synthesis, as nucleotide incorporation efficiency was saturated at 10 μM (Figure 3.7). These data clearly demonstrate that human telomerase repeat addition was stimulated specifically by increased concentrations of dGTP, and not dATP or dTTP. The increased ratio of higher over lower M.W. products could arise from an increase in the processivity and/or the rate of repeat addition, two independent attributes of the telomerase enzyme (Drosopoulos et al, 2005; Xie et al, 2010). To investigate the underlying mechanism for dGTP-stimulation of telomerase repeat addition, we employed two specific telomerase activity assays to measure separately processivity from rate of repeat addition in the presence of elevated dGTP concentrations.

To specifically measure the processivity of telomerase repeat addition, we designed a telomerase product release assay that quantitates repeat addition processivity based on the distribution of DNA products released from the enzyme (Figure 3.8A). Enzyme-bound DNA products are still undergoing additional rounds of

repeat addition and the inclusion of these premature intermediates would influence the measurement of telomerase repeat addition processivity. For this assay, human telomerase was reconstituted in HEK 293FT cells and the immuno-purified enzyme bound to beads was incubated with the telomeric DNA primer (TTAGGG)3 in the presence of different concentrations of dGTP or dATP. The DNA products released from the immobilized telomerase enzyme were isolated from the supernatant and analyzed to determine the probability of each successive DNA repeat addition. This probability was calculated from the slope of 'products left behind' (Latrick & Cech, 2010) by plotting the intensity of major DNA products with the number of repeats (3-12) added (Figure 3.8A and 3.8B). The slope of the plot corresponds to the repeat addition processivity and was used to compare the relative repeat addition processivity across different assay conditions (Figure 3.8B). The results of this product release assay found that increasing dGTP concentration from 10 to 100 μM resulted in a 2-fold increase in processivity, while increasing dATP concentrations to 100 μM had no significant effect on processivity (Figure 3.8C). Thus, high dGTP concentration effectively stimulates the processivity of human telomerase repeat addition.

We next investigated the effects of elevated dGTP concentrations on the rate of repeat addition. To specifically measure repeat addition rate, we employed a pulse-chase time course assay to track the increasing size of the DNA products undergoing processive repeat addition over time (Figure 3.8D). For this pulse-chase assay, immuno-purified telomerase was initially incubated exclusively with ^{32}P-dTTP to radioactively label the DNA primer and this pulsed reaction was chased with cold nucleotides to track the processive enzyme-DNA complexes over time. The repeat

addition rate was 0.86 repeat/min measured under the chase condition with 10 μM dGTP and 100 μM of dTTP and dATP. However, when chased with the dGTP concentration increased to 100 μM, the repeat addition rate nearly doubled to 1.45 repeat/min (Figure 3.8E, left panel). In contrast, when the reaction was chased with either 10 or 100 μM dATP, in the presence of 100 μM dGTP and dTTP, the repeat addition rate remained unchanged at 1.21 or 1.27 repeat/min, respectively (Figure 3.8E, right panel). Thus, dGTP concentration is a crucial determinant for the rate, in addition to processivity, of human telomerase repeat addition.

First nucleotide incorporation following template translocation mediates nucleotide-specific stimulation of telomerase repeat addition.

The synthesis of a telomeric DNA repeat comprises three dG incorporations: dG^1, dG^2 and dG^6 (Figure 3.9A). We hypothesized that the high dGTP concentration stimulated telomerase repeat addition by overcoming the high K_M for dG^1 incorporation. To determine whether the dG^1 incorporation is specifically responsible for the dGTP-stimulation of telomerase repeat addition, we generated three hTR template mutants hTR-51U, -50U and -46/52U that individually altered the three dG nucleotide incorporations to dA^1, dA^2 and dA^6, respectively. We reconstituted these telomerase template mutants in human HEK293 cells and assayed the immuno-purified enzyme by conventional telomerase primer-extension assay in the presence of ^{32}P-dTTP with either 10 or 100 μM of dGTP or dATP. Remarkably, of these three mutants, only the hTR-51U mutant had a pronounced increase of the higher M.W. products with increased dATP (Figure 3.9B, lanes 4 and 5), and was unaffected by increased dGTP (Figure 3.9B, lanes 4 and 6). Similar to wild-type, the hTR-50U and -46/52U mutant telomerases had increased repeat addition efficiencies with increased

dGTP, and were unaffected by increased dATP (Figure 3.9B, lanes 6-12). It is interesting to note that the hTR-46/52U mutant telomerase had significantly lower repeat addition efficiency, producing less high M.W. products (Figure 3.9B, lanes 1 and 10). This was likely due to the less stable dA:rU base-pairing located at the end of the primer/template duplex, which would negatively impact primer realignment efficiency during template translocation. Noticeably, the hTR-51U and -50U mutant telomerases generated DNA products with altered banding profiles (Figure 3.9B). This is seeming due to the substitution of a dA instead of a dG residue at the specified template positions affecting nucleotide incorporation efficiency, as it has been reported that telomerase is sensitive to the template sequence alterations (Drosopoulos et al, 2005; Gilley et al, 1995). The template mutant hTR-50U appeared to have a lower incorporation efficiency for dG^{6} residue, resulting accumulation of the DNA product after dA^{5} incorporation visible as an additional band (Figure 3.9B, lanes 7 and 8), which was effectively alleviated by high dGTP (Figure 3.9B, lane 9). Nonetheless, by changing the nucleotide incorporation from dG^{1} to dA^{1} with the hTR-51U template mutation, we effectively changed the stimulation of human telomerase repeat addition from dGTP to dATP-dependent. This further supports the hypothesis that the dG^{1} nucleotide incorporation is a critical step for human telomerase repeat addition.

We next sought to determine whether the dATP-dependent stimulation of hTR-U51 mutant telomerase affects specifically the processivity and/or the rate of repeat addition. We examined the repeat addition processivity of the hTR-51U mutant with our product release assay (Figure 3.10A). As expected, the hTR-51U mutant had a 35% increase of telomerase repeat addition processivity in the presence of 100 μM dATP and no effect with 100 μM dGTP (Figure 3.10A-C). This result indicates that

the first nucleotide incorporation in the telomerase catalytic cycle is an important determinant for repeat addition processivity. Following this, we then examined the contribution of the first nucleotide incorporation efficiency on the repeat addition rate. We performed a pulse-chase time course assay with the hTR-51U mutant to measure the repeat addition rate in the presence of either 10 or 100 μM of dATP or dGTP (Figure 3.10D). When the reactions were chased with 100 μM dATP, the repeat addition rate was dramatically increased to 3.15 repeat/min from 1.27 repeat/min with 10 μM dATP—a near 2-fold increase (Figure 3.10E). In contrast, increasing dGTP from 10 to 100 μM did not increase the repeat addition rate of hTR-51U mutant which remained similar from 2.99 to 2.95 repeat/min (Figure 3.10E). Our data indicate that the concentration of the nucleotide incorporated as the first residue of a telomeric DNA repeat is crucial for the processivity as well as the rate of human telomerase repeat addition.

Telomerase can incorporate deoxynucleoside diphosphates as substrate

It was previously reported that *Tetrahymena* telomerase accumulates high M.W. DNA products in the presence of elevated dGTP, dGDP, or even dGMP, leading to the hypothesis that a secondary guanosine binding site was responsible for the dGTP-dependent repeat addition stimulation (Hardy et al, 2001). However, our hTR51U telomerase mutant exhibited dATP-dependent stimulation of repeat addition processivity, opposing a secondary guanosine binding site in human telomerase. To investigate the possibility of a more general purine nucleoside binding site for repeat addition stimulation, we examined whether dGMP or dGDP stimulates human telomerase repeat addition. Our result showed that dGMP, at either 10 or 100 μM, failed to stimulate telomerase repeat addition in a reaction containing 10 μM dGTP,

10 μM dTTP and 100 μM dATP (Figure 3.11A, lanes 1 and 2). Interestingly, increasing dGDP concentrations from 10 to 100 μM generated a noticeable increase in telomerase repeat addition efficiency (Figure 3.11A, lanes 3 and 4). To investigate this dGDP-dependent stimulation of repeat addition, we examined whether dGDP functions as a substrate for nucleotide incorporation by telomerase. By replacing dGTP with either dGDP or dGMP in the telomerase reaction, we showed that human telomerase can effectively incorporate dGDP as substrate for telomeric DNA synthesis (Figure 3.11A, lanes 8-9), and not dGMP (Figure 3.11A, lanes 6-7). We further examined telomerase for utilizing dADP as substrate. Similarly, human telomerase can effectively incorporate dADP, and not dAMP (Figure 3.12A-B). To eliminate the possibility of γ-phosphate transfer from dATP in the reaction to dGDP, we performed a telomerase reaction lacking any nucleoside triphosphates using a ^{32}P-end labeled DNA primer with exclusively deoxynucleoside diphosphates: dGDP, dADP and dTDP as substrates (Figure 3.12C). This deoxynucleoside diphosphates-only telomerase reaction generated a significant level of repeat addition activity (Figure 3.12D, lanes 1-2) which however was consistently lower than the activity from the deoxynucleoside triphosphates reaction (Figure 3.12D, lanes 3-4). These results suggest that deoxynucleoside diphosphates are sufficient substrates, yet less effective than deoxynucleoside triphosphates for human telomerase DNA synthesis.

We sought to assess the pervasiveness of DNA polymerases for utilizing deoxynucleoside diphosphates for DNA synthesis. In addition to telomerase examined in this study, it has been previously reported that the HIV RT and a bacteriophage DNA polymerase are capable of using deoxynucleoside diphosphates as substrate (Garforth et al, 2008; Yang et al, 2002). We examined three RTs: TF telomerase,

AMV and TGIRT III group II intron RTs, and three DNA-dependent DNA polymerases: Taq, T4 and the Klenow fragment, for incorporating dGDP into DNA products using corresponding DNA/RNA or DNA/DNA duplex substrates and labeling ^{32}P-dATP (Figures 3.11B-C and 3.11). Except for the T4 DNA polymerase (Figure 3.13, lane 7), all other examined enzymes showed significant incorporation of dGDP and not dGMP as substrate (Figure 3.11B, lane 4 and 8; Figure 3.11C, lanes 3; and 7; Figure 3.13, lane 3). All enzymes analyzed showed template-directed nucleotide incorporations lacking non-specific terminal transferase activities. Therefore, the utilization of deoxynucleoside diphosphate as substrate for DNA synthesis is ubiquitous amongst DNA polymerases. Moreover, the dGDP-dependent stimulation of human telomerase repeat addition is likely from active incorporation of dGDP as substrate rather than secondary-site binding.

Removal of the template-embedded pause signal eliminates dGTP-specific stimulation of human telomerase repeat addition.

With our TF telomerase system, we showed that the template-embedded pause signal is responsible for the high K_M of the dG^1 incorporation (Figure 3.1E), a crucial determinant for repeat addition processivity and rate (Figure 3.8). To assess whether the pause signal limits repeat addition in a processive telomerase reaction, we generated a human telomerase template mutant, termed Δpause, that lacks the pause signal by mutating the four rA residues (nt positions 48, 49, 54 and 55) in the template to rU residues (Figure 3.14A). Our previous study indicated that each of the rA residues in the TR template must be altered to completely eliminate the pause signal (Brown et al, 2014). We reconstituted wild-type and the Δpause mutant human telomerase in HEK293 cells and assayed the immuno-purified enzyme with

corresponding DNA primers and a titration of dGTP from 10 to 50 μM (Figure 3.14B). In sharp contrast to the wild-type telomerase that had the expected dGTP-dependent stimulation of repeat addition activity (Figure 3.14B, lanes 1-3), the Δpause mutant had strikingly high repeat addition activity with only 10 μM dGTP, which remained unchanged with 100 μM dGTP (Figure 3.14B, lanes 4-6). Interestingly, the Δpause template mutant had an altered major banding pattern compared with the wild-type enzyme, which was presumably due to a shift of the limiting nucleotide incorporation from dG^1 to the three dA residues for the mutant enzyme (Figure 3.14B, lane 4). We then analyzed the Δpause mutant for repeat addition processivity and rate separately (Figure 3.15). The Δpause mutant had an approximately 1-fold greater processivity at either 10 or 100 μM dGTP compared to the wild-type enzyme at 10 μM dGTP (Figure 3.15A-C). The repeat addition rate of the Δpause mutant was found to be 1.70 repeat/min at 10 μM dGTP and 1.65 repeat/min with 100 μM dGTP (Figure 3.15D-E), which is significantly higher than the 0.7 and 1.3 repeat/min of the wild-type enzyme at 10 and 100 μM dGTP, respectively (Figure 3.8D-E). These results strongly support the pause signal is responsible for the intrinsically low processivity and rate, as well as the dGTP-specific stimulation of human telomerase repeat addition.

dGTP-specific processivity stimulation is mediated by the sequence-defined pause and not template translocation.

Template translocation efficiency has long been viewed as the key determinant of telomerase repeat addition processivity (Lue, 2004). This was supported by the assumption that failed template translocation was responsible for DNA product release giving rise to the characteristic six-nucleotide ladder banding pattern of

telomerase activity (Greider, 1991). The physical template boundary alone does not prevent mis-incorporations using the template flanking non-telomeric residues in the hTR-T6 template permutation mutant (Figure 3.16). The contribution, and even the existence, of the hTR template-embedded pause signal was obscured by the precise overlap of the pause site with the physical template boundary and the position for template translocation (Figure. 3.17A). Thus, the sequence-defined pause site would need to be separated from the template physical boundary and the ensuing template translocation. To determine the individual contributions of (1) template translocation efficacy compared to (2) the sequence-defined pausing for telomerase processivity, we uncoupled the pause site from the physical boundary defined by TR structural elements (Chen & Greider, 2003). We generated the hTR template mutant T6 with a permuted template sequence, 3'-CCAAUCCCAAU-5', one-residue offset from the wild-type sequence 3'-CAAUCCCAAUC-5' (Figure 3.17A). The hTR-T6 template permutation delays the sequence-defined pause of DNA synthesis, resulting in template translocation occurring at the physical boundary and reaching the pause site after a single nucleotide addition (Figure 3.17B). This uncoupling separates the dG residue incorporated immediately following template translocation from a distinct dG residue incorporated immediately following the pause site. To discern amongst these two dG residues, we introduced mutations, T6-51U and T6-50U, into the hTR-T6 permuted template sequence to alter individually one of the two dG residues to dA (Figure 3.17C). We then reconstituted hTR-T6 mutant telomerases for processivity stimulation analysis with ^{32}P-dTTP and increased dGTP or dATP concentrations. Similar to the wild-type enzyme, the telomerase hTR-T6 template permutation mutant exhibited dGTP-specific processivity stimulation (Figure 3.17D and 3.17E).

Strikingly, the T6-51U mutant retained dGTP-specific processivity stimulation, suggesting that the first nucleotide incorporated following template translocation was not responsible for processivity stimulation. In contrast, the T6-50U mutant showed dATP-specific stimulation, demonstrating that the first nucleotide incorporated following the pause site was critical for processivity stimulation (Figure 3.17D and 3.17E). Interestingly, the hTR-T6 template permutation mutants generated products with banding patterns identical to the wild-type telomerase, suggesting that the telomeric DNA products were released at the sequenced-defined pause site and not at the physical template boundary (Figures 3.9B and 3.17D).

3.5 Discussion

Telomerase is an RNA-dependent DNA polymerase specialized in adding telomeric DNA repeats onto chromosome ends (Podlevsky & Chen, 2016). Apart from other DNA polymerases, telomerase employs a highly orchestrated, yet poorly understood, catalytic cycle to regenerate the RNA template for processive synthesis of multiple telomeric DNA repeats (Wu et al, 2017). The total number of DNA repeats added by a given telomerase enzyme in a single turnover is determined by the two tangibly separate attributes of the telomerase enzyme: the processivity and the rate of repeat addition (Podlevsky & Chen, 2012; Schmidt & Cech, 2015). The processivity of telomerase repeat addition corresponds to the probability of continuous DNA repeat synthesis over complete product release following each catalytic cycle of six nucleotide incorporations. Distinct from processivity, the rate of repeat addition corresponds to the number of telomeric repeat synthesized per unit time. The repeat addition rate is contributed by: (i) the rate of individual nucleotide additions to the primer and (ii) the rate of template regeneration by template translocation. In this

work, we discovered a previously unknown role of the telomerase template-embedded pause signal for inhibiting the dG^1 incorporation step, the first nucleotide of each telomeric DNA repeat. This slow dG^1 incorporation is a decisive step that affects the rate of the telomerase reaction. Failure to incorporate the dG^1 residue prevents processive additional cycles of repeat synthesis, which prompts complete DNA product release and terminates the reaction (Figure. 3.18).

As depicted in our working model of the telomerase catalytic cycle (Figure 3.18), each repeat synthesis comprises the addition of six nucleotides to the 3' hydroxyl of the DNA primer and then arrested at the 5' end of the hTR template by the physical boundary element (Chen & Greider, 2003) and the unique template-embedded pause signal (Brown et al, 2014). Following each repeat synthesis, telomerase regenerates the template through a template translocation step, which has recently been shown to be a rapid process (Parks & Stone, 2014) with a rate about 100-fold faster than the overall repeat addition rate measured (Latrick & Cech, 2010). Thus, the template translocation step is unlikely a major determinant for the rate of repeat addition (Figure 3.18). Moreover, the high repeat addition activity and the lack of product release after the dG^6 incorporation with the Δpause mutant suggest that template translocation is efficient (Figure 3.14B, lane 4). Recently, two models have been proposed for the mechanism of template translocation: single-stranded DNA retention by DNA-protein interactions (Wu et al, 2017) and DNA hairpin formation (Yang & Lee, 2015). Each of these models are possible for template translocation, yet additional work is necessary to establish the definitive mechanism. The data presented herein centers on DNA synthesis post template translocation and neither supports nor negates these proposed models. However, mutations across the template that alter the

telomeric DNA sequence do not affect the functionality of the pause signal (Brown 2014), which would imply that the putative DNA hairpin is largely unaffected by the DNA sequence or is not critical for pause-signal mediated arrest of DNA synthesis. A myriad of intrinsic and extrinsic factors contribute synergistically to template translocation efficiency and repeat addition processivity. These intrinsic factors include the template length that affects template/primer realignment (Chen & Greider, 2003), TERT anchor sites that bind DNA to prevent complete DNA dissociation (Akiyama et al, 2015; Finger & Bryan, 2008; Jacobs et al, 2006; Wyatt et al, 2007; Zaug et al, 2008), or TERT motifs that enable stable retention of the realigned DNA/RNA hybrid in the active site (Huard et al, 2003; Lue et al, 2003; Qi et al, 2012; Wu et al, 2017; Xie et al, 2010). Moreover, telomerase accessory proteins, POT1 (Protection Of Telomeres 1) and TPP1 (TIN2 and POT1-interacting Protein 1), have been found to increase processivity by delaying product release through DNA-protein interactions (Latrick & Cech, 2010; Lingner et al, 1997). These DNA-protein interactions promote progression into the next cycle of repeat synthesis and augments telomerase repeat addition processivity (Figure 3.18). In addition to the intrinsic factors, extrinsic factor such as ionic strength, temperature, nucleotide and primer concentrations (Sun et al, 1999). The sheer number of distinct factors that affect telomerase repeat addition processivity underlie the excessive complexity of template translocation.

After a successful template translocation event, the template is regenerated and ready for further nucleotide addition (Figure 3.18). Nevertheless, the pause signal remains effective following template translocation and inhibits the incorporation of the dG^{1} residue through an excessively high K_M for this incorporation (Figure 3.1C).

Our K_M measurements for nucleotide incorporation at specific positions across template were only feasible by using the non-processive TF telomerase (Qi et al, 2012) and specifically designed DNA/RNA hybrid substrates with permuted sequences (Figure 3.3); these measurements were otherwise challenging and complex with a processive telomerase enzyme. By measuring individual nucleotide incorporation efficiencies with the TF telomerase, we found that removing the pause signal in the DNA/RNA hybrid effectively lowers the high K_M of the dG^1 incorporation to a value comparable to other positions across template, suggesting that the pause signal is responsible for this inhibitory effect (Figures 3.1E and 3.5). For the processive wild-type telomerase enzyme, the removal of the pause signal from the hTR template dramatically increases repeat addition activity even in the presence of low dGTP concentration at 10 μM (Figure 3.14B). This suggests that the dG^1 incorporation is no longer the limiting step for processive repeat addition. The template mutations introduced in the Δpause mutants modified the sequence of the DNA products, which may affect DNA-protein interactions with TERT anchor sites or accessory proteins. While altering DNA-enzyme binding affinity has the potential to augment repeat addition processivity, it is unlikely that this would simultaneously enhance the rate of repeat addition (Figure 3.15). Therefore, it is more feasible that the increased rate of repeat addition with the Δpause mutant was caused by the lower K_M of the dG^1 incorporation. Under saturating dGTP concentrations, the Δpause mutant and wild-type telomerases had equally high repeat addition activity (Drosopoulos et al, 2005), supporting our hypothesis that the dramatically high repeat addition activity of the Δpause mutant at low dGTP was mainly due to the alleviated dG^1 incorporation. Moreover, the loss of the pause signal noticeably altered the

banding pattern of DNA products, which was presumably from new limiting nucleotide incorporations at other template positions and premature product releases.

Upon recognition of the pause signal in the DNA/RNA hybrid, telomerase stalls DNA synthesis precisely at the pause site by the elevated K_M for nucleotide incorporation (Figure 3.1C). While the underlying mechanism for pause-signal recognition requires further investigation, we speculate that pause-signal recognition induces a subtle conformational change in the DNA/RNA hybrid binding site and/or the catalytic site within the TERT protein that manifests as the elevated K_M for nucleotide incorporation. Supporting this hypothesis, previous structural and biochemical studies suggest that telomerase undergoes conformational changes at distinct steps of catalytic cycle (Mitchell et al, 2010; Parks et al, 2017; Tomlinson et al, 2015). However, determining the exact mechanism for pause-signal mediated arrest of DNA synthesis would require high-resolution structures of the telomerase enzyme complexed with various DNA/RNA hybrids and even the incoming nucleotide bound within the active site.

Beyond compensating for the high K_M of the dG^1 incorporation, high dGTP concentrations have no exotic stimulatory effects on human telomerase. Our results demonstrate that altering the dG^1 incorporation to dA^1 effectively shifted the stimulation of repeat addition processivity and rate from dGTP- to dATP-dependent for human telomerase (Figures 3.9 and 3.10). However, the ciliate *Tetrahymena thermophila* telomerase has been reported to have repeat addition processivity stimulated by high concentrations of dGTP, dGDP or even dGMP (Hardy et al, 2001). In contrast, our assays with human telomerase failed to show dGMP-dependent stimulation of repeat addition activity (Figure 3.11A). Thus, the effects of elevated

dGTP concentrations on ciliate telomerases appear esoteric with an underlying mechanism distinct from human telomerase. It was interesting to observe that, in addition to dGTP, elevated dGDP also stimulates telomerase repeat addition (Figure 3.11A, lane 3). Rather than an allosteric effect from a secondary guanosine binding site, dGDP was directly utilized as substrate and effectively increased overall nucleotide concentrations (Figure 3.11A, lanes 8-9). Furthermore, telomerase assayed with solely deoxynucleoside diphosphates generated a significant amount of DNA products (Figure 3.12D, lane 2), eliminating the possibility of phosphate transfer from deoxynucleoside triphosphates to diphosphates. Nonetheless, deoxynucleoside diphosphates are a poorer substrate to telomerase with 5-10-fold lower concentrations in cells than deoxynucleoside triphosphates (Bradshaw & Samuels, 2005). Thus, we do not expect telomerase to utilize deoxynucleoside diphosphates as substrate under cellular conditions. In addition to telomerase, all other RTs and most DNA-dependent DNA-polymerases examined in this study are capable to incorporate dGDP into DNA products (Figures 3.11B-C and 3.13). This however is not entirely unexpected as deoxynucleoside triphosphates and diphosphates both permit the same DNA polymerase catalysis with the 3' hydroxyl of the DNA primer attacking the α-phosphate of the incoming deoxynucleotide and the release of inorganic pyrophosphate or monophosphate, respectively (Kornberg, 1969). Interestingly, the Klenow fragment of *Escherichia coli* DNA polymerase that showed dGDP utilization activity in our assay (Figure 3.11C) has been previously reported inert with deoxynucleoside diphosphates (Garforth et al, 2008; Kornberg, 1957). This discrepancy is likely due to the lower nucleotide concentration used in previous studies.

Under estimated intracellular nucleotide concentrations (Bradshaw & Samuels, 2005), telomerase would be efficient for the synthesis of a single repeat, yet limited for the processive synthesis of multiple repeats through multiple catalytic cycles. Conventional telomerase assays have been performed under exceptionally high concentrations of dATP and dTTP in the range of 100 to 1,000 µM, with the radiolabeled dGTP in the very low µM range (Greider, 1991; Huard et al, 2003; Latrick & Cech, 2010; Wu et al, 2017). These skewed assay conditions lead to significant DNA synthesis arrest at the end of catalytic cycle and generated the characteristic six-nucleotide ladder banding pattern, a hallmark of telomerase activity. Reducing individual nucleotide concentrations below 5 µM results in intermediate DNA repeat products accumulation due to the stalling of nucleotide addition before reaching the end of the template (Figure 3.7). The incorporation of dG^1 is presumably slow under the low nucleotide concentrations *in vivo*, telomerase would predominately release DNA products terminating with dG^6 prior to the dG^1 incorporation. The analysis of chromosome terminal sequences found a sharp increase of the specific dG^6 terminal sequence from about 25% in telomerase-null cells to about 40% in telomerase-positive cells (Sfeir et al, 2005), which is consistent with our hypothesis that telomerase generates DNA products with this terminal sequence.

In contrast to the slow dG^1 addition, the remaining five nucleotide incorporations appear to be efficient without accumulation of any significant intermediate products (Figure 3.8A, lane 4). However, in our telomerase product release assay, an intermediate DNA product with only three residues, dG^1, dG^2 and dT^3, added was observed in the enzyme-bound fraction (Figure 3.8A, lane 1), and not in the released product fraction (Figure 3.8A, lane 4). This intermediate DNA product

likely resulted from a slightly slower incorporation of dT^4. In support of the slower rate of the dT^4 incorporation, increasing dTTP concentration to above 10 μM indeed increases repeat addition rate and generates products with a greater number of repeats added (Figure 3.6C, lanes 2 and 3), which is consistent with a previous report (Drosopoulos & Prasad, 2010). Together, these results support that the incorporation efficiencies of the remaining five residues, dG^2, dT^3, dT^4, dA^5 and dG^6, minimally contribute to the overall repeat addition rate. The dG^1 incorporation efficiency is the key determinant for both the processivity and the rate of telomerase repeat addition.

Elucidating the mechanism by which telomerase undergoes processive synthesis of hundreds of telomeric DNA repeats has remained challenging. The unique telomerase catalytic cycle relies on a highly-orchestrated arrangement of TERT, TR, and accessory proteins to facilitate DNA product retention and effective template regeneration for processive repeat addition. Our findings herein redefine the telomerase catalytic cycle as three critical and distinct steps: (i) rapid template translocation followed by (ii) slow dG^1 incorporation and (iii) efficient addition of the five remaining residues dG^2, dT^3, dT^4, dA^5 and dG^6 (Figure 3.10). DNA synthesis arrest at the slow dG^1 incorporation step promotes product release and limits processive repeat synthesis. The intrinsic low processivity of human telomerase is beneficial as it affords repeat addition regulation through DNA-protein interactions with TERT anchor sites and telomerase accessory proteins to control product release (Figure 3.18). Moreover, our findings suggest that telomerase products are released mainly from unsuccessful dG^1 incorporation, instead of failed template translocation. Thus, the slow dG^1 incorporation step and the inhibitory effect of the pause-signal

limit the processivity and rate of telomerase repeat addition, representing prime targets for therapeutic regulation of telomerase function.

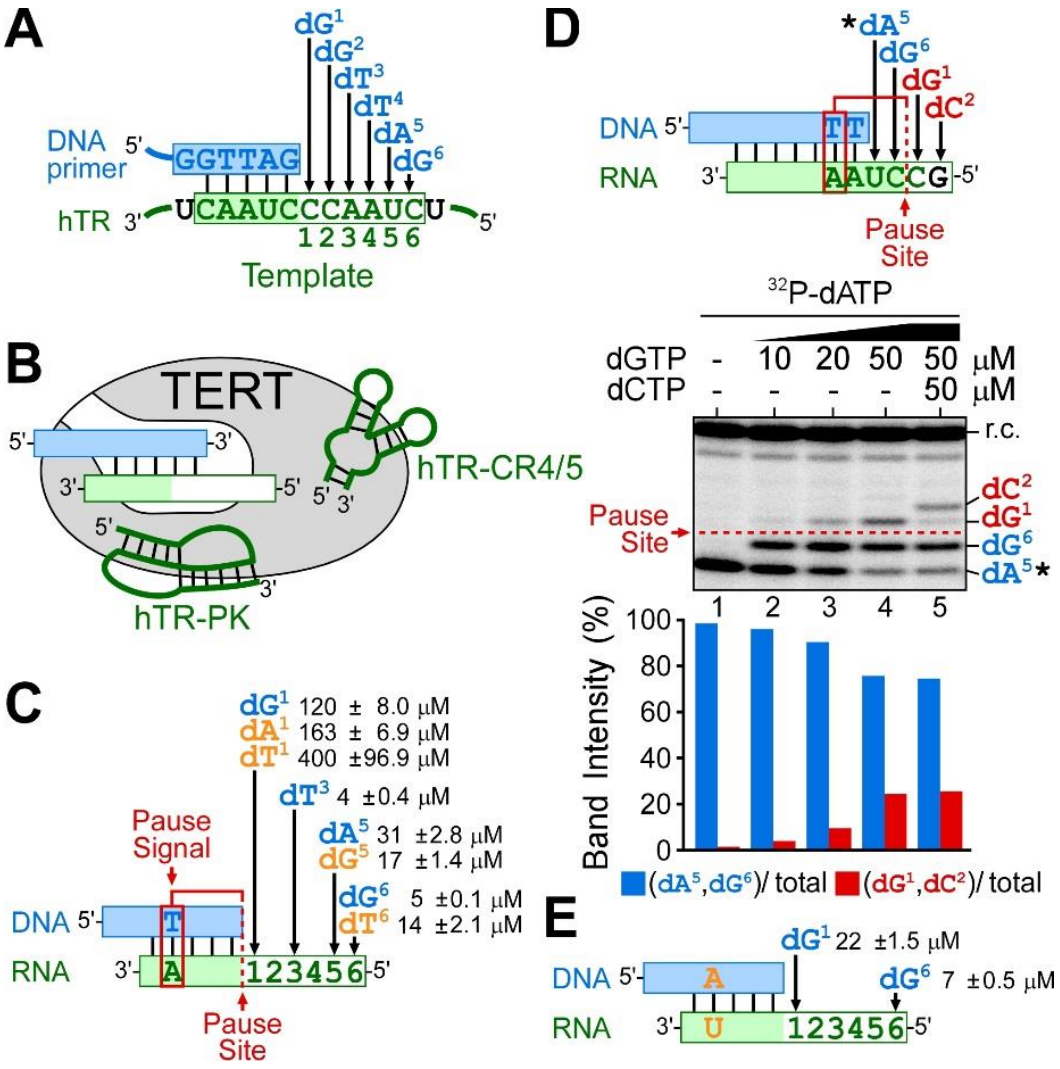
A
dG1
dG2
dT3
dT4
dA5
dG6
DNA primer 5'
GGTTAG
hTR 3'
UCAAUCCCAAUCU
5'
1 2 3 4 5 6
Template
B
TERT
5'
3'
3'
5'
5'
3'
5'
3'
hTR-CR4/5
hTR-PK
C
dG1 120 ± 8.0 μM
dA1 163 ± 6.9 μM
dT1 400 ±96.9 μM
dT3 4 ±0.4 μM
dA5 31 ±2.8 μM
dG5 17 ±1.4 μM
dG6 5 ±0.1 μM
dT6 14 ±2.1 μM
Pause Signal
DNA 5'
T
RNA 3'
A
123456
5'
Pause Site
D
*dA5
dG6
dG1
dC2
DNA 5'
TT
RNA 3'
AAUCCG
5'
Pause Site
32P-dATP
dGTP - 10 20 50 50 μM
dCTP - - - - 50 μM
r.c.
dC2
dG1
dG6
dA5*
Pause Site
1 2 3 4 5
Band Intensity (%)
100
80
60
40
20
0
(dA5,dG6)/ total
(dG1,dC2)/ total
E
dG1 22 ±1.5 μM
dG6 7 ±0.5 μM
DNA 5'
A
RNA 3'
U
123456
5'

Figure 3.1. An elevated K_M for the dG1 nucleotide incorporation by human telomerase. (A). Schematic of the six nucleotide incorporations catalyzed by human telomerase. Human telomerase catalyzes incorporations of six deoxynucleotides, dG1, dG2, dT3, dT4, dA5 and dG6, directed by the integral hTR template (green box). The hTR template contains two regions: an alignment sequence (shaded) for base-pairing with the DNA primer and the actual templating sequence for specifying DNA polymerization. Numbers below the hTR template region denote the order and position of the six deoxynucleotide incorporations. (B). Composition of template-free (TF) telomerase. TF telomerase was reconstituted by assembling *in vitro* expressed human TERT protein with the two essential hTR fragments, CR4/5 and the pseudoknot (PK) that had the template region excised. Pre-annealed DNA primer (blue box) and RNA template (green box) hybrids are used as substrates for the TF telomerase activity assay. (C). K_M for incorporating nucleotides dG1, dT3, dA5, and dG6 by TF telomerase. The dG1 incorporation is located adjacent to the pause site (red dashed line) specified by the pause signal (red box), a dT:rA base-pair in the DNA/RNA hybrid. For measuring the K_M of specific nucleotide incorporations, different DNA/RNA hybrid substrates with permuted sequences were used (Figure 3.4). The K_M for incorporating non-telomeric nucleotides (orange) with corresponding template mutations are denoted. (D) High dGTP concentrations overcome the pause signal mediated DNA synthesis arrest. Primer extension assays performed using the TF telomerase and a DNA/RNA hybrid substrate in the presence of 0.165 μM ^{32}P-dATP (asterisk) with a titration of dGTP (10, 20 and 50 μM). The DNA/RNA hybrid substrate allows for the incorporation of four nucleotides: dA5, dG6, dG1, dC2, as depicted. The pause signal (red box) and the pause site (red dashed line) in the DNA/RNA substrate arrests DNA synthesis after the incorporation of dA5 and dG6 (blue) reducing the incorporation efficiency for dG1 (red). A radiolabeled DNA recovery control (r.c.) was added before product purification and precipitation. Nucleotide incorporation beyond the pause site was quantitated by the intensity of dG1 and dC2 products (red) over the total intensity of products. (E) Removal of pause signal decreases K_M for dG1 incorporation. The DNA/RNA hybrid substrates with the pause signal dT:rA mutated to dA:rU (orange) were used to determine K_M for nucleotide incorporation at positions dG1 and dG6 (Figure 3.5).

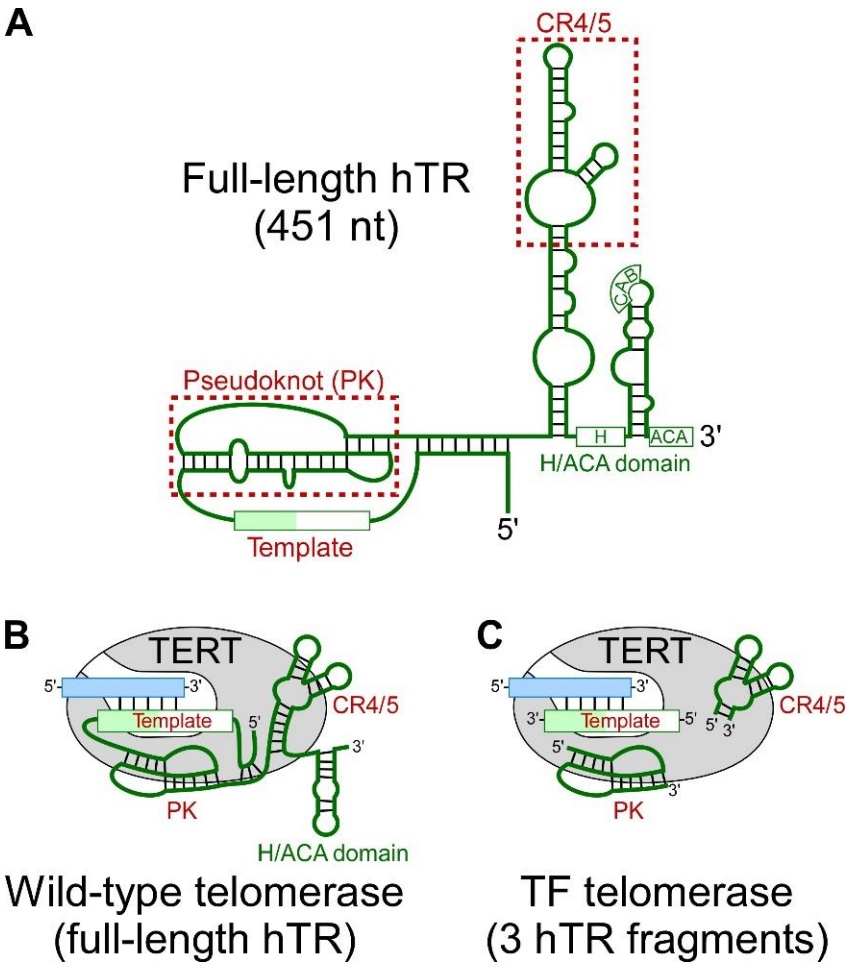

Figure 3.2. Comparison of wild-type and template-free (TF) telomerase reconstitution systems. (A) Schematic of the 451 nt full-length hTR. The hTR secondary structure comprises three major structural domains: the pseudoknot (PK), conserved regions 4/5 (CR4/5) and box H/ACA domain. The template region and the two structural domains, PK, and CR4/5 (red), are minimally required for reconstituting telomerase activity *in vitro*. (B) The wild-type telomerase core enzyme comprises the full-length hTR (green) and the catalytic TERT protein (grey). The substrate for wild-type telomerase is a single-stranded DNA primer (blue). (C) TF telomerase comprises the minimally required PK and CR4/5 hTR fragments (green). The substrate for TF telomerase is duplex of a single-stranded DNA primer (blue) pre-annealed with an RNA template.

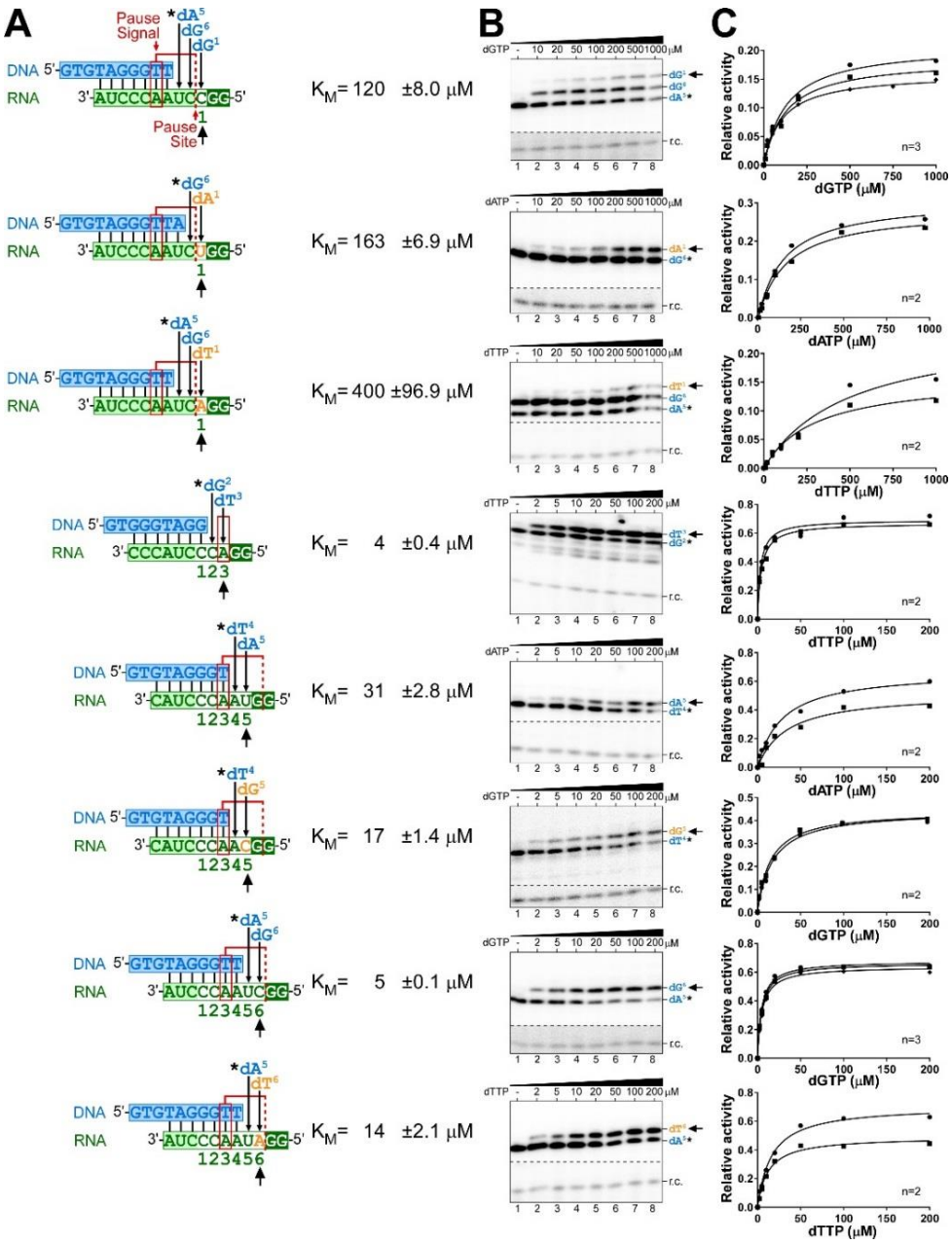
A
B
C
Pause Signal
Pause Site
DNA 5'-GTGTAGGGTTT
RNA 3'-AUCCCAAUCCGG-5'
K_M= 120 ±8.0 μM
DNA 5'-GTGTAGGGTTTA
RNA 3'-AUCCCAAUCUGG-5'
K_M= 163 ±6.9 μM
DNA 5'-GTGTAGGGTTT
RNA 3'-AUCCCAAUCAGG-5'
K_M= 400 ±96.9 μM
DNA 5'-GTGGGTAGG
RNA 3'-CCCAUCCCAGG-5'
K_M= 4 ±0.4 μM
DNA 5'-GTGTAGGGT
RNA 3'-CAUCCCAAUGG-5'
K_M= 31 ±2.8 μM
DNA 5'-GTGTAGGGT
RNA 3'-CAUCCCAACGG-5'
K_M= 17 ±1.4 μM
DNA 5'-GTGTAGGGTTT
RNA 3'-AUCCCAAUCGG-5'
K_M= 5 ±0.1 μM
DNA 5'-GTGTAGGGTTT
RNA 3'-AUCCCAAUAGG-5'
K_M= 14 ±2.1 μM
dGTP
dATP
dTTP
r.c.
Relative activity
dGTP (μM)
dATP (μM)
dTTP (μM)
n=3
n=2

Figure 3.3. K_M measurement for nucleotide incorporations at specific template positions. (A) Sequences of the DNA/RNA hybrid substrates and positions of the pause site. *In vitro* reconstituted template-free (TF) telomerase were analyzed with specific DNA/RNA hybrid substrates to determine the apparent K_M for each nucleotide incorporation. Numbers below DNA/RNA duplexes indicate positions corresponding to the telomerase template and order of nucleotides incorporated. Non-telomeric template residues (orange) are indicated. The K_M^{app} values measured for the nucleotide incorporation at the indicated position (black arrow) with each hybrid substrate are listed to the right. The nucleotides added (black) to the DNA in the hybrid are shown, with the first incorporation a ^{32}P-dNTP (circled). (B) Representative gels for K_M^{app} measurements. A ^{32}P end-labeled DNA recovery control (r.c.) was added before product purification and precipitation. (C) Plots derived from the normalized intensity of the +2 or +3 product over the total intensity of products for the specified nucleotide concentration. The Michaelis–Menten equation, $Y=Vmax*X/(K_M+X)$, was used to fit the nonlinear curve to determine the K_M^{app}. Two or three replicates were performed for each measurement.

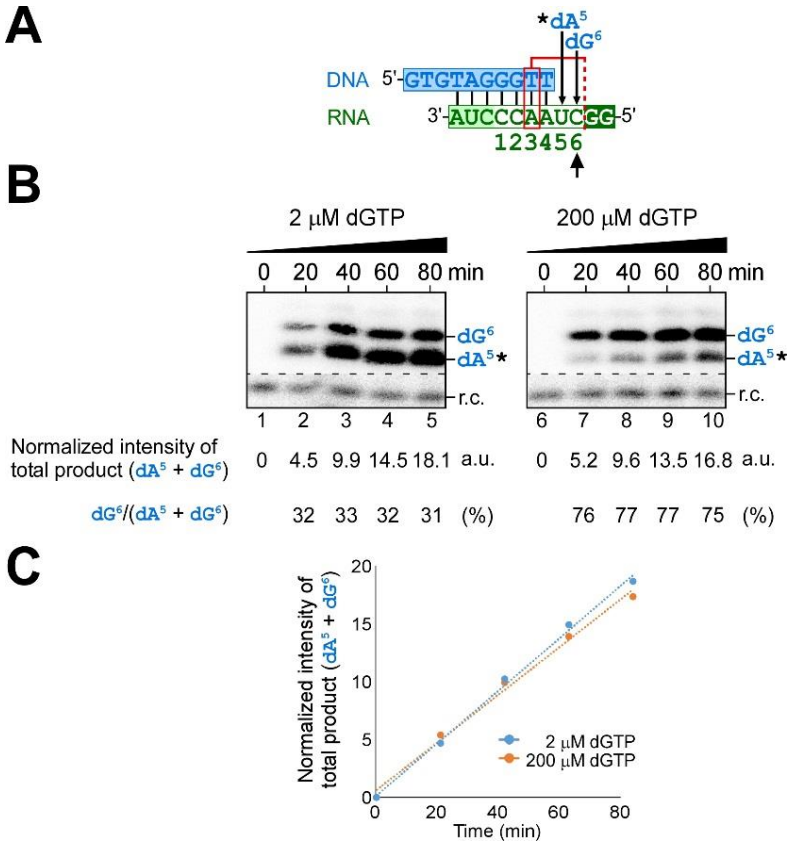

Figure 3.4. Time course analysis of telomerase primer-extension assay at 2 and 200 μM. (A) Sequence of the DNA/RNA hybrid substrate, position of the pause signal and pause site (red). *In vitro* reconstituted template-free (TF) telomerase were analyzed with specific DNA/RNA hybrid substrate to determine linear product formation for the K_M measurements of nucleotide incorporation over time (0, 20, 40, 60, and 80 min). Numbers below the DNA/RNA duplex indicate positions corresponding to the telomerase template and the order of nucleotides incorporated. The nucleotide incorporation K_M values measured are indicated (black arrow). The DNA products were labeled by incorporating a ^{32}P-dATP (0.166 μM, asterisk) prior to the K_M measurement. (B) Representative gel for linear product formation for the K_M measurements of nucleotide incorporation over time. A ^{32}P end-labeled DNA recovery control (r.c.) was added before product purification and precipitation. The intensity of total product formation (dA5 and dG6) at various times were normalized to the loading control were measured with arbitrary units (a.u.) and were linear. The ratio intensity of dG6 over total (dA5 and dG6) was unchanged with time. (C) Plots derived from the normalized intensity of total product formation (dA5 and dG6) at various times revealed a linear relationship between product formation and time.

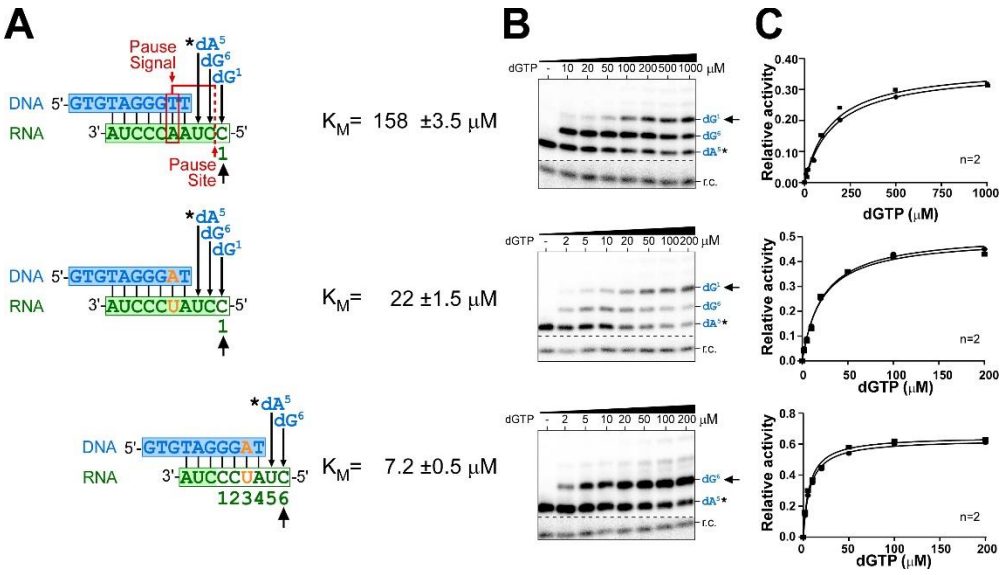

Figure 3.5. K_M measurement for nucleotide incorporations in the presence or absence of the pause signal. (A) Sequences of the DNA/RNA hybrid substrates and the position of the pause signal mutation. *In vitro* reconstituted template-free telomerase (TF) were analyzed with specific DNA/RNA hybrid substrates to determine the apparent K_M for each nucleotide incorporation. (B) Representative gels for K_M^{app} measurements. An ^{32}P end-labeled DNA recovery control (r.c.) was added before product purification and precipitation. (C) Plots derived from the normalized intensity of the +2 or +3 product over the total intensity of products for the specified nucleotide concentration. The Michaelis–Menten equation, $Y=Vmax*X/(K_M+X)$, was used to fit the nonlinear curve to determine the K_M^{app}. Two or three replicates were performed for each measurement.

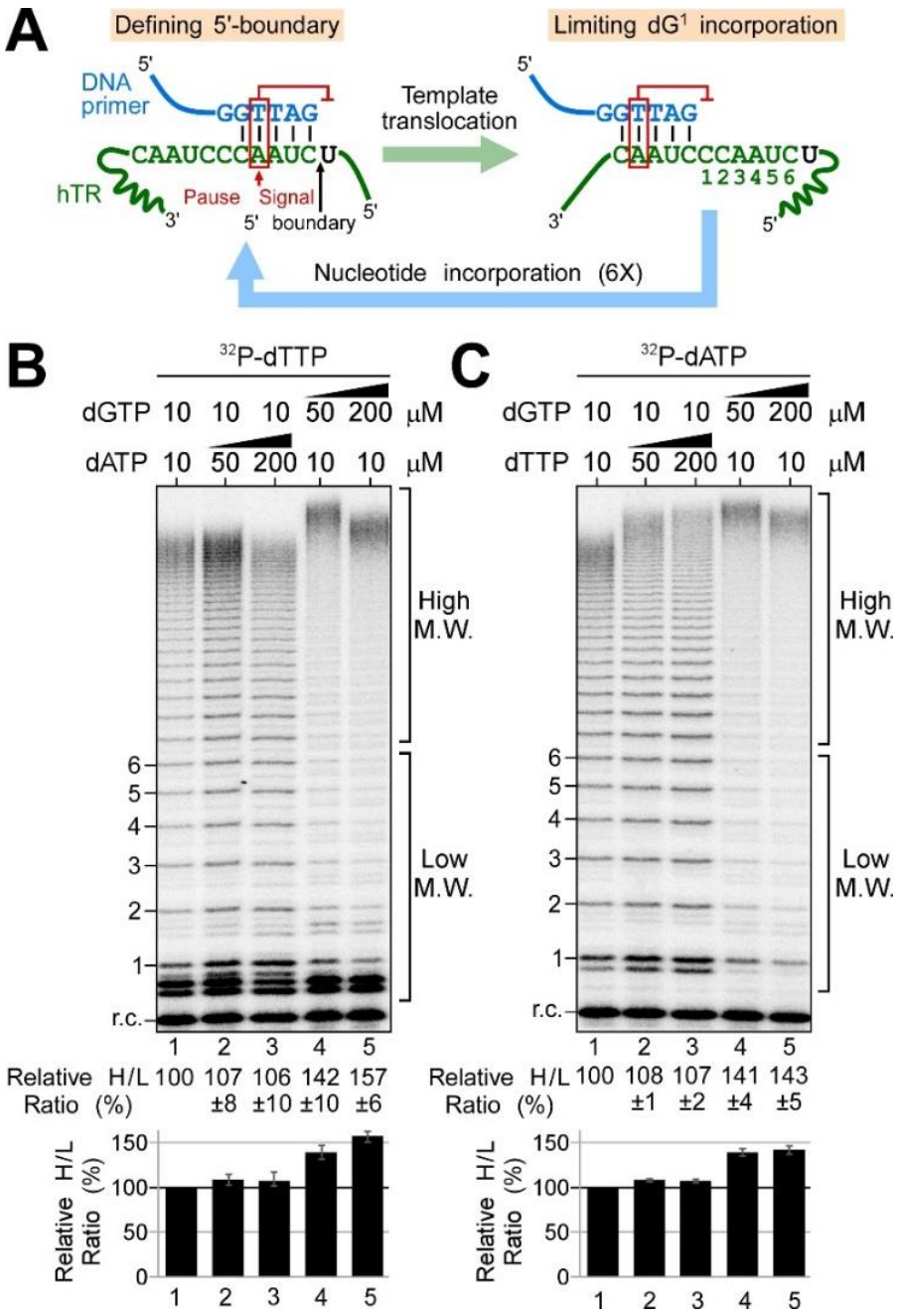
A
Defining 5'-boundary
Limiting dG1 incorporation
DNA primer
GGTTAG
CAAUCCCAAUCU
hTR
Pause
Signal
5' boundary
Template translocation
123456
Nucleotide incorporation (6X)
B
32P-dTTP
dGTP 10 10 10 50 200 μM
dATP 10 50 200 10 10 μM
High M.W.
Low M.W.
r.c.
Relative H/L Ratio (%) 100 107 ±8 106 ±10 142 ±10 157 ±6
C
32P-dATP
dGTP 10 10 10 50 200 μM
dTTP 10 50 200 10 10 μM
Relative H/L Ratio (%) 100 108 ±1 107 ±2 141 ±4 143 ±5

Figure 3.6. dGTP-dependent repeat addition stimulation of human telomerase. (A) Schematic of the dual function of the template-embedded pause signal (red box). The pause signal defines the 5' template boundary (black arrow) by inhibiting non-telomeric DNA synthesis beyond the template boundary (Brown et al, 2014b). A putative additional function of the pause signal is to limit dG^{1} incorporation post template translocation. (B, C) Direct primer extension assays were performed with telomerase enzyme reconstituted *in vivo* and immuno-purified. Telomerase was assayed in the presence of either (B) 0.165 µM ^{32}P-dTTP, 10 µM dTTP and a range of dGTP or dATP concentrations, or (C) 0.165 µM ^{32}P-dATP, 10 µM dATP and a range of dGTP or dTTP concentrations. A radiolabeled DNA recovery control (r.c.) was added before product purification and precipitation. Numbers to the left of the gel denote the number of repeats added to the telomeric primer. Ratio as a percent for the intensity of high over low M.W. DNA products generated relative to the reaction with the low nucleotide concentrations. A bar graph of the relative ratio of high/low M.W. DNA products are shown below the gel. The error bars represent standard error of the mean determined from three independent replicates.

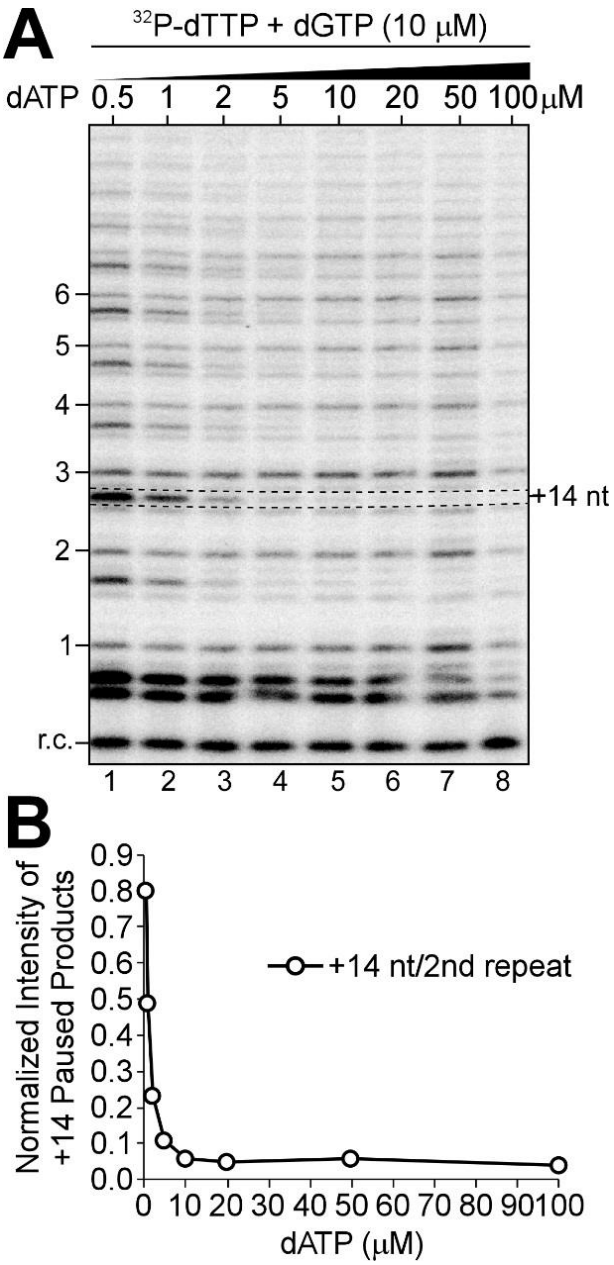

Figure 3.7. Effects of dATP concentration on nucleotide incorporation. (A) Direct primer extension assays were performed with native telomerase reconstituted *in vivo* and immuno-purified. The DNA primer substrate was extended in the presence of ^{32}P-dTTP, 10 μM dGTP and a range of dATP concentrations (0.5, 1, 2, 5, 10, 20, 50 and 100 μM). (B) Quantitation of intermediate product accumulation from dATP insufficiency. Plot of band intensity for the stalling DNA product (+14 nt) with 14 nucleotides added (two repeats plus 4 nucleotides) over the major product (+2 repeats) with two repeats added and normalized for total telomerase activity.

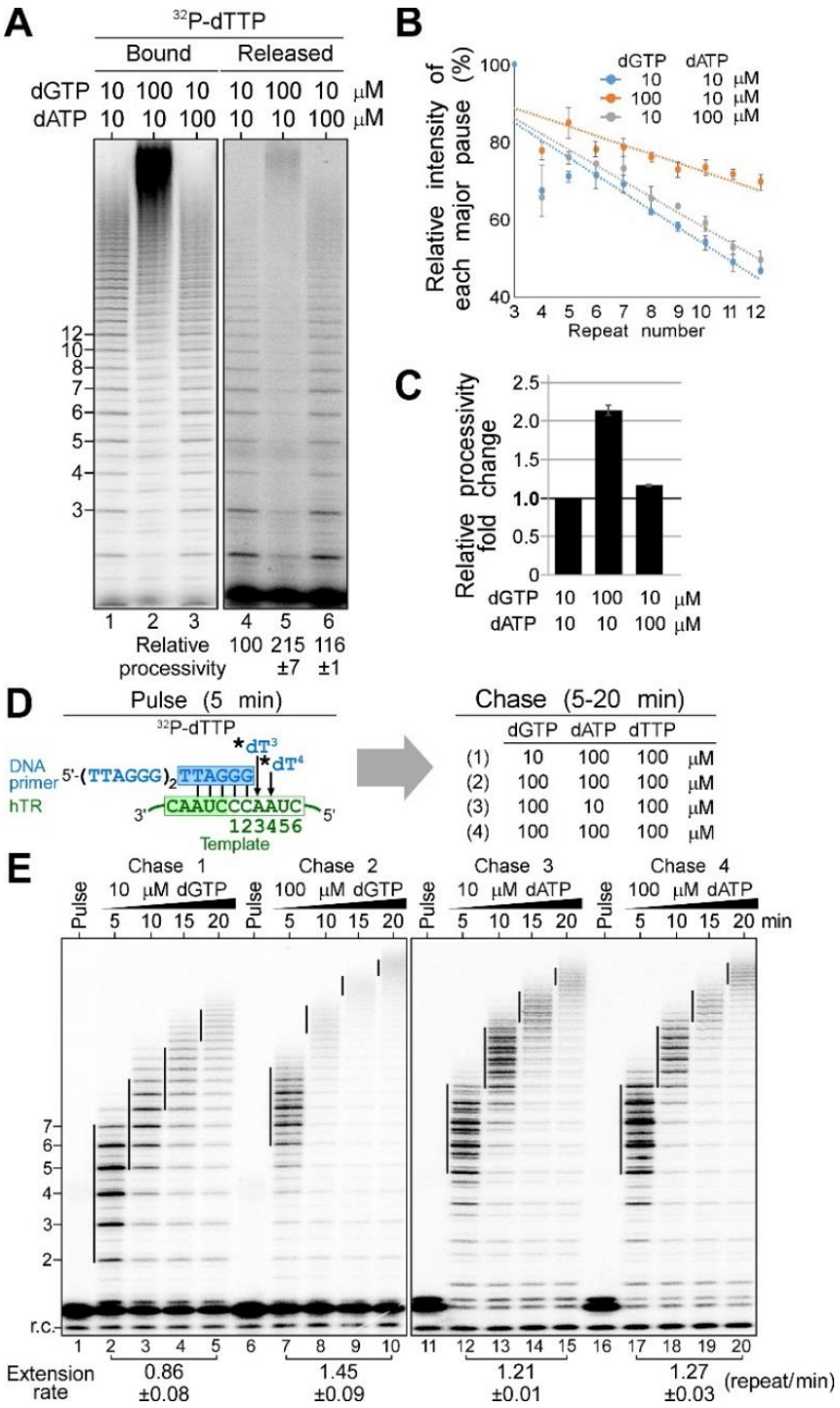
A
32P-dTTP
Bound
Released
dGTP 10 100 10 10 100 10 μM
dATP 10 10 100 10 10 100 μM
12
10
8
7
6
5
4
3
1 2 3 4 5 6
Relative processivity 100 215 ±7 116 ±1
B
dGTP dATP
10 10 μM
100 10 μM
10 100 μM
Relative intensity of each major pause (%)
100
80
60
40
3 4 5 6 7 8 9 10 11 12
Repeat number
C
Relative processivity fold change
2.5
2.0
1.5
1.0
0.5
0
dGTP 10 100 10 μM
dATP 10 10 100 μM
D
Pulse (5 min)
32P-dTTP
*dT3
*dT4
DNA primer 5'-(TTAGGG)2TTAGGG
hTR 3' CAAUCCCAAUC 5'
123456
Template
Chase (5-20 min)
dGTP dATP dTTP
(1) 10 100 100 μM
(2) 100 100 100 μM
(3) 100 10 100 μM
(4) 100 100 100 μM
E
Chase 1
10 μM dGTP
Chase 2
100 μM dGTP
Chase 3
10 μM dATP
Chase 4
100 μM dATP
Pulse
5 10 15 20 min
7
6
5
4
3
2
r.c.
1 2 3 4 5 6 7 8 9 10 11 12 13 14 15 16 17 18 19 20
Extension rate
0.86 ±0.08
1.45 ±0.09
1.21 ±0.01
1.27 ±0.03
(repeat/min)

Figure 3.8. Effects of dGTP on repeat addition processivity and rate. (A) Stimulation of repeat addition processivity with dGTP. *In vivo* reconstituted telomerase enzyme was assayed by the product release analysis in the presence of 0.165 μM ^{32}P-dTTP, 10 μM dTTP as well as either 10 or 100 μM of dGTP and dATP. The enzyme-bound and released DNA products were separated and individually analyzed. (B) Quantitation of repeat addition processivity. The intensities of the released DNA products with 3-12 repeats added were quantitated and normalized to the intensity of the product with 3 repeats added. The relative intensities of major bands were plotted against the number of repeats added to determine slopes that correspond to the relative processivity from each reaction (see Materials and Methods section). (C) Relative repeat addition processivity under different nucleotide concentrations. A bar graph indicates the fold change of the relative repeat addition processivity under either 10 or 100 μM of dGTP and dATP. The error bars represent standard error of the mean determined from two independent replicates. (D) Schematic of pulse-chase time course analysis. During the pulse reaction, the DNA primer $(TTAGGG)_3$ was labeled with 0.165 μM ^{32}P-dTTP (asterisk) by the telomerase enzyme. During the chase reaction, the enzyme-bound radiolabeled DNA primer was extended processively with telomeric repeats under 100 μM cold dTTP as well as either 10 or 100 μM of dGTP and dATP for 5, 10, 15 or 20 mins. (E) Repeat addition rate measured by the pulse-chase time course analysis under differing nucleotide concentrations. The vertical lines on the gel indicate the major bands of telomere products synthesized during the chase reactions. Repeat addition rates are expressed as repeats per minute (see Materials and Methods) and indicated below the gel. The standard error of the mean was determined from two independent replicates.

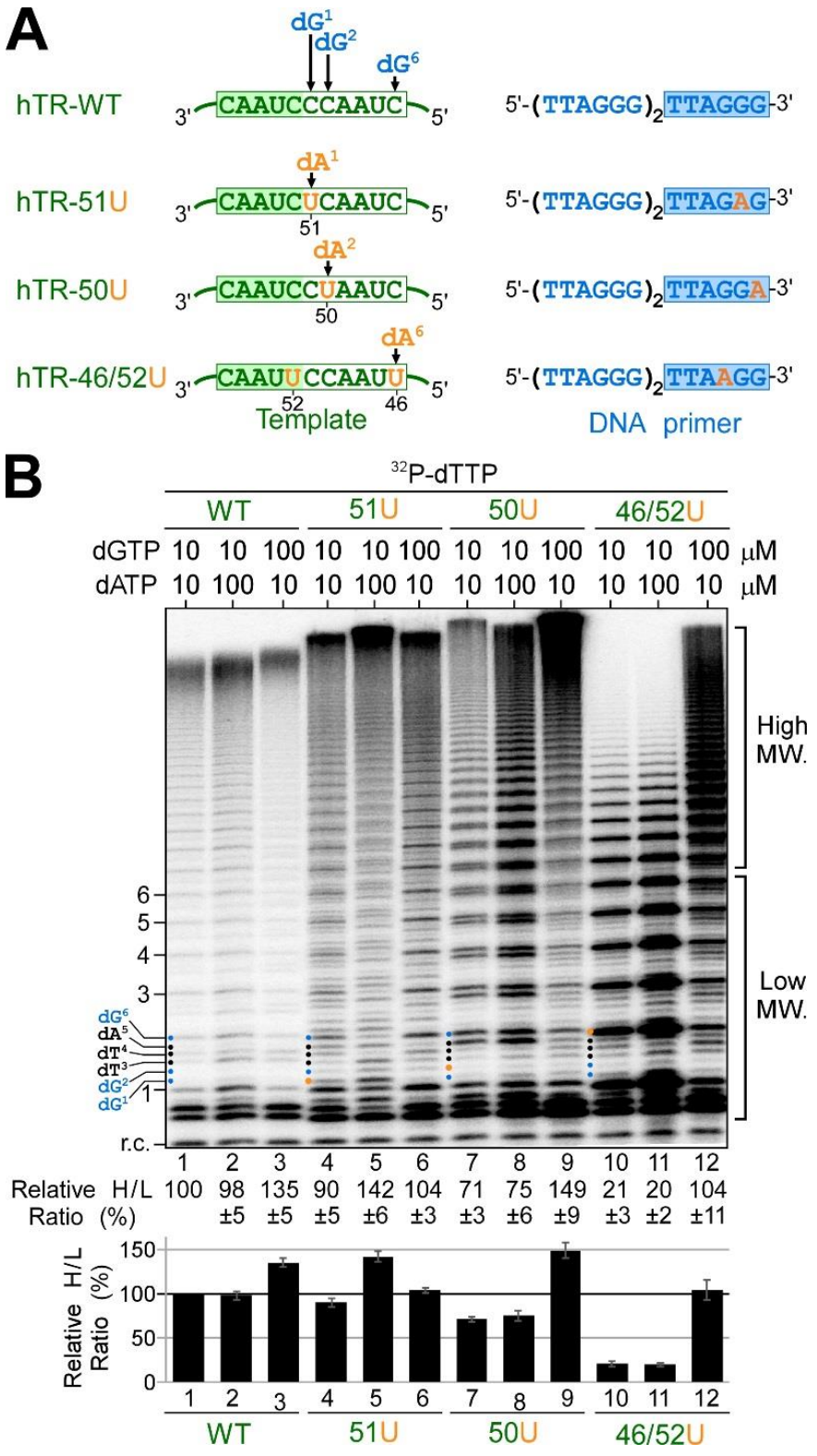
A
dG1
dG2
dG6
hTR-WT
3' CAAUCCCAAUC 5'
5'-(TTAGGG)2TTAGGG-3'
dA1
hTR-51U
3' CAAUCUCAAUC 5'
51
5'-(TTAGGG)2TTAGAG-3'
dA2
hTR-50U
3' CAAUCCUAAUC 5'
50
5'-(TTAGGG)2TTAGGA-3'
dA6
hTR-46/52U
3' CAAUUCCAAUU 5'
52
46
5'-(TTAGGG)2TTAAGG-3'
Template
DNA primer
B
32P-dTTP
WT
51U
50U
46/52U
dGTP 10 10 100 10 10 100 10 10 100 10 10 100 μM
dATP 10 100 10 10 100 10 10 100 10 10 100 10 μM
High MW.
Low MW.
6
5
4
3
dG6
dA5
dT4
dT3
dG2
dG1
1
r.c.
1 2 3 4 5 6 7 8 9 10 11 12
Relative H/L Ratio (%) 100 98 ±5 135 ±5 90 ±5 142 ±6 104 ±3 71 ±3 75 ±6 149 ±9 21 ±3 20 ±2 104 ±11
Relative H/L Ratio (%)
150
100
50
0
1 2 3 4 5 6 7 8 9 10 11 12
WT
51U
50U
46/52U

Figure 3.9. The dG^1 incorporation and telomerase repeat addition activity. (A). Sequences of hTR mutant templates and DNA primers used in this assay. The wild-type hTR template specifies for the incorporation of three dG residues, dG^1, dG^2, and dG^6. The mutant hTR templates, 51U, 50U and 46/52U, harbor rC-to-rU template mutations (orange) that specify incorporations of non-telomeric dA^1, dA^2 and dA^6 (orange), respectively. The telomerase template mutants were assayed with corresponding DNA primers as depicted. (B) Direct primer extension assays of telomerase template mutants. Wild-type and mutant telomerases were reconstituted *in vivo* and the immuno-purified enzymes were assayed in the presence of 0.165 µM ^{32}P-dTTP, 10 µM dTTP as well as either 10 or 100 µM of dGTP and dATP. Ratio as a percent for the intensity of high over low M.W. DNA products generated relative to the wild-type telomerase reaction with the low nucleotide concentrations. A bar graph of the relative ratio of high/low M.W. DNA products are shown below the gel. Standard error of the mean was determined from three independent replicates.

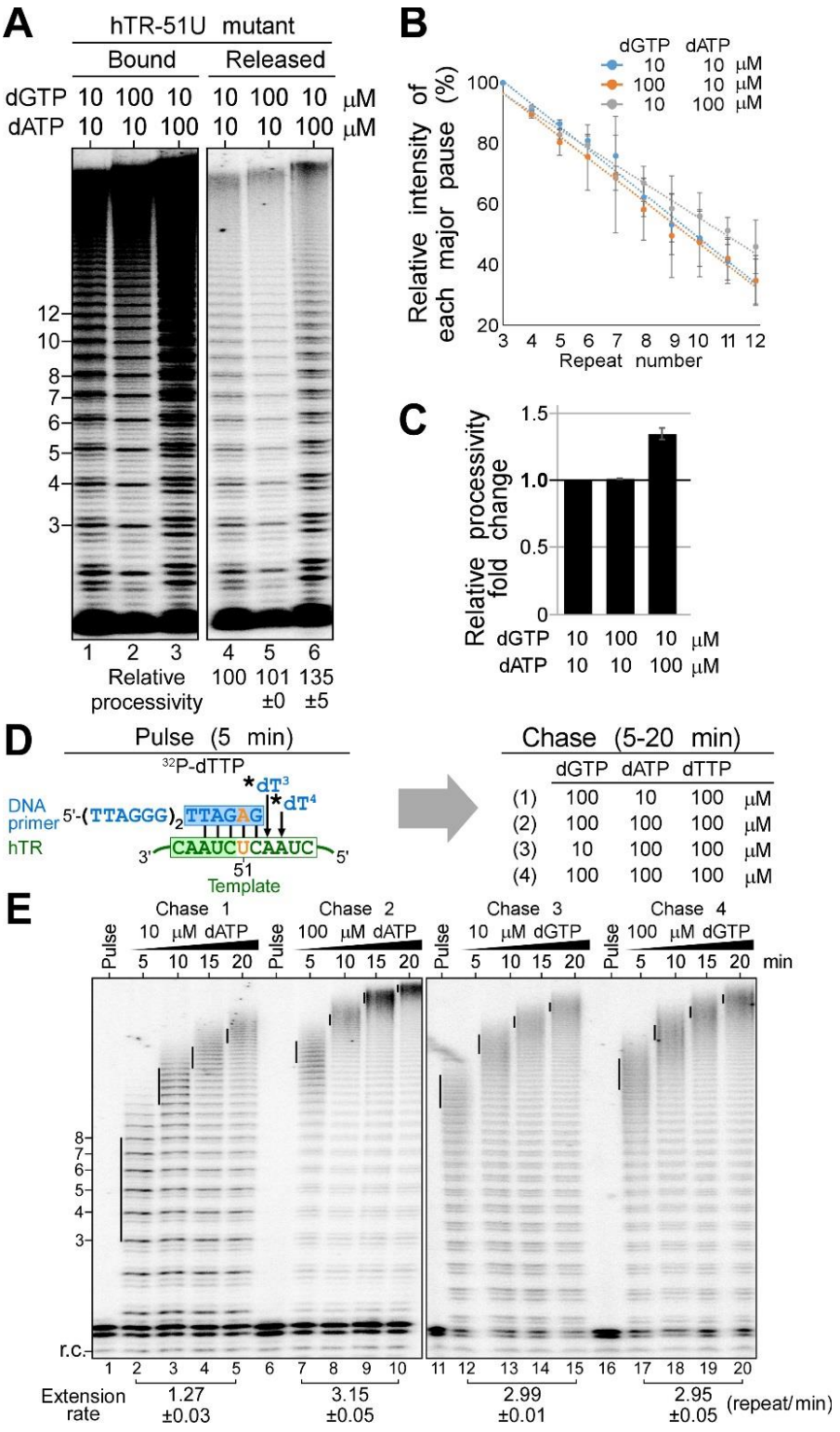
A
hTR-51U mutant
Bound
Released
dGTP 10 100 10 10 100 10 μM
dATP 10 10 100 10 10 100 μM
12
10
8
7
6
5
4
3
1 2 3 4 5 6
Relative processivity
100 101 ±0 135 ±5
B
dGTP dATP
10 10 μM
100 10 μM
10 100 μM
Relative intensity of each major pause (%)
100
80
60
40
20
3 4 5 6 7 8 9 10 11 12
Repeat number
C
Relative processivity fold change
1.5
1.0
0.5
0
dGTP 10 100 10 μM
dATP 10 10 100 μM
D
Pulse (5 min)
32P-dTTP
*dT3
*dT4
DNA primer
5'-(TTAGGG)2TTAGAG
hTR
3'
CAAUCUCAAUC
5'
51
Template
Chase (5-20 min)
dGTP dATP dTTP
(1) 100 10 100 μM
(2) 100 100 100 μM
(3) 10 100 100 μM
(4) 100 100 100 μM
E
Chase 1
10 μM dATP
Chase 2
100 μM dATP
Chase 3
10 μM dGTP
Chase 4
100 μM dGTP
Pulse
5 10 15 20 min
8
7
6
5
4
3
r.c.
1 2 3 4 5 6 7 8 9 10 11 12 13 14 15 16 17 18 19 20
Extension rate
1.27 ±0.03
3.15 ±0.05
2.99 ±0.01
2.95 ±0.05
(repeat/min)

Figure 3.10. Effects of dATP on repeat addition processivity and rate for the telomerase mutant hTR-51U. (A) dATP-dependent stimulation of repeat addition processivity with the hTR-51U mutant. *In vivo* reconstituted telomerase enzyme was assayed by the product release analysis in the presence of 0.165 μM ^{32}P-dTTP, 10 μM dTTP as well as either 10 or 100 μM of dGTP and dATP. The enzyme-bound and released DNA products were separated and individually analyzed. (B) Quantitation of repeat addition processivity. The intensities of the released DNA products with 3-12 repeats added were quantitated and normalized to the intensity of the product with 3 repeats added. The relative intensities of major bands were plotted against the number of repeats added to determine the slopes that correspond to the relative processivity from each reaction. (C) Relative repeat addition processivity under different nucleotide concentrations. A bar graph indicates the fold change of the relative repeat addition processivity under either 10 or 100 μM of dGTP and dATP. The error bars represent standard error of the mean determined from two independent replicates. (D) Schematic of the pulse-chase time course analysis for the telomerase mutant hTR-51U. During the pulse reaction, the DNA primer (TTAGGG)2TTAGAG was labeled with 0.165 μM ^{32}P-dTTP (asterisk) by the telomerase hTR-51U enzyme. During the chase reaction, the enzyme-bound radiolabeled DNA primer was extended processively with telomeric repeats under 100 μM cold dTTP as well as either 10 or 100 μM dGTP and dATP for 5, 10, 15 or 20 mins. (E) Repeat addition rate measured by the pulse-chase time course analysis under differing nucleotide concentrations. A radiolabeled DNA recovery control (r.c.) was added before product purification and precipitation. The vertical lines on the gel indicate the major bands of telomere products synthesized during the chase reactions. Repeat addition rates are expressed as repeats per minute and indicated below the gel. The standard error of the mean was determined from two independent replicates.

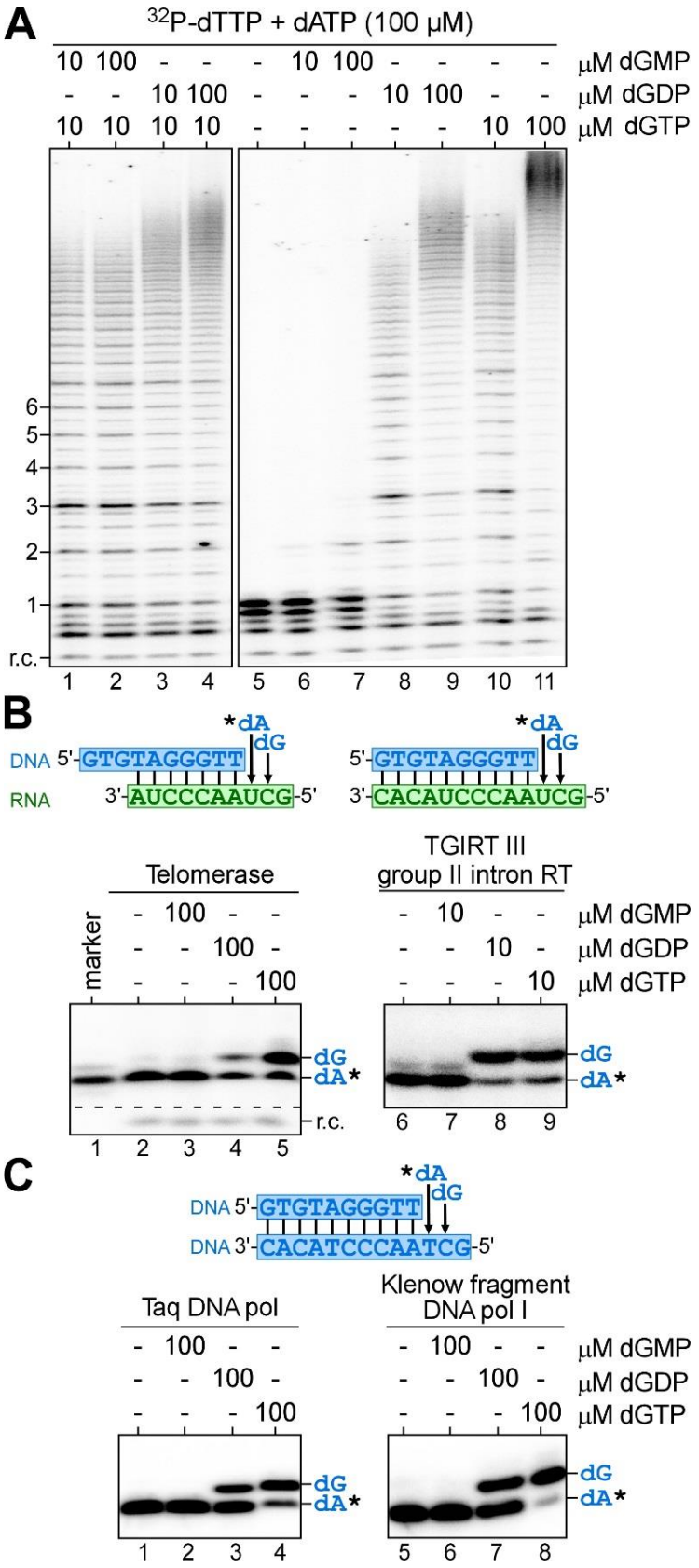
A
32P-dTTP + dATP (100 μM)
10 100 - - - 10 100 - - - - μM dGMP
- - 10 100 - - - 10 100 - - μM dGDP
10 10 10 10 - - - - - 10 100 μM dGTP
6
5
4
3
2
1
r.c.
1 2 3 4 5 6 7 8 9 10 11
B
*dA
dG
DNA 5'-GTGTAGGGTT
RNA 3'-AUCCCAAUCG-5'
5'-GTGTAGGGTT
3'-CACAUCCCAAUCG-5'
Telomerase
TGIRT III
group II intron RT
marker
- 100 - - μM dGMP
- - 100 - μM dGDP
- - - 100 μM dGTP
- 10 - - μM dGMP
- - 10 - μM dGDP
- - - 10 μM dGTP
dG
dA*
r.c.
1 2 3 4 5
6 7 8 9
C
*dA
dG
DNA 5'-GTGTAGGGTT
DNA 3'-CACATCCCAATCG-5'
Taq DNA pol
Klenow fragment
DNA pol I
- 100 - - μM dGMP
- - 100 - μM dGDP
- - - 100 μM dGTP
dG
dA*
1 2 3 4
5 6 7 8

Figure 3.11. Telomerase utilizes deoxynucleoside diphosphates as substrate. (A) Direct primer extension assays were performed with telomerase enzyme reconstituted *in vivo* and immuno-purified. Telomerase was assayed in the presence of 0.165 µM ^{32}P-dTTP, 10 µM dTTP, 100 µM dATP as well as combinations of either 10 or 100 µM of dGMP, dGDP or dGTP. (B) Utilization of dGDP by RTs. Specific DNA/RNA hybrid substrates depicted harbor a template sequence for the incorporation of a single dA and a dG residue. (C) Utilization of dGDP by DNA-dependent DNA polymerases. A DNA/DNA hybrid substrate depicted harbor a template sequence to allow for incorporation of a single dA and a dG residue. Taq DNA polymerase (pol) and the Klenow fragment of DNA polymerases I were assayed in the presence of 0.165 µM ^{32}P-dATP (asterisk) and either dGMP, dGDP or dGTP. Numbers to the right of the gel denote the identity of nucleotides added.

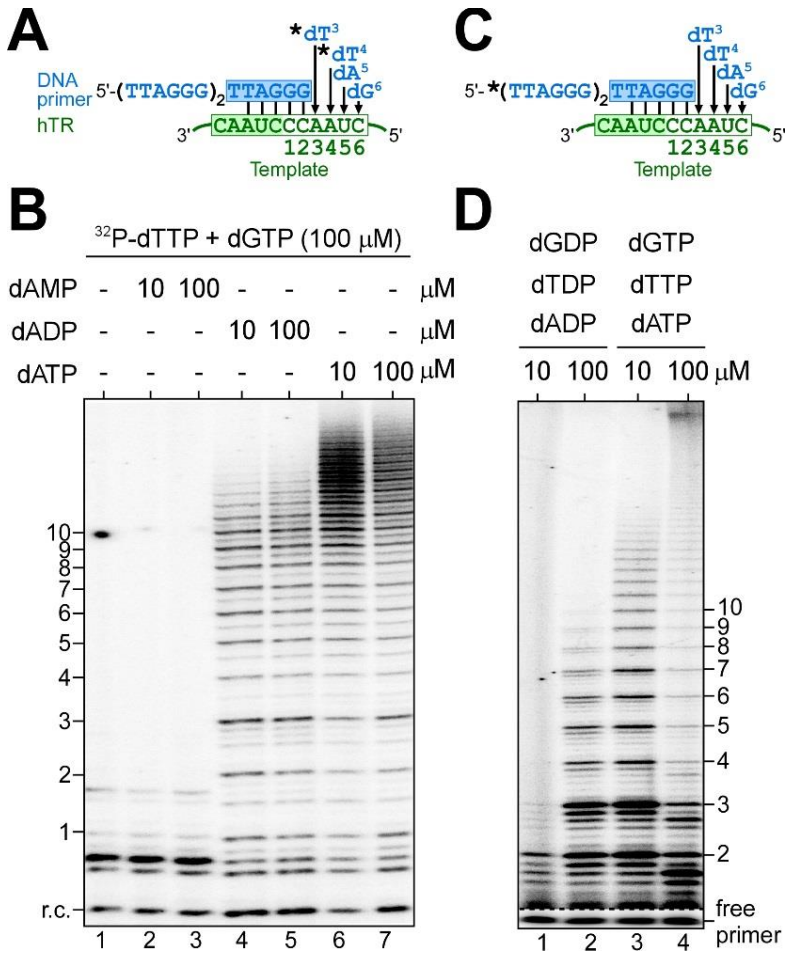

Figure 3.12. **The utilization of deoxynucleoside diphosphates as substrate for telomerase nucleotide addition.** (A) Schematic of nucleotide addition with native telomerase. The order of the nucleotides, TTAG, added prior to first template translocation was depicted. The DNA products were labeled with ^{32}P-dTTP (circled). (B) Telomerase was assayed in the presence of ^{32}P-dTTP and 100 μM dGTP with either 10 or 100 μM of dAMP, dADP and dATP. An ^{32}P end-labeled DNA recovery control (r.c.) was added before product purification and precipitation. (C) Schematic of nucleotide addition with a ^{32}P-end-labeled DNA primer and native telomerase. The order of the nucleotides, TTAG, added prior to first template translocation was depicted. The DNA primer was ^{32}P end-labeled to eliminate the need of including ^{32}P-dTTP in the dNDP-only reaction. (D) Telomerase was assayed in the presence of either 10 or 100 μM deoxynucleoside diphosphates (dGDP, dTDP, dADP) or deoxynucleoside triphosphates (dGTP, dTTP, dATP). Direct primer extension assays were performed with telomerase enzyme reconstituted *in vivo* and immuno-purified.

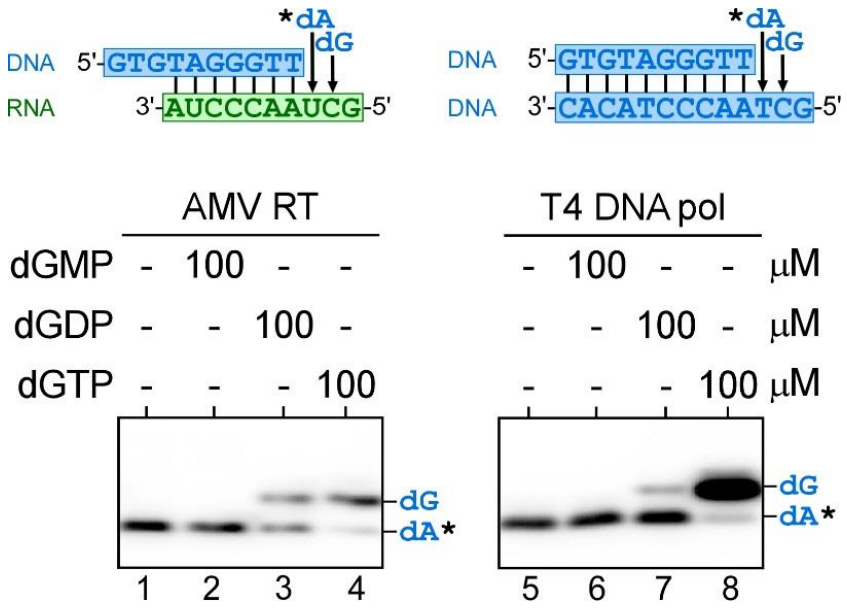

Figure 3.13. Utilization of dGDP as substrate by the AMV RT and T4 DNA polymerase. Sequences of the DNA/RNA or DNA/DNA hybrid substrates are shown above the gels. The templates of the substrates specify incorporation for a dA and a dG residue. The enzymes were assayed with 0.166 μM ^{32}P-dATP (asterisk) and either dGMP, dGDP or dGTP at 100 μM.

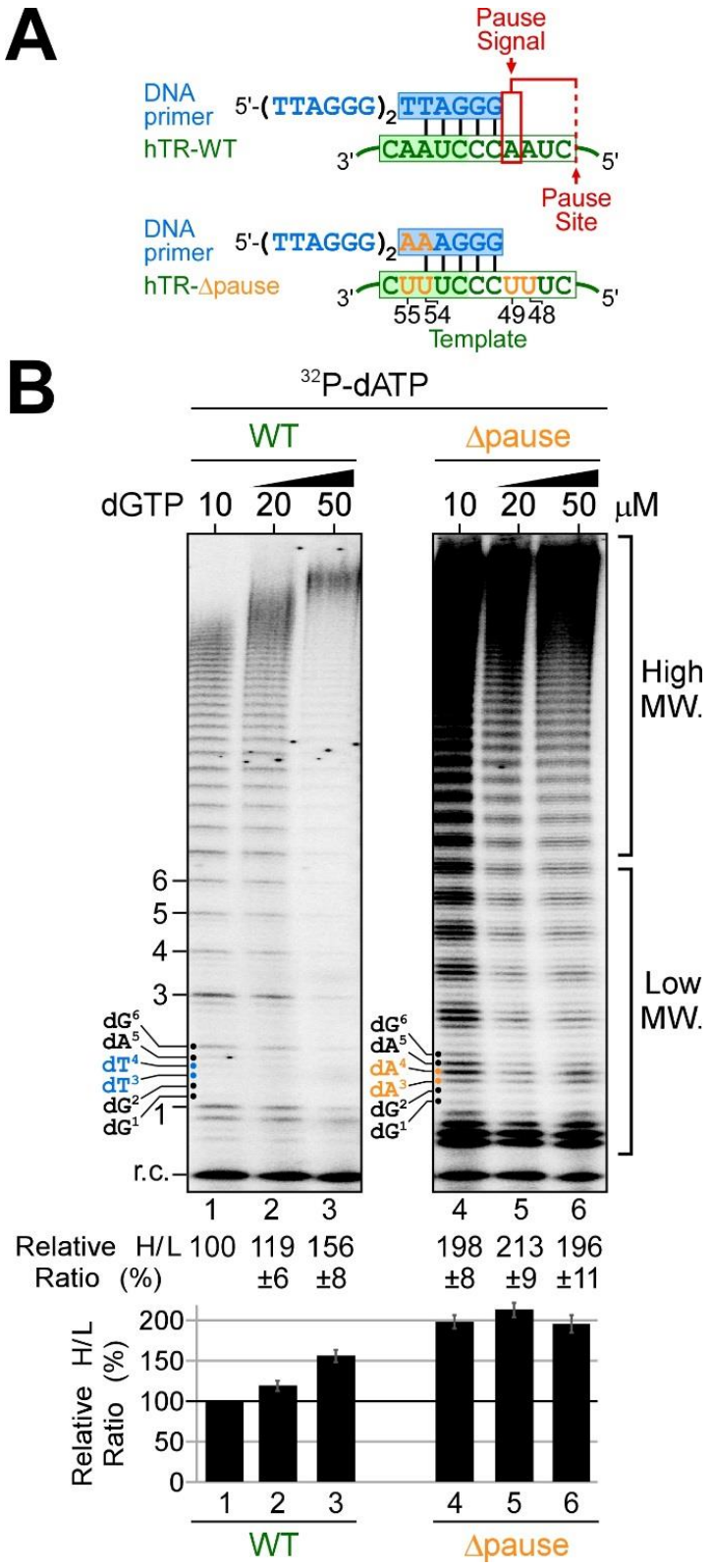
A
Pause Signal
DNA primer
5'-(TTAGGG)2TTAGGG
hTR-WT
3'
CAAUCCCAAUC
5'
Pause Site
DNA primer
5'-(TTAGGG)2AAAGGG
hTR-Δpause
3'
CUUUCCCUUUC
5'
55 54 49 48
Template
B
32P-dATP
WT
Δpause
dGTP 10 20 50
10 20 50 μM
High MW.
Low MW.
6
5
4
3
1
r.c.
dG6
dA5
dT4
dT3
dG2
dG1
dA4
dA3
1 2 3 4 5 6
Relative H/L Ratio (%)
100
119 ±6
156 ±8
198 ±8
213 ±9
196 ±11
200
150
100
50
0
WT
Δpause

Figure 3.14. Effects of pause signal removal on telomerase repeat addition. (A) Schematic of wild-type and hTR Δpause template mutant telomerase with corresponding DNA primers. The hTR Δpause template mutant harbors rA-to-rU mutations (orange) at four residues: 48, 49, 54, and 55 to eliminate the template-embedded pause signal (red box). (B) Direct primer extension assays for the telomerase Δpause template mutant. Wild-type and mutant telomerases were reconstituted *in vivo* and the immuno-purified enzymes were assayed in the presence of 0.165 μM ^{32}P-dATP, 10 μM dATP as well as either 10, 20 or 50 μM of dGTP. Relative repeat addition activity was presented as the ratio of the intensity of high over low M.W. DNA products generated in each reaction normalized to the wild-type enzyme reaction with 10 μM dGTP. A bar graph of the relative ratio of high/low M.W. DNA products are shown below the gel. Standard error of the mean was determined from three independent replicates.

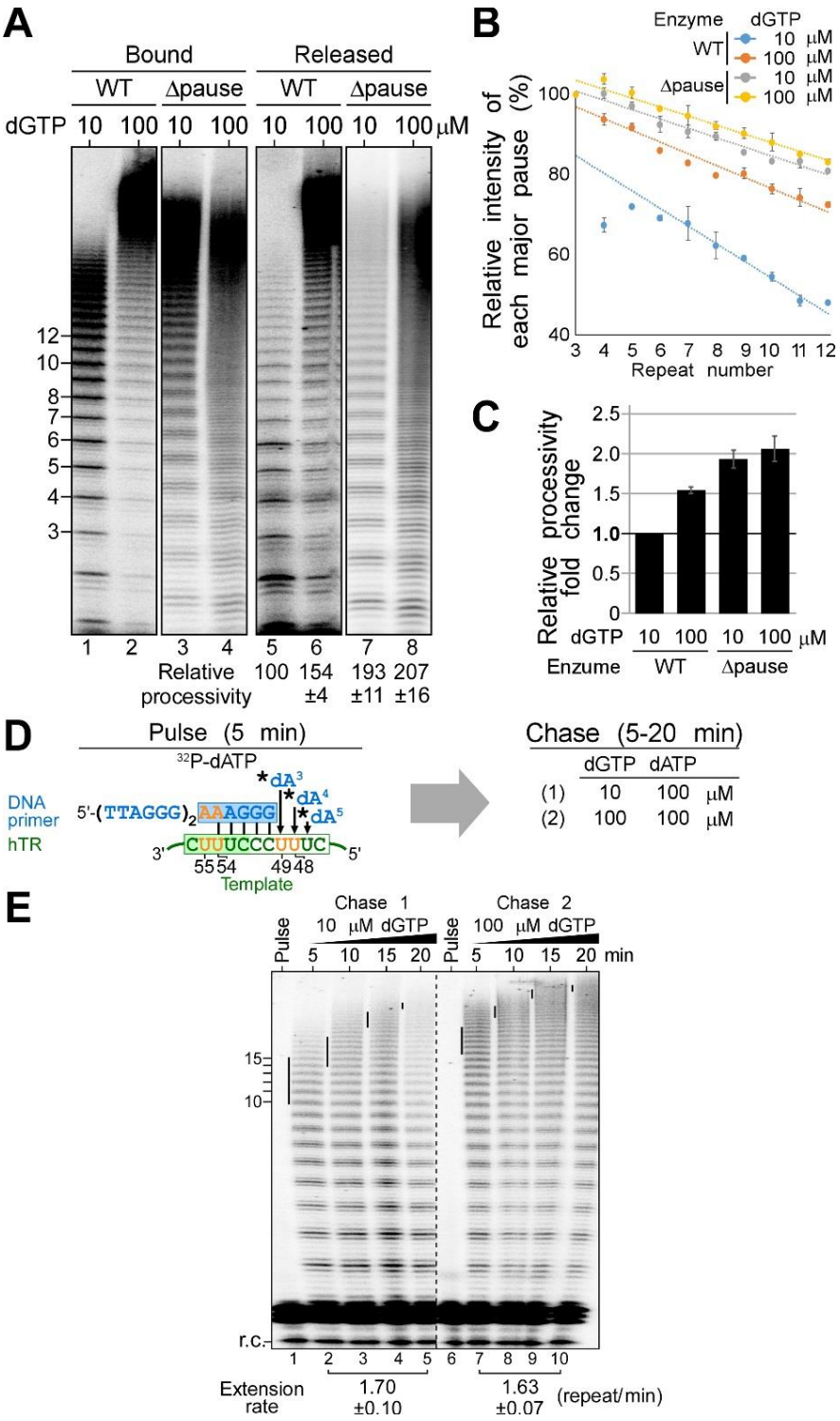
A
Bound
Released
WT
Δpause
WT
Δpause
dGTP 10 100 10 100 10 100 10 100 μM
12
10
8
7
6
5
4
3
1 2 3 4 5 6 7 8
Relative processivity 100 154 ±4 193 ±11 207 ±16
B
Enzyme dGTP
WT 10 μM
100 μM
Δpause 10 μM
100 μM
Relative intensity of each major pause (%)
100
80
60
40
3 4 5 6 7 8 9 10 11 12
Repeat number
C
Relative fold change processivity
2.5
2.0
1.5
1.0
0.5
0
dGTP 10 100 10 100 μM
Enzume WT Δpause
D
Pulse (5 min)
32P-dATP
DNA primer
hTR
5'-(TTAGGG)2AAAGGG
*dA3
*dA4
*dA5
3' CUUUCCCUUUC 5'
55 54 49 48
Template
Chase (5-20 min)
dGTP dATP
(1) 10 100 μM
(2) 100 100 μM
E
Chase 1
10 μM dGTP
Chase 2
100 μM dGTP
Pulse
5 10 15 20 min
15
10
r.c.
1 2 3 4 5 6 7 8 9 10
Extension rate
1.70 ±0.10
1.63 ±0.07
(repeat/min)

Figure 3.15. Effects of dGTP on repeat addition processivity and rate of the hTR-Δpause mutant telomerase. (A) Lack of stimulation of repeat addition processivity with dGTP for the telomerase mutant hTR-Δpause. *In vivo* reconstituted telomerase enzyme was assayed by the product release analysis in the presence of 0.165 µM ^{32}P-dATP, 10 µM dATP as well as either 10 or 100 µM of dGTP. The enzyme-bound and released DNA products were separated and individually analyzed. (B) Quantitation of repeat addition processivity. The intensities of the released DNA products with 3-12 repeats added were quantitated and normalized to the intensity of the product with 3 repeats added. The relative intensities of major bands were plotted against the number of repeats added to determine the slopes that correspond to the relative processivity from each reaction. (C) Relative repeat addition processivity under different nucleotide concentrations. A bar graph indicates the fold change of the relative repeat addition processivity under either 10 or 100 µM of dGTP for wild-type and the hTR-Δpause mutant. The error bars represent standard error of the mean determined from two independent replicates. (D) Schematic of the pulse-chase time course analysis for the telomerase mutant hTR-51U. In the pulse reaction, the DNA primer (TTAGGG)2AAAGGG was labeled with 0.165 µM ^{32}P-dATP (asterisk) by the telomerase hTR-Δpause enzyme. During the chase reaction, the enzyme-bound radiolabeled DNA primer was extended processively with telomeric repeats under 100 µM cold dATP as well as either 10 or 100 µM dGTP for 5, 10, 15 or 20 mins. (E) Repeat addition rate measured by the pulse-chase time course analysis under differing nucleotide concentrations. A radiolabeled DNA recovery control (r.c.) was added before product purification and precipitation. The vertical lines on the gel indicate the major bands of telomere products synthesized during the chase reactions. Repeat addition rates are expressed as repeats per minute and indicated below the gel. The standard error of the mean was determined from two independent replicates.

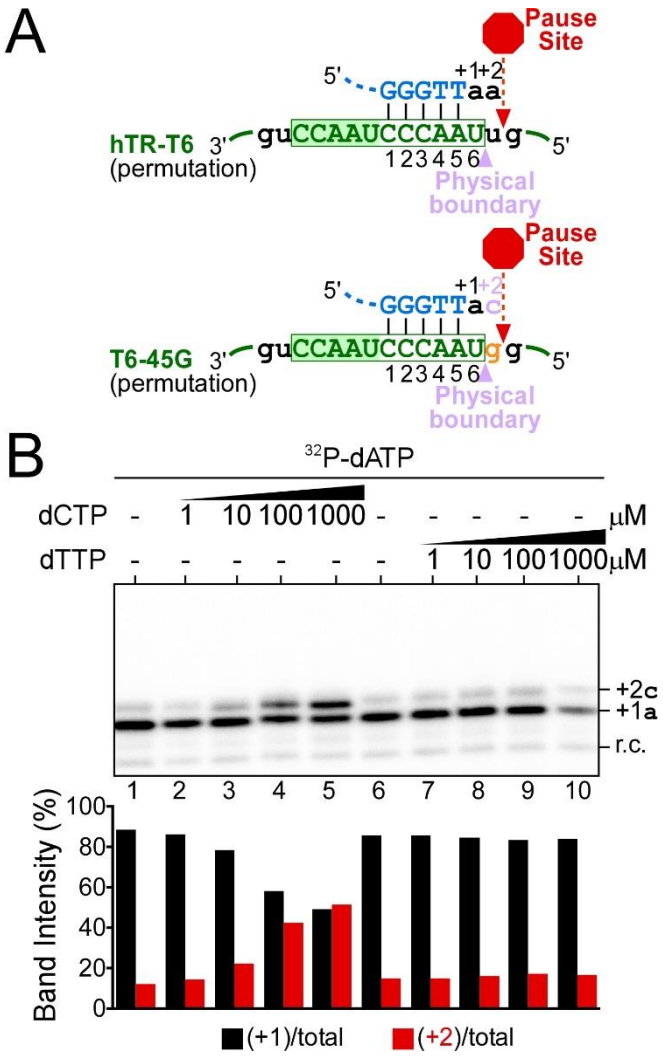

Figure 3.16. The template immediately-adjacent non-telomeric-encoding nucleotide is accessible at the end of telomeric DNA repeat synthesis. (A) Schematic of hTR-T6 template permutation shifting the pause site (red hexagon) one nucleotide after the physical template boundary (violet triangle). Within the hTR-T6-45G template mutant, the template immediately-adjacent non-telomeric-encoding nucleotide at the 5'-end of the template is mutated from an rU to an rG (orange lowercase) to monitor for template bypass in the presence of dCTP in the reaction. (B) Direct activity assay with *in vivo* reconstituted hTR-T6-45G telomerase in the presence of ^{32}P-dATP with a range of dCTP concentrations or as a control for mis-incorporation or terminal transferase activity a range of dTTP concentrations. Quantitation of band intensity before (+1, black) and after (+2, red) the physical template boundary over total activity.

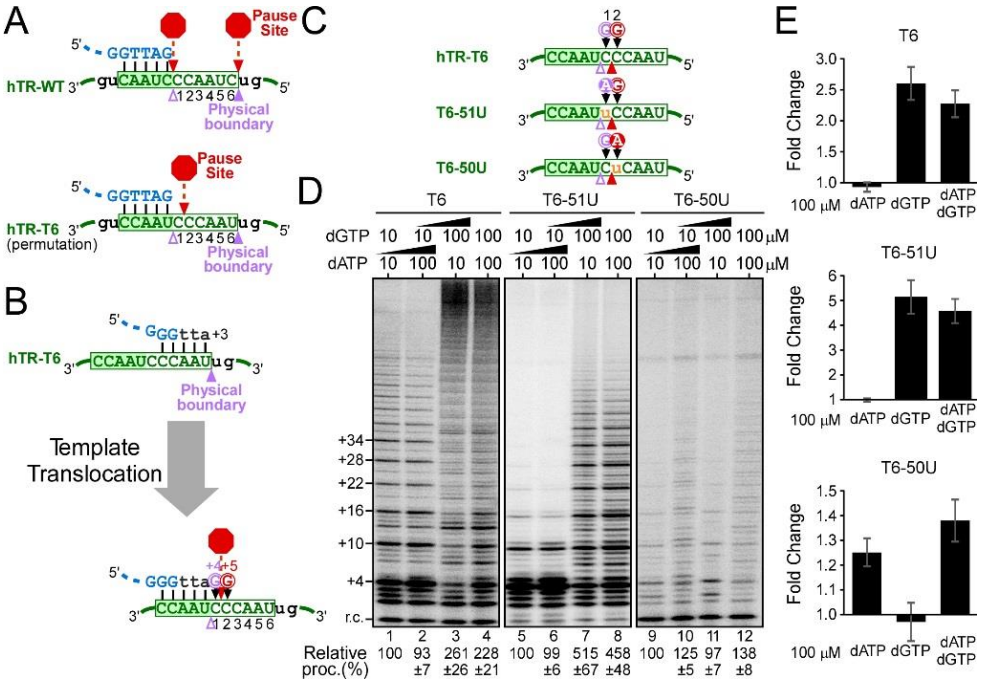
A
Pause Site
5′ GGTTAG
hTR-WT 3′ guCAAUCCCAAUCug 5′
Δ123456
Physical boundary
Pause Site
5′ GGTTAG
hTR-T6 3′ guCCAAUCCCAAUug 5′
(permutation)
Δ123456
Physical boundary
B
5′ GGGtta+3
hTR-T6 3′ CCAAUCCCAAUug 3′
Physical boundary
Template Translocation
+4+5
5′ GGGttaCG
3′ CCAAUCCCAAUug 3′
Δ123456
C
12
hTR-T6 3′ CCAAUCCCAAU 5′
T6-51U 3′ CCAAUuCCAAU 5′
T6-50U 3′ CCAAUCuCAAU 5′
D
T6
T6-51U
T6-50U
dGTP 10 10 100 100 10 10 100 100 10 10 100 100 μM
dATP 10 100 10 100 10 100 10 100 10 100 10 100 μM
+34
+28
+22
+16
+10
+4
r.c.
1 2 3 4 5 6 7 8 9 10 11 12
Relative proc.(%) 100 93 ±7 261 ±26 228 ±21 100 99 ±6 515 ±67 458 ±48 100 125 ±5 97 ±7 138 ±8
E
T6
Fold Change
3.0
2.5
2.0
1.5
1.0
100 μM dATP dGTP dATP dGTP
T6-51U
Fold Change
6
5
4
3
2
1
100 μM dATP dGTP dATP dGTP
T6-50U
Fold Change
1.5
1.4
1.3
1.2
1.1
1.0
100 μM dATP dGTP dATP dGTP

Figure 3.17. The sequence-defined pause, and not template translocation process, underlies dGTP-specific processivity stimulation. (A) Uncoupling the sequence-defined pause site from the physical boundary. In the wild-type hTR template, the pre-translocation pause site (red hexagon) and physical boundary boundary (violet triangle) coincide at the end of the template. The post-translocation pause site (red hexagon) coincides with the position of first nucleotide incorporation. The sequence permutation in the hTR-T6 template mutant shifted the pause site one nucleotide downstream from the physical boundary and the position of first nucleotide incorporation. (B) Schematic of the telomerase catalytic cycle with the hTR-T6 template mutant. After reaching the physical template boundary, the hTR-T6 mutant undergoes template translocation and incorporates a dG residue (+4, violet) as the first nucleotide, followed by a second dG residue (+5, red) at the shifted pause site. (C) Schematic of hTR-T6 template mutations, T6-U51 and -U50, that alter the first or second nucleotide incorporated from dG to dA (shaded) immediately following template translocation. The mutated residues in the hTR-T6 template are indicated (orange lowercase). The first (violet) and second (red) residues incorporated following template translocation are also denoted. (D) Altering the nucleotide incorporated following the pause signal—and not the template translocation—shifts the nucleotide-specific processivity stimulation. Direct activity assay of the hTR-T6 telomerase template mutants. The assays were performed in the presence of ^{32}P-dTTP with either 10 or 100 μM dGTP and dATP. An end-labeled DNA recovery control (r.c.) was added before product purification and precipitation. Relative processivity is shown below the gel. (E) The bar graph of fold change compared to the low-nucleotide-concentration reaction. The error bars represent standard error of the mean determined from three replicates.

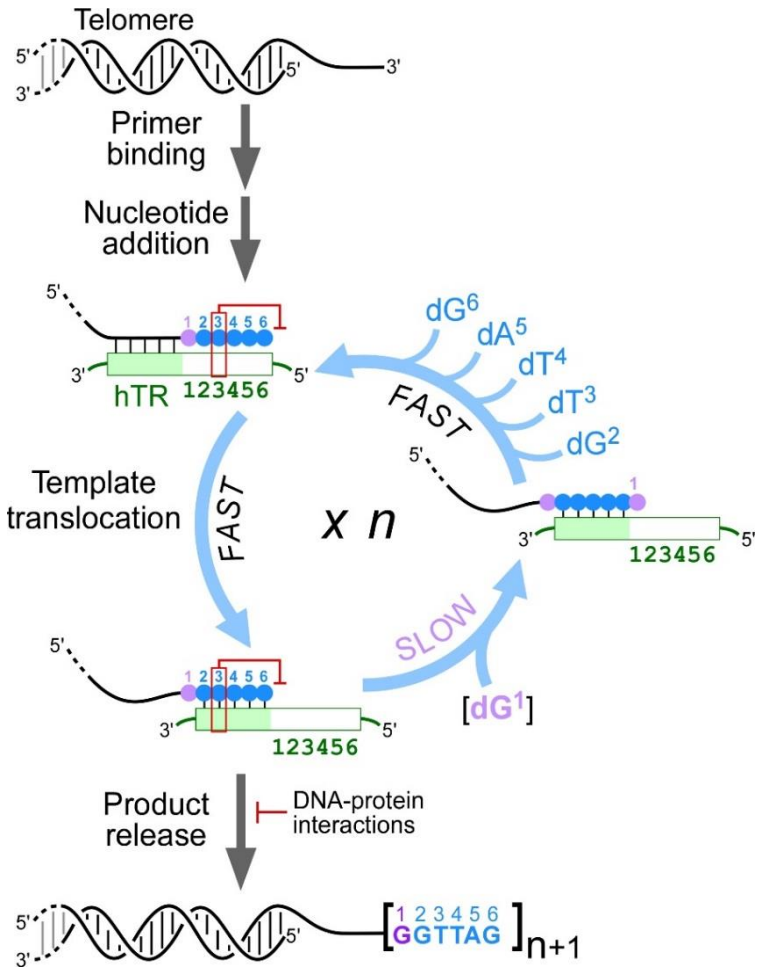
Telomere
5'
3'
3'
5'
Primer binding
Nucleotide addition
5'
1 2 3 4 5 6
3'
5'
hTR 123456
dG6
dA5
dT4
dT3
dG2
FAST
5'
1
3'
5'
123456
Template translocation
FAST
x n
5'
1 2 3 4 5 6
3'
5'
123456
SLOW
[dG1]
Product release
DNA-protein interactions
5'
3'
5'
1 2 3 4 5 6
GGTTAG
n+1

Figure 3.18. A working model of the telomerase catalytic cycle. Following telomerase binding the 3'-end of the telomere, nucleotide addition of six residues (violet and blue circles) proceeds to the end of the template and is arrested by the pause signal (red box) at the pause site. A fast template translocation process regenerates the template by realigning the template relative to the 3'-end of the DNA primer. Progression to the next catalytic cycle is impeded by the still active pause signal from the DNA/RNA hybrid, causing a slow dG^1 residue incorporation (violet) at the pause site. Failure to incorporate the dG^1 residue promotes product release, which is counteracted by DNA-protein interactions through the TERT anchor sites and telomerase accessory POT1-TPP1 protein complex. Successful dG^1 residue incorporation is proceeded by the rapid incorporation of five additional residues, dG^2, dT^3, dT^4, dA^5, and dG^6 (blue), completing a telomerase catalytic cycle. The number of repeats added corresponds to the number of catalytic cycles completed before complete disassociation of the telomeric DNA from the telomerase enzyme. Increasing the dGTP concentration increases the rate of the slow dG^1 residue incorporation, which increases telomerase repeat addition processivity and rate.

CHAPTER 4

THE MOLECULAR MECHANISM UNDERLYING THE TELOMERASE MOTIF T K570A MUTATION

4.1 Abstract

Linear chromosomal ends in eukaryotes are protected by telomeres, a nucleoprotein structure that contains repetitive telomeric DNA sequences and associated proteins. Telomerase is an RNA-dependent DNA polymerase that adds telomeric DNA repeats to the 3' ends of chromosomes to offset the loss of terminal DNA repeats during DNA replication. It consists of two core components: a telomerase reverse transcriptase (TERT) and a telomerase RNA (TR). Even though the crystal structures of TERT and TR domains have provided important structural information a co-crystal ribonucleoprotein structure is lacking still. The telomerase RNA binding domain (TRBD) of TERT contains a unique motif T, which is conserved universally among TERTs, but not in conventional reverse transcriptase. Motif T folds into a β-loop structure and is located facing the binding pocket of the substrate DNA and template RNA duplex based on the crystal structure of *Tribolium* TERT. Comprehensive alanine screening mutagenesis identified residue K570 in motif T crucial for telomerase enzymatic function. The positive charge as well as the position of this residue is indispensable for nucleotide addition in human telomerase. We also demonstrated that the K570A mutant shows binding defects with the telomeric DNA substrate as well as DNA/RNA duplex in the active site, thus increasing the apparent K_m^{app} of the incorporation of nucleotide for DNA synthesis. The results from these experiments will add to our current understanding of TERT structure/function relationships and the molecular mechanism of telomerase action.

4.2 Introduction

Telomerase is a unique reverse transcriptase crucial for the de novo synthesis of telomeric DNA repeats onto chromosomal termini to counter progressive telomere shortening resulting from incomplete end replication (Ohki et al, 2001). Highly proliferative cells, including germline and stem cells, require telomerase for proper telomere length maintenance (Shawi & Autexier, 2008). Telomerase is undetectable in human somatic cells, but up-regulated in nearly 90% of cancer cells (Shay & Keith, 2008). Some inherited human diseases, such as aplastic anemia, dyskeratosis congenita and idiopathic pulmonary fibrosis, have been linked to telomerase gene mutations that result in telomere shortening and growth defects in stem cells (Armanios, 2009; Armanios et al, 2007). The telomerase core enzyme is minimally composed of the catalytic telomerase reverse transcriptase (TERT) and the integral telomerase RNA (TR) (Collins, 2006). TR varies greatly in size between organisms ranging from 159 nt to over 2000 nt (Qi et al, 2013). In contrast, TERT is highly conserved among different species. The TERT protein contains four structural domains, including the TERT essential N-terminal domain (TEN), the Telomerase RNA binding domain (TRBD), the reverse transcriptase domain (RT) and the C-terminal extension (CTE). Due to the low abundance of telomerase in human cells and difficulties in over-expression of soluble full length TERT protein, structural determination of the telomerase ribonucleoprotein complex has been limited to individual domains of TERT and TR (Miracco et al, 2014). The recently solved crystal structure of the TRBD from *Takifugu rubripes* and *Oryzias latipes* indicate that the structures have mainly alpha helical topology, similar to *Tribolium castaneum* TRBD and *Tetrahymena thermophila* TRBD (Harkisheimer et al, 2013; Huang et al,

2014; Mitchell et al, 2010; Rouda & Skordalakes, 2007). TRBD contains an indentation on its surface formed by two conserved motifs, motif T and CP (Harkisheimer et al, 2013; Huang et al, 2014).

The motif T, which lies within the telomerase RNA binding domain of hTERT was recognized as being highly conserved and telomerase specific. Based on the crystal structure of *Tribolium castaneum* TERT (tcTERT) complexed with a synthetic RNA/DNA duplex showed that the 5' end of the RNA template is located at the entry site of the T-CP pocket (Mitchell et al, 2010). The motif T is the first non-RT motif shown to be necessary for telomerase activity (Nakamura et al, 1997). The T motif is encoded by amino acids 547–594 in human, within which lies a near-universally conserved sequence motif, FYXTE. Mutagenesis of residues within this motif results in varying degrees of reduced telomerase activity, as well as significantly increased telomere extension rates, without affecting either hTR binding or enzyme processivity (Drosopoulos & Prasad, 2010). Use of the telomerase repeat amplification protocol (TRAP) to functionally analyze the mutated residue (K570N) demonstrated a drastic reduction in telomerase activity, correlating with severely shortened telomere length (Xin et al, 2007). Two motif T variants, T567M and K570N, identified in dyskeratosis congenita patients have been demonstrated to reduce telomerase repeat addition processivity (Gramatges et al, 2013).

Recently it was found that telomerase with the T-motif loop substitution K570A failed to protect a substantial amount of product telomeric DNA from exonucleases. It was proposed the T-motif loop cooperates with the thumb loop and thumb helix to contribute to a ssDNA retention surface (SRS) that overlaps the binding surface of the DNA strand of template duplex (Wu et al, 2017). Our data

support the biological importance of K570 residue for the efficiency of nucleotide addition by binding to DNA/RNA duplex close to the active site, which is necessary for the maintenance of telomeres. The aim of this study is to understand the structure/function relationship of how telomerase handles the substrate and how it affects telomerase repeat addition processivity. In addition, a cellular limit on active telomerase level appears necessary for normal telomere length homeostasis. Elucidation of telomerase function could potentially facilitate the development of effective treatments for telomerase-related diseases.

4.3 Material and Methods

Plasmid construction and mutagenesis.

Specific mutations in the human TERT genes were introduced into the pNFLAG-hTERT by site directed mutagenesis using overlapping PCR strategy (Ge & Rudolph, 1997). Intended mutations were confirmed by sequencing.

In vitro reconstitution of human telomerase.

Human TERT protein was expressed in rabbit reticulocyte lysate (RRL) from the pNFLAG-hTERT plasmid DNA using the TnT T7 Quick Coupled transcription/translation kit (Promega) following manufacturer's instructions (Xie et al, 2010). For quantitation, hTERT was synthesized in the presence of ^{35}S-Methionine (>1000 Ci/mmol, 10.2 mCi/ml, Perkin-Elmer) and analyzed by SDS–PAGE. The hTR pseudoknot (residues 32–195) and CR4/5 (residues 239–328) fragments were *in vitro* transcribed, gel purified, and assembled together with the TERT protein in RRL for 30 min at 30°C at a final concentration of 1.0 μM (Brown et al, 2014; Qi et al, 2012). For template free human telomerase, the hTR pseudoknot (residues 64–184) and CR4/5 (residues 239–328) fragments were *in vitro* transcribed, gel purified, and

assembled together with the TERT protein in RRL for 30 min at 30°C at a final concentration of 1.0 μM (Brown et al, 2014; Qi et al, 2012).

In vivo reconstitution of human telomerase.

HEK 293FT cells were grown in DMEM medium (Corning) supplemented with 10% FBS (Atlanta Biological), 1x Penicillin-Streptomycin-Amphotericin B mix (Lonza) and 5% CO_2 at 37°C to 80–90% confluency. Cells in a 6-well plate were transfected with 0.4 μg of pcDNA-nFLAG-hTERT wild type or K570A mutant, 1.6 μg of pBS-U1-hTR wildtype or template mutants using 6 μL of Fugene HD transfection reagent (Promega) following manufacturer's instruction. Cells were harvested 48 hours post transfection, homogenized in HEPES lysis buffer (20 mM HEPES-KOH, pH 7.9, 400 mM NaCl, 0.2 mM EGTA, 2 mM $MgCl_2$, 10% glycerol, 5 mM β-mercaptoethanol and 1x complete protease inhibitor cocktail (Roche), 1 mM PMSF), incubated on ice for 30 min and the lysate clarified by centrifugation. Two hundred microliters of cell lysate were combined with 30 μL Anti-FLAG® M2 Beads (Sigma) pre-washed with 1X TBS buffer (50 mM Tris-HCl, pH 7.4 and 150 mM NaCl) and incubated at 4°C with gentle rotation for 1 hour. The beads were washed three times with 100 μL of 1x TBS buffer and once with 50 μL 1x telomerase reaction buffer (50 mM Tris-HCl, pH 7.5, 3 mM $MgCl_2$, 50 mM KCl, 2 mM DTT and 1 mM spermidine), followed by activity assay.

Telomerase direct primer-extension assay.

Two microliters *in vitro* reconstituted telomerase enzyme or 20 μL of immuno-purified *in vivo* reconstituted telomerase enzyme on beads was assayed in a 10 μL reaction containing 1x telomerase reaction buffer, 1 μM DNA primer, specified dNTPs and 0.165 μM of the denoted α-^{32}P-dNTP. Reactions were incubated at 30°C

for 60 min and terminated by phenol/chloroform extraction, followed by ethanol precipitation. The DNA products were resolved on a 10% (wt/vol) polyacrylamide/8 M Urea denaturing gel, dried, exposed to a phosphorstorage screen and imaged on a Bio-Rad FX-Pro phosphorimager.

K_M^{app} measurement using native telomerase.

Twenty microliters of immuno-purified *in vivo* reconstituted telomerase enzyme on beads was assayed in a 10 μL reaction containing 1x telomerase reaction buffer, 1 μM DNA primer, specified dNTP or ddNTPs and 0.165 μM of the denoted α-^{32}P-dNTP. For measuring the K_M^{app} values, the activity assays were performed with deoxynucleotide or dideoxynucleotide concentrations varying from 0 to 200 μM, or up to 1 mM for high K_M measurement. Reactions were incubated at 30°C for 60 min and terminated by phenol/chloroform extraction, followed by ethanol precipitation. The DNA products were resolved on a 10% (wt/vol) polyacrylamide/8 M urea denaturing gel, dried, exposed to a phosphorstorage screen and imaged on a Bio-Rad FX-Pro phosphorimager. The intensities of specific products were normalized to the total product intensity and plotted against the nucleotide concentrations with the Michaelis-Menten equation, Y=Vmax*X/(Km+X), used to fit the nonlinear curve to determine the K_M^{app} (Prism 5, Graphpad Software).

Duplex K_M measurement using TF telomerase.

One microliter of RRL reconstituted TF telomerase enzyme was assayed in a 10 μL reaction containing 1X telomerase reaction buffer, specified dNTPs and 0.165 μM of the denoted α-^{32}P-dNTP. For measuring the K_M values of the duplex, the activity assays were performed with DNA/RNA duplex concentrations varying from 0 to 200 μM. Reactions were incubated at 30°C for 60 min and terminated by

phenol/chloroform extraction, followed by ethanol precipitation. The DNA products were resolved on a 15% (wt/vol) polyacrylamide/8 M urea denaturing gel, dried, exposed to a phosphorstorage screen and imaged on a Bio-Rad FX-Pro phosphorimager. The quantification is same as described above.

N. crassa telomerase and T. brucei in vitro reconstitution and telomerase activity assay.

The *N. crassa* and *T. brucei* telomerases were *in vitro* reconstituted as previously described (Bley et al, 2011; Podlevsky et al, 2016; Qi et al, 2013). Recombinant *nc*TERT and *tbr*TERT protein were synthesized from pCITE-NFLAG-*N.crassa* and pCITE-NFLAG-*T.brucei* in a 10 µL reaction of TnT Quick-coupled transcription/translation kit (Promega) at 30°C for 60 min, following the manufacturer's instructions. *N. crassa* TERT was assembled with *N. crassa* TR RNA fragments T/PK (nt 225- 1515, Δ463-1288/GGAC, Δ256-433/GAAA) and TWJ (nt 1813-1877); and *T.brucei* TERT was assembled with *T.brucei* TR RNA fragments template core (nt 279-414) and eCR4/5 (nt 781-819). RNA fragments were *in vitro* transcribed, gel purified, and added at a final concentration of 1 µM to assemble with *tbr*TERT in RRL.

The telomerase assay was carried out with 2 µl of *in vitro* reconstituted telomerase in a 10 µl of reaction. For *N. crassa* and *T.brucei* telomerase assays, the reaction contained 1x reaction buffer (50 mM Tris- HCl (pH 8.0), 0.5 mM $MgCl_2$, 1 mM spermidine, 2 mM DTT), 100 µM dATP, 1 µM dTTP, 5 µM dGTP, 0.165 µM α-^{32}P-dGTP (3000 Ci/mmol, 10 mCi/ml, PerkinElmer) and 1 µM DNA primer 5'-$(TTAGGG)_3$-3'. The reactions were incubated at 30°C for 60 min and terminated by phenol/chloroform extraction, followed by ethanol precipitation. Telomerase extended

products were resolved on a denaturing 8M urea/10% polyacrylamide gel. The dried gel was exposed to a phosphor storage screen and analyzed with a Bio-Rad FX Pro Molecular Imager.

K_{off} measurements using native telomerase.

Twenty microliters of immuno-purified *in vivo* reconstituted telomerase enzyme on beads was assayed in an 8 µL reaction containing 1x telomerase reaction buffer, 0.1 µM DNA primer $(TAGGGT)_3$ for 10 min at 30 °C. Then addition of the 1 µL $(TAGGGT)_4$ challenge primer (10 µM). At times denoted added to 1 µL 0.165 µM α-^{32}P-dTTP (3000 Ci/mmol, 10 mCi/ml, PerkinElmer) and labeled for 10 min at 30 °C. Reactions were terminated by phenol/chloroform extraction, followed by ethanol precipitation. The DNA products were resolved on a 10% (wt/vol) polyacrylamide/8 M urea denaturing gel, dried, exposed to a phosphorstorage screen and imaged on a Bio-Rad FX-Pro phosphorimager. The intensities of initial primer products were normalized to the total product intensity. The rate constants were determined by fitting the data to the equation $y=Aexp^{(-kt)}$ (where A represents the amount of primer in complex at time zero, k is the rate constant, and t is the time in minutes), using the Prism software package (Prism 5, Graphpad Software).

4.4 Results

Alanine mutagenesis of motif T residue K570 displays defects in telomerase function.

The telomerase specific motif T, located in the TRBD domain of TERT was previously found to contain a universally conserved sequence "FYXTE" within a β-loop structure in many species (Figure 4.1A). Two disease mutations were discovered in the motif T region of human TRBD: T567M and K570N (Gramatges et al, 2013). The defects of these mutants were consistent with previous results that have shown a

conserved region inside motif T affect repeat addition rate (Drosopoulos & Prasad, 2010). To experimentally determine the function of motif T, comprehensive alanine screening mutagenesis on each residue of motif T was performed. Coding sequence mutations were created by overlap extension PCR (from residue 561- 577). These motif T mutants were expressed and reconstituted in RRL with *in vitro* transcribed hTR for activity and processivity assays. The activity of each mutant was normalized by ^{35}S-labeled hTERTs. While various mutations showed different levels of telomerase activity, the K570A mutant, like the K570N disease mutant previously described, had dramatically decreased repeat addition processivity. (Figure 4.1B) These differences could not be accounted for by differences in hTERT expression levels. A similar processivity defect of K570A mutant was observed using telomerase reconstituted *in vivo* (Figure 4.2). The telomeric DNA substrate can be extended to reach the end of the template (+4) by K570A mutant, but the activity significantly decreases after the first repeat. The intermediate bands before reaching the end of the template (+4) means more product release during the nucleotide addition. It suggests that K570 residue in hTERT plays an important role for telomerase catalytic function. *Different substitutions or position of K570 affects telomerase activity and processivity.*

To further investigate the possible roles of the motif T regulate telomerase enzymatic function, based on a homology threading model made of *Takifugu rubripes* TERT using *Tribolium* TERT DNA/RNA duplex co-crystal and *Takifugu rubripes* TRBD crystal structure. Motif T is located close to a substrate duplex in the active site (Harkisheimer et al, 2013). The position of motif T in this model makes it possible to directly interact with the duplex in the active site or with the single

stranded DNA to facilitate template translocation. It is also easy to imagine that motif T may interact with the 5' region of the single stranded RNA template. According to the threading model of hTRBD through *tr*TRBD with DNA/RNA duplex, K570 is located in the middle of the β-loop and is very close to the 3' end of the DNA substrate or 5' end of the RNA template. (Figure 4.3A)

To investigate a possible role of K570 interacting with DNA/RNA duplex within the active site, we created various substitutions of K570 and assayed telomerase function. The mutants were reconstituted in RRL with hTR for activity assays and normalized by ^{35}S-labeled hTERTs. The wild type hTERT as well as mutants of flanking residues of K570 was used as a control. The substitutions of K570 to neutral residues (glutamine or asparagine) showed the same phenomenon as K570A, which decreased processivity significantly to only completing one repeat addition (+4). (Figure 4.3B) The K570D and K570E mutants showed worst defects in nucleotide addition with neither of them unable to reach the end of the template. Intriguingly, K570R mutant showed nearly native telomerase activity. The arginine is the only substitution which can rescue the telomerase processivity while histidine failed (Figure 4.3B). Both arginine and lysine are positively charged amino acids with a linear side chain, this suggests that the positively charged linear side chain of this residue is required for telomerase activity, which may interact with the negatively charged DNA/RNA duplex in the active site. Additionally, the insertion or deletion of residues flanking K570, drastically reduced telomerase processivity similar to the K570A mutant (Figure 4.3B). This indicates that the position of K570 residue is vital for telomerase activity. Altered position of K570 residue could disrupt the local structure near the active site, thus hindering the interaction of K570 residue with the

hybrid duplex. Furthermore, motif T mutants in *N. crassa* and *T. brucei* were tested via alanine screening mutagenesis as well. Residues corresponding to K570 (hTERT) based on amino acid sequence alignments, also showed processivity defects (Figure 4.4). This indicates evolutionarily conservation of the charge and position of the residue is critical for telomerase enzymatic function.

K570A mutants are defective in utilizing short DNA primers.

The K570A mutant that disrupted telomerase processivity, presumably affected either the template realignment or product release during template translocation. Collectively, the information from the crystal structure and functional assays suggest that K570 may interact with DNA/RNA duplex close to the catalytic active site to regulate template translocation. To test this, various short primers that can base pair with RNA template, but leave no single stranded overhang for the TEN domain anchor site to bind have been analyzed. This assay eliminates discounts the effect of the TEN domain on substrate binding (Lue et al, 2003). To study the specific function of K570, other TERT mutants were used as controls: mutations N95A in the TEN domain and L980A in CTE have been previously shown to reduce telomerase processivity (Huard et al, 2003; Lue et al, 2003; Moriarty et al, 2005). Mutations D682A and D684A in motif 3 have been demonstrated to respectively decrease and increase processivity by interacting with DNA/RNA duplex (Xie et al, 2010). Upon feeding a short 8 mer telomeric DNA substrate, the K570A mutant completely fails to synthesize a single repeat (Figure 4.5). While wild type telomerase can utilize all primers and exhibit similar activity. The K570A as well as D682A and L980A mutations cannot use the short primer as substrate. D682A and L980A have been shown to compromise the ability of TERT in promoting DNA/RNA duplex formation

or positioning the duplex to the active site for the first repeat synthesis. While the N95A mutant, having low processivity, can extend the short primer efficiently shows that TEN domain does not play a role in facilitating primer/template realignment but in preventing product release during template translocation. This indicates K570 may act together with any other residues of motif 3 and CTE to interact with the DNA/RNA duplex for template translocation.

The K570A mutants retain stimulation by elevated dGTP concentration

It has been previously reported that elevated dGTP concentrations positively correlate with a repeat addition processivity for human telomerase. To investigate whether K570A mutant telomerase activity could be affected by nucleotide concentration, I performed telomerase primer extension assays in the presence of ^{32}P-dGTP with increasing concentrations (10, 50 and 200 μM) of the individual dTTP or dATP nucleotides or unlabeled dGTP (5, 10 and 20 μM) (Figure 4.6). Since K570A mutant is not processive, we use the intensity of product released after second repeat (+10) / intensity of the product released after the first repeat (+4) to evaluate the repeat addition efficiency. In the wild type human telomerase, it is consistent with previous results that the elevation of dGTP concentration increased the band intensity ratio +10: +4, while the concentration of dATP and dTTP had no significant effect on repeat addition efficiency. Meanwhile, elevated dGTP concentrations at 10 and 20 μM significantly increased the ratio of +10 over +4 of K570A mutant by approximately 2 and 3 folds compared to 5 μM dGTP. This indicates that the motif T mutant, K570A, does not abrogate the stimulation in processive repeat synthesis with elevated dGTP concentration.

Position specific deficiency of K570A mutant for nucleotide incorporation.

During the extension of telomeric DNA substrate, the reaction with *in vivo* reconstituted K570A mutant showed much stronger intermediate bands compared to wild type before reaching the end of the template (Figure 4.7). This indicates that the mutant may have nucleotide incorporation defects. To investigate the nucleotide addition efficiency of K570A mutants we measured the apparent K_M (K_M^{app}) value of nucleotide incorporation. I reconstituted human telomerases *in vivo* in human HEK293 cells, following by assays on immuno-purified enzyme with $(TAGGGT)_3$ DNA primers in the presence of ^{32}P-dTTP and titration of dATP. K_M^{app} for dATP incorporation was approximately 0.5 μM for native wild type enzyme, compared to the remarkably high 8.5 μM in K570A mutant (Figure 4.8A). The extra band shown from wild type telomerase at high concentration of the dATP could be due to mis-incorporation or terminal transferase activity (Lue et al, 2005) (Figure 4.9). To eliminate the extra-band and test the K_M^{app} at other positions, permutated telomeric DNA primers are employed in the presence of varying ^{32}P-dNTP and titration of ddNTP for K_M^{app} measurement. K_M^{app} for ddATP incorporation was about 0.76 μM for wild type enzyme, compared to 11 μM in K570A mutant (Figure 4.8A). The mutant still has much higher K_M^{app} compared to the wild type enzyme, and both values are close to that of dATP. It suggests that ddNTP could be used to estimate the incorporation nucleotide at other positions of the template, where K_M^{app} measurements with dNTP titration is technically challenging. The result demonstrates that K_M^{app} for ddGTP at the end of the template (hTR 46) is 0.3 μM for the wild type telomerase and 9 μM for K570A. Interestingly, the K_M^{app} for the first dT (hTR 49) is comparable between wild type and mutant enzymes, which is 2.5 μM and 3 μM respectively (Figure 4.8A). However, the hTR 49U mutant shows the same

phenomenon. The K_M^{app} for wild type TERT with hTR 49U mutation is 1.1 μM and 0.7 μM for K570A with hTR 49U mutation (Figure 4.8B). It indicates that K570A mutant has position specific nucleotide incorporation defects, instead of bias on purine over pyrimidine. Particularly, the middle position of the template, the apparent K_M is less affected in the mutant. It suggests that the K570A mutant may play a role for type I template translocation for nucleotide repeat addition when reaching the end of the hTR template by handling DNA/RNA duplex. This is further verified by the comparison of K_M^{app} value between the wild type hTERT and K570A with hTR 46A mutant (Figure 4.8B).

The K570A mutant shows substrate binding affinity deficiency.

It has been shown the motif T mutant K570A failed to protect the DNA substrate from exonuclease digestion (Wu et al, 2017). The defect of binding affinity of K570A to DNA substrate could contribute to the higher K_M^{app} value. To determine the binding affinity, we measured the K_{off} value of telomeric DNA for wild type telomerase and K570A mutant. Initially, a saturating concentration of the 18 mer $(TAGGGT)_3$ was incubated with *in vivo* reconstituted immuno-purified enzymes. After reaching equilibrium, the enzyme-primer complex was challenged with a large excess of a competitive 24 mer $(TAGGGT)_4$ primer, having a different length than the original one. Aliquots were removed at different time points and labeled with ^{32}P-dTTP, which resulted in either the original primer or the competitive primer producing a discrete end-labeled product (Figure 4.10A). The intensity of the lower band (18+1) representing the product of the initial enzyme-primer complex decreases as a function of time. A concomitant increase in the upper band representing the product of the competitive primer can also be observed (Figure 4.10B). The ratio of

product resulting from the initial enzyme-primer complex over total is assigned the value of 100% bound (time zero). Remaining complexes at subsequent times is expressed as a fraction of that initial amount (Figure 4.10C). It is noteworthy that a major increase of the K_{off} value of K570A mutant is observed at 0.23 min^{-1} ($t_{1/2}$ ~3 min) compared with the wild type enzyme which has 0.03 min^{-1} ($t_{1/2}$ ~22 min). This affinity difference may be attributed to its defects in the ability to incorporate incoming nucleotide.

In template free system K570A mutant shows deficiency to use DNA/RNA duplex in the active site.

The active site of telomerase intrinsically binds the DNA/RNA duplex. The binding affinity of DNA/RNA duplex has been shown to correlate with repeat addition processivity and template translocation efficiency. To further study the interaction of K570 residue with DNA/RNA hybrid in active site, we measured the apparent Michaelis constant (K_M) value of the DNA/RNA duplex in the template-free human telomerase system which lacks the template sequence in the hTR component. The wild type human telomerase and K570A mutant were reconstituted in RRL with *in vitro* transcribed template free hTR fragments. The K570A mutant compared to the wild type enzyme showed generally lower activity. The activities were normalized by ^{35}S-labeled hTERTs (Figure 4.11). The mutant had an apparent K_M value of 50 μM, which was considerably higher than the 13 μM for the wild-type enzyme (Figure 4.11). A lower affinity for the hybrid substrate is expected to result in nucleotide addition processivity deficiency. This data is consistent with the K_{off} value of the K570A mutant which shows defects in binding to the DNA substrate in the catalytic site.

4.5 Discussion

Repeat addition processivity is a unique property of telomerase, which requires repetitive regeneration of the short hTR template. The telomerase catalytic-cycle transitions through states with many specializations of substrate handling required for processive repeat synthesis. Specific interactions between hTERT and hTR define the template region, allowing stable active site engagement of the short duplex formed in the realignment region, dissociate duplex at the template 5' end, and retain ssDNA during template translocation. Based on the high-resolution structure of *Tribolium castaneum* TERT bound to a model DNA–RNA duplex (Mitchell et al, 2010), some TERT specific motifs could potentially contact either template strand on hTR or telomeric DNA substrate. Including telomerase specific motif T in TRBD, motif 3 in RT domain, the thumb helix region in CTE and thumb loop linking the RT and CTE domains (Figure 4.12). With mutagenesis studies, substitution of some of residues led to decrease in repeat addition processivity for human telomerase, such as N666A, L681A, G682A, I686A on motif 3 (Xie et al, 2010); L859, L980A, K981A on CTE (Huard et al, 2003); and K570A on motif T. It has also been shown TERT-mutant enzymes with substitutions in the T-motif loop, thumb loop, and thumb helix all failed to unpair protected product from the template 3' end (Wu et al, 2017). The T-motif loop, thumb loop, and thumb helix are deep within the active-site cleft where they could potentially discriminate the sequence of the final base-pairs of template 5' end duplex to execute sequences-specified template 5' boundary definition (Brown et al, 2014). It has been proposed that these residues in hTERT may interact with ssDNA as well as the DNA/RNA duplex to create a large surface for ssDNA retention during template translocation (Wu et al, 2017). The conformation of the motif T β-loop is not

determined at atomic resolution, but its general location suggests that it may clamp around the DNA 3' end on the face opposite the thumb helix to stabilize bound duplex.

The T motif was the first conserved element to be described that is unique to TERTs, identified via the nearly universal conserved the "FYXTE" telomerase signature sequence to the N terminal of the beta-sheet (Nakamura et al, 1997). Within this telomerase signature sequence, it also has a remarkable influence of telomerase repeat extension rate. Data from primer direct extension assays indicates that mutants of this sequence fail to alter repeat addition processivity (Figure 4.1). It is consistent with previous targeted mutagenesis of this region showing only significant alteration of extension rate but not processivity. It could be achieved via the repeat translocation rate by interaction with the template region of the TR at its 5' end (Drosopoulos & Prasad, 2010). The loop of motif T is conserved among species, according to sequence alignments and secondary structure prediction, even with various residues. The K570A mutant in human hTERT as well as the corresponding mutants in *N. crassa* and *T. brucei* showed significant decrease in repeat addition processivity (Figure 4.4). Defects are rescued by K570R mutant in human telomerase for processivity supports that a positively charged residue is critical for repeat addition processivity via interactions with negatively charged DNA/RNA duplex in the catalytic active site. The position of the K570 residue is also important since modifying the location of this residue by insertion or deletion abolished repeat addition processivity. The relatively weak processivity of N571A mutant could also be due to the larger side chain of asparagine than alanine that help to position K570 (Figure 4.3).

Additionally, K570A failed to utilize a short primer (8mer) as substrate indicating the deficiency of the mutant in interacting with the duplex in the active site. It shows a similar phenomenon like the D682A and L980A on motif 3 and CTE respectively, both of which have been demonstrated to have defects for duplex handling in the active site (Huard et al, 2003; Xie et al, 2010). It is solely the contribution of mutants in facilitating formation, or recognition, of the short DNA/RNA duplex inside the active site. This assay thus discounts the effect of the TEN domain on substrate binding, since the TEN domain N95A mutant can extend both the short 8 mer or 12 mer DNA substrate efficiently (Figure 4.5). This phenomenon is consistent with previous reports that TEN domain binding to the longer DNA primer facilitates template translocation (Moriarty et al, 2005). Meanwhile, the short 5' end of the DNA overhang may interact with hTERT protein or hTR via a yet unclear mechanism to facilitate telomerase extension, which evidenced by alleviating the template embedded pause signal in template free system (Brown et al, 2014). The short 5' end DNA overhang is indispensable for nucleotide incorporation of the K570A mutant since it is unable to bind the DNA/RNA duplex in the active site.

Telomerase has to interact with both of its substrate, the telomeric DNA and the incoming nucleotide for nucleotide incorporation. Interestingly, the K570A showed significantly higher K_M^{app} for the incorporation of ddATP and ddGTP, but not ddTTP. This suggests that the mutant may disrupt a specific conformation of the protein structure proximal to the active site at a certain stage of nucleotide addition, which is required for type I translocation, thus failing to bind the duplex at certain positions. According to the accordion model of template positioning by telomerase,

the TR contributes to the template positioning within the active site, it requires unknown specific interaction with TERT when reaching the 5' end of the template (Berman et al, 2011). K570 could be part of the surface area of hTERT to handle the DNA/RNA duplex for type I template translocation during each round of nucleotide extension.

K570A mutant has similar K_M^{app} value compared with the wild type enzyme for the incorporation of 1st T (or A after mutate 49rA to rU on hTR template), which ruled out the binding deficiency of the mutant to the nucleotide (Figure 4.8). The binding affinity of telomerase with its DNA substrate can be assessed from the dissociation constant (K_D). The K_D for a given substrate can be determined by titration its concentration and measuring the quantity bound to enzyme as a function of its concentration. Alternatively, the dissociation rate (K_{off}) of enzyme bound substrates can be used to determine relative affinities of the substrates for the enzyme. Measuring the K_{off} is often a much more experimentally tractable approach, especially when it is hard to get a large amount of telomerase enzyme. K_{off} was chosen when determining primer affinities for telomerase. The higher K_{off} and lower $t_{1/2}$ of K570A provided direct evidence that the binding deficiency of K570A to the telomeric DNA substrate and consistent with the result of exonuclease protection assays (Wu et al, 2017). The higher K_M^{app} of nucleotide could because of the weak binding affinity of the mutant to DNA substrate. For the phenotype, it could be the mechanism of the K570N mutant, which have been found in patients with aplastic anemia and dyskeratosis congenital, for the shorten of telomere. With deeper understanding the mechanism of the mutants could be helpful for the diagnose and therapy strategy for the disease (Gramatges et al, 2013; Xin et al, 2007).

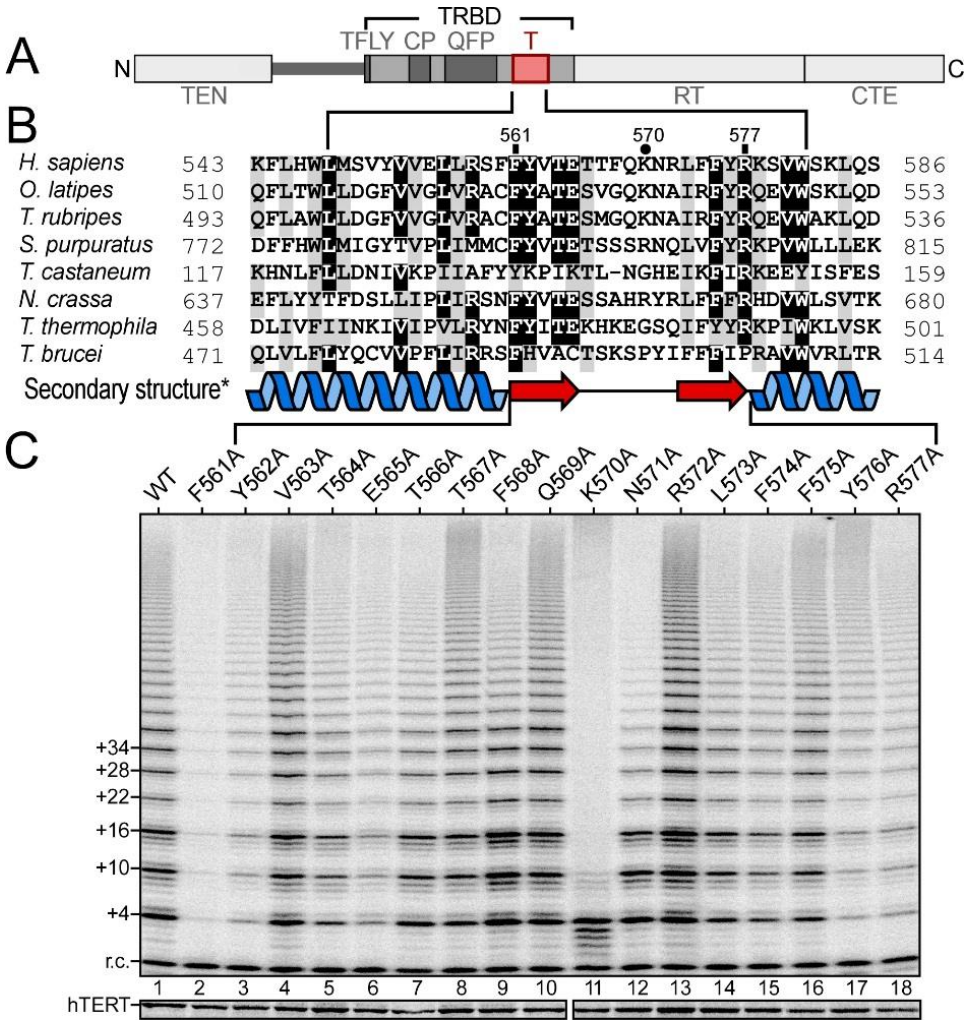

Figure 4.1. Alanine substitution screening of motif T. (A) Schematic of domain and motif organization of human TERT protein. Telomerase specific motif T is colored (red). (B) Sequence alignment of TERT motif T from vertebrates, invertebrates, fungi, plants and ciliates. Darker shading indicates greater identity conservation with the human sequence (<30% light, 30–60% medium and >60% dark). (C) Activity assay of the motif T mutants. Human telomerases with alanine substitutions in motif T were reconstituted in vitro and assayed for activity. (TTAGGG)3 was used as DNA substrate and ^{32}P-dGTP for labeling with unlabeled other nucleotides. Numbers on the left (+4, +10, +16, etc.) of the gel indicate the number of nucleotides added to the primer in each major band. r.c.: recovery control, a ^{32}P-end-labeled 18-nt DNA oligonucleotide. Below the gel, the [^{35}S] methionine labeled TERTs analyzed by SDS–PAGE for quantitation are shown.

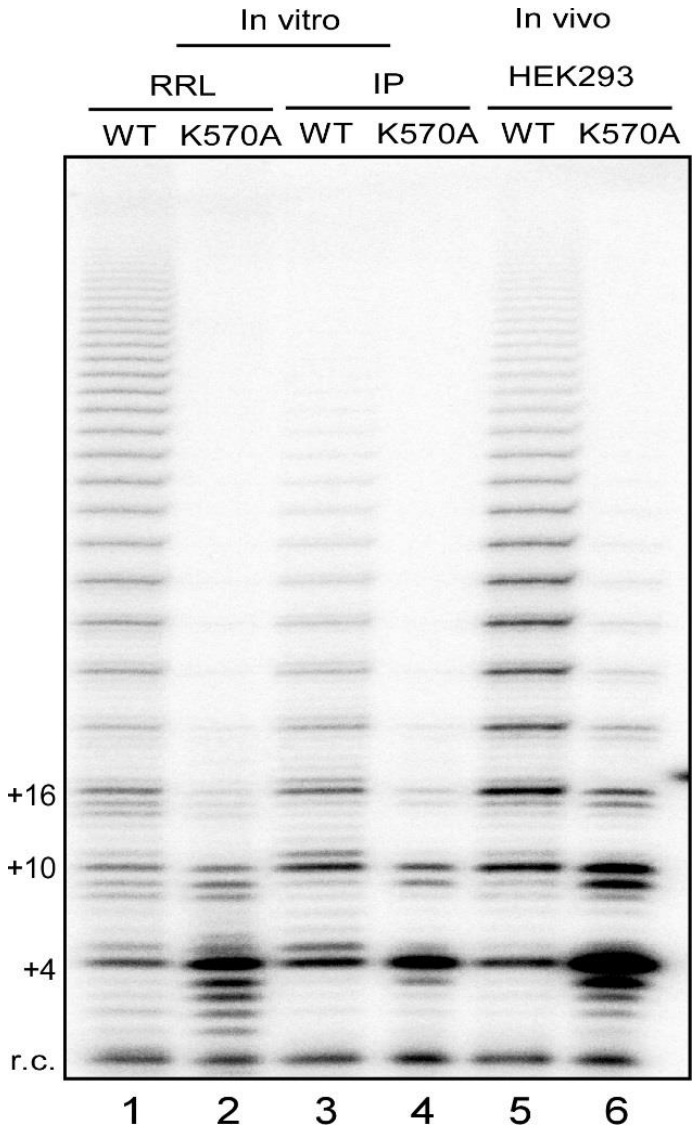

Figure 4.2. Both *in vitro* as well as *in vivo* reconstituted K570A mutant showed defect of repeat addition processivity. Wild type or K570A mutant TERT was reconstituted in RRL or HEK293FT cell with hTR for activity assay. $(TTAGGG)_3$ is used as DNA substrate and ^{32}P-dGTP for labeling with unlabeled other nucleotides. Numbers on the left (+4, +10, +16) of the gel indicate the number of nucleotides added to the primer in each major band. r.c.: recovery control, a ^{32}P-end-labeled 18-nt DNA oligonucleotide.

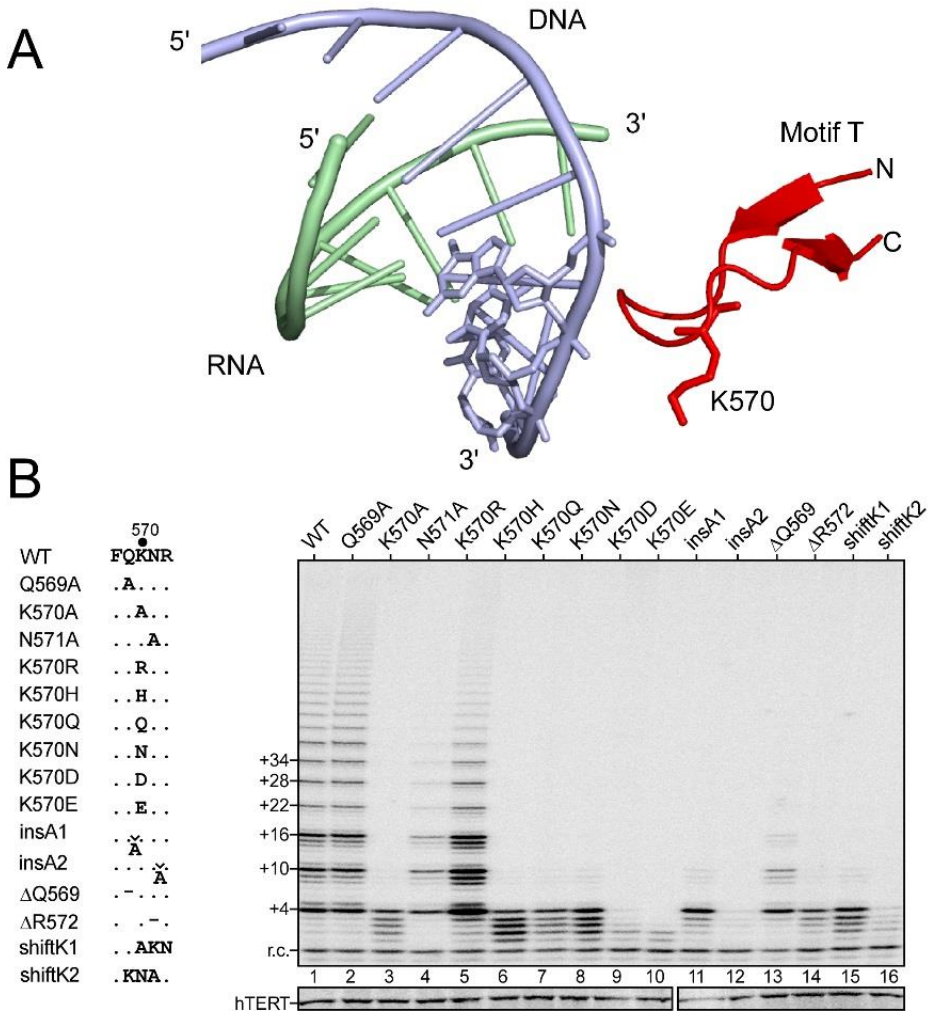

Figure 4.3. Substitutions, deletion and insertion mutants of motif T. (A) Structural model of motif T β-loop interacting with an RNA/DNA duplex. A model derived from *Takifugu rubripes* TRBD crystal structure (PDB: 4MLO) and *Tribolium castaneum* TERT RNA/DNA duplex co-crystal structure (PDB: 3KYL). (B) Left: the list of different mutants of K570 and flanking residues in motif T. Right: Activity assays of the motif T mutants. Human telomerases with substitutions of K570 as well as insertion or/and deletion next to K570 in motif T were reconstituted *in vitro* and assayed for activity. Numbers on the left (+4, +10, +16, etc.) of the gel indicate the number of nucleotides added to the primer in each major band. r.c.: recovery control, a ^{32}P-end-labeled 18-nt DNA oligonucleotide. Below the gel, the [^{35}S] methionine labeled TERTs analyzed by SDS–PAGE for quantitation are shown.

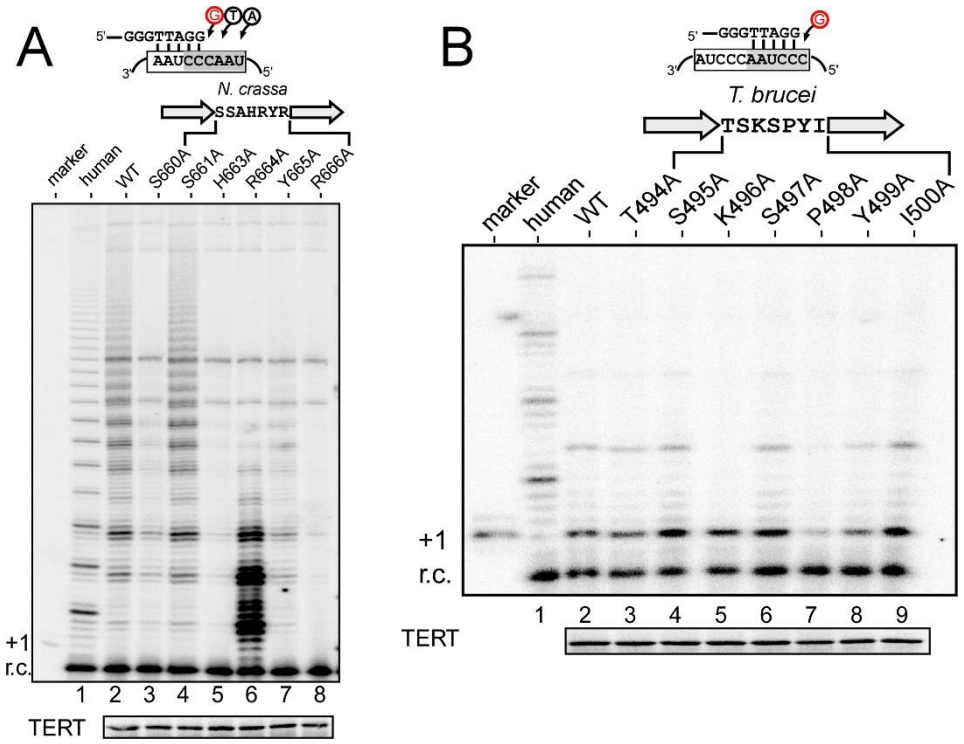

Figure 4.4. Evolutionary conservation of the hTERT K570 residue function. Alanine substitution screening of the motif T β-loop in *N. crassa* (A) and *T. brucei* (B). $(GTTAGG)_3$ was used as substrates for activity assay with ^{32}P-dGTP and other unlabeled dNTPs. The DNA primers $(GTTAGG)_3$ extended by one ^{32}P-dGTP with terminal deoxynucleotidyl transferase (TdT) were included as size markers. Human telomerase reconstituted in RRL used as control. r.c.: recovery control, a ^{32}P-end-labeled 18-nt DNA oligonucleotide. Below the gel, the [^{35}S] methionine labeled TERTs analyzed by SDS–PAGE for quantitation are shown.

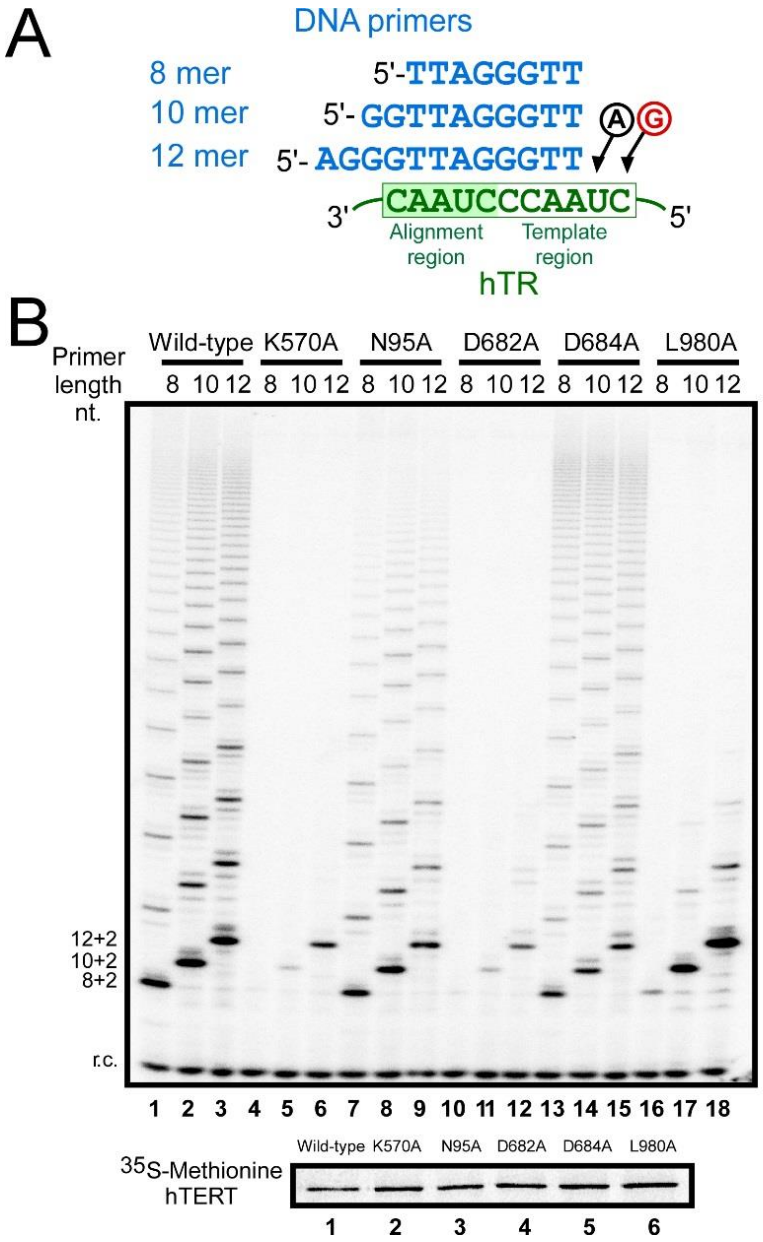

Figure 4.5. Activity assay of telomerase mutants using primers with various lengths. (A) The 3 different primers are aligned with hTR template sequence. (B) Telomerases with specific mutations in TERT indicated were assayed for activity using telomere primers, tel8, tel10 or tel12, with length ranging from 8 to 12 nt. The numbers (8+2, 10+2, 12+2, etc.) labeled on the left of the gel indicate the length of the primer plus the number of nucleotides added. r.c.: recovery control, a ^{32}P-end-labeled 7-nt DNA oligonucleotide. Below the gel, the [^{35}S] methionine labeled TERTs analyzed by SDS–PAGE for quantitation are shown.

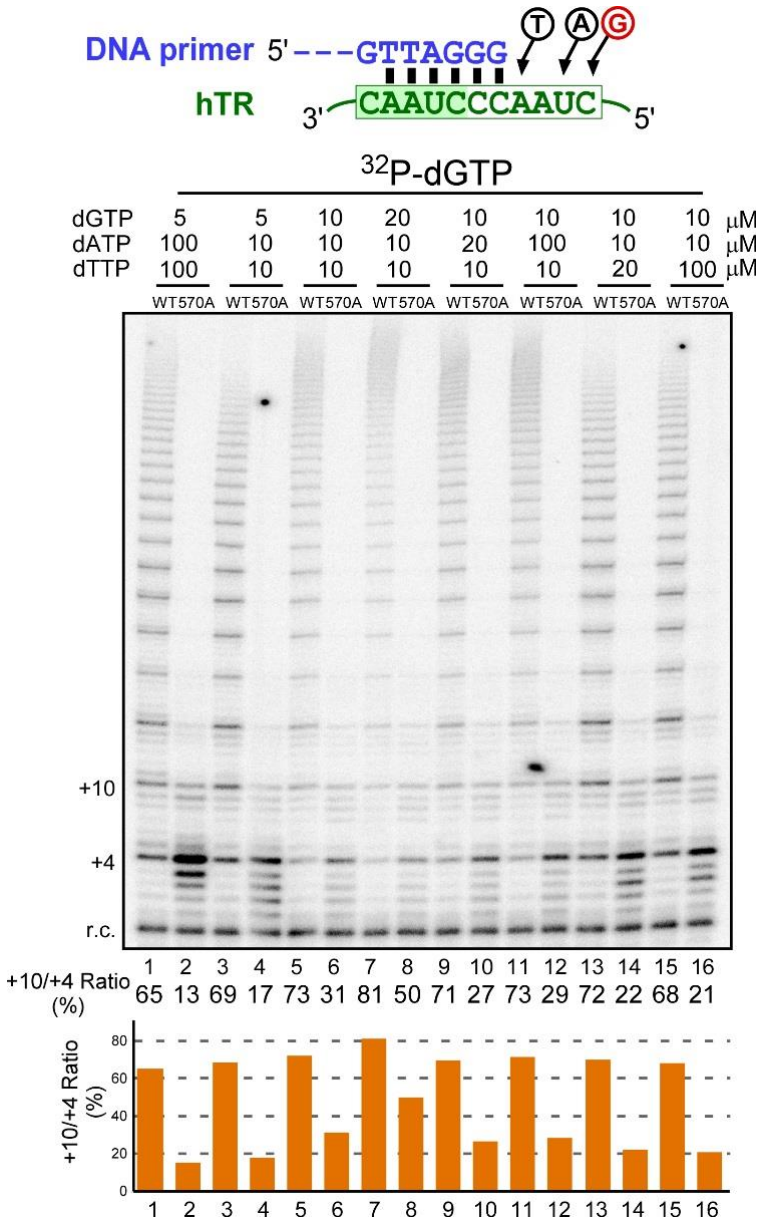

Figure 4.6. Effects of nucleotide concentration on telomerase repeat addition activity for K570A mutant and wild type enzyme. Direct primer extension assays were performed with telomerase enzyme reconstituted *in vitro*. Top: Sequences of the DNA primer and the hTR template for telomerase direct assay. Middle: Telomerase was assayed in the presence of either ^{32}P-dGTP with a range of dGTP, dATP and dTTP concentrations. A radiolabeled DNA 18 mer recovery control (r.c.) was added before product purification and precipitation. Numbers to the left of the gel denote the number of nucleotide added to the telomeric primer. Ratio as a percent of the intensity of +10 over +4 DNA products. Bottom: A bar graph of the relative ratio of +10/+4 DNA products are shown below the gel.

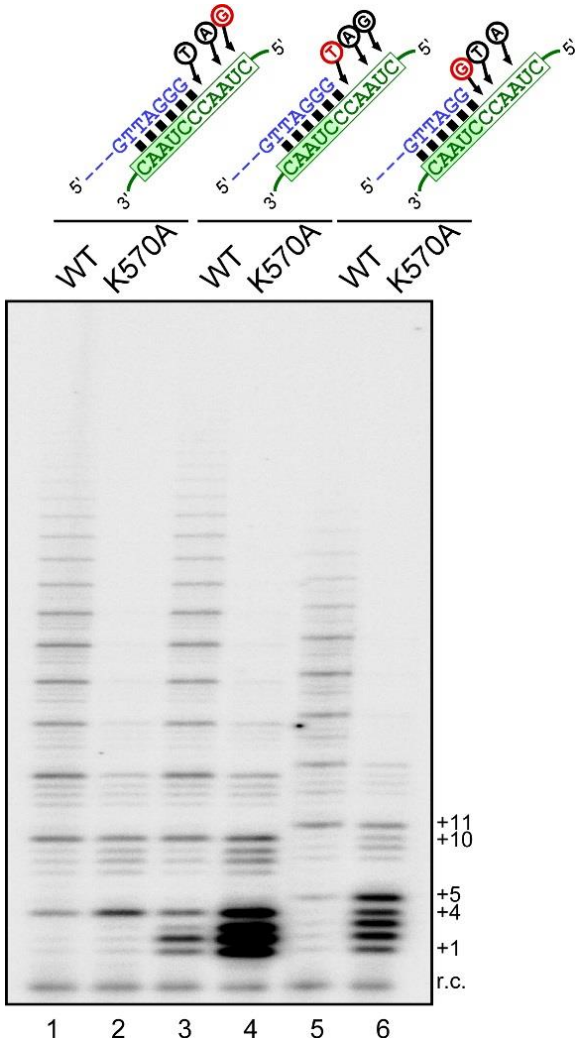

Figure 4.7. Nucleotide addition defect of K570A mutant. Wild type or K570A mutant hTERT was *in vivo* reconstituted and immune-purified for activity assay. $(TTAGGG)_3$ or $(GTTAGG)_3$ is used as DNA substrate respectively and labeled with denoted ^{32}P-dNTP with unlabeled other nucleotides. Numbers on the right (+1, +4, +5 etc.) of the gel indicate the number of nucleotides added to the primer in each major band. r.c.: recovery control, a ^{32}P-end-labeled 18-nt DNA oligonucleotide.

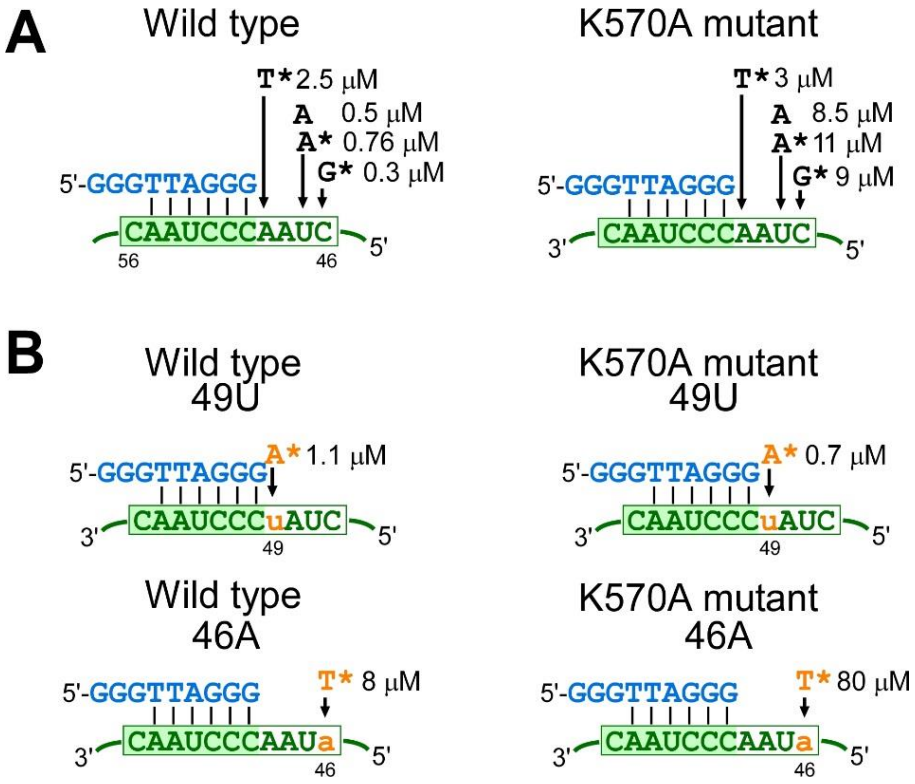

Figure 4.8. K570A deficiency on nucleotide incorporation kinetics. (A). The K_M^{app} for nucleotide addition at positions 46,47, and 49 were measured using wild type and K570A mutant telomerases reconstituted *in vivo* and the immuno-purified and various DNA substrates (Figure 4.8 & Figure 4.13). Position 47 of hTR was incorporating dATP as well as ddATP (marked with *). The 46 and 49 was incorporate with ddGTP or ddTTP (marked with *). The K_M^{app} for incorporating nucleotides are denoted. (B). Mutation at position 46 and 49 of hTR, rC mutated rA and rA mutated to rU respectively (orange), keep the same trend for the nucleotide incorporation efficiency between wild type and K570A mutant (Figure 4.14).

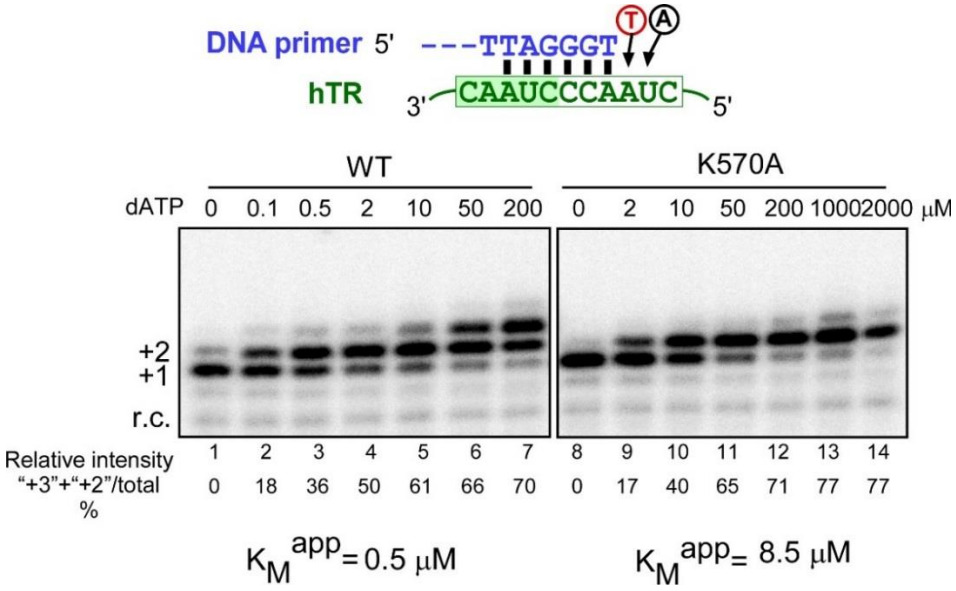

Figure 4.9. Defect of K570A mutant on K_M^{app} for dATP incorporation. *In vivo* reconstituted telomerases were immune-purified and analyzed with $(TAGGGT)_3$ substrates and labeled with ^{32}P-dTTP to determine the apparent K_M for dATP. Numbers on the left (+1, +2) of the gel indicate the number of nucleotides added to the primer. A ^{32}P end-labeled DNA recovery control (r.c.) was added before product purification and precipitation. At the bottom of the gel is the quantification of the intensity of the +2 and +3 products over the total intensity of products for the specified nucleotide concentration. The Michaelis–Menten equation, $Y=V_{max}*X/(K_M+X)$, was used to fit the nonlinear curve to determine the K_M^{app}.

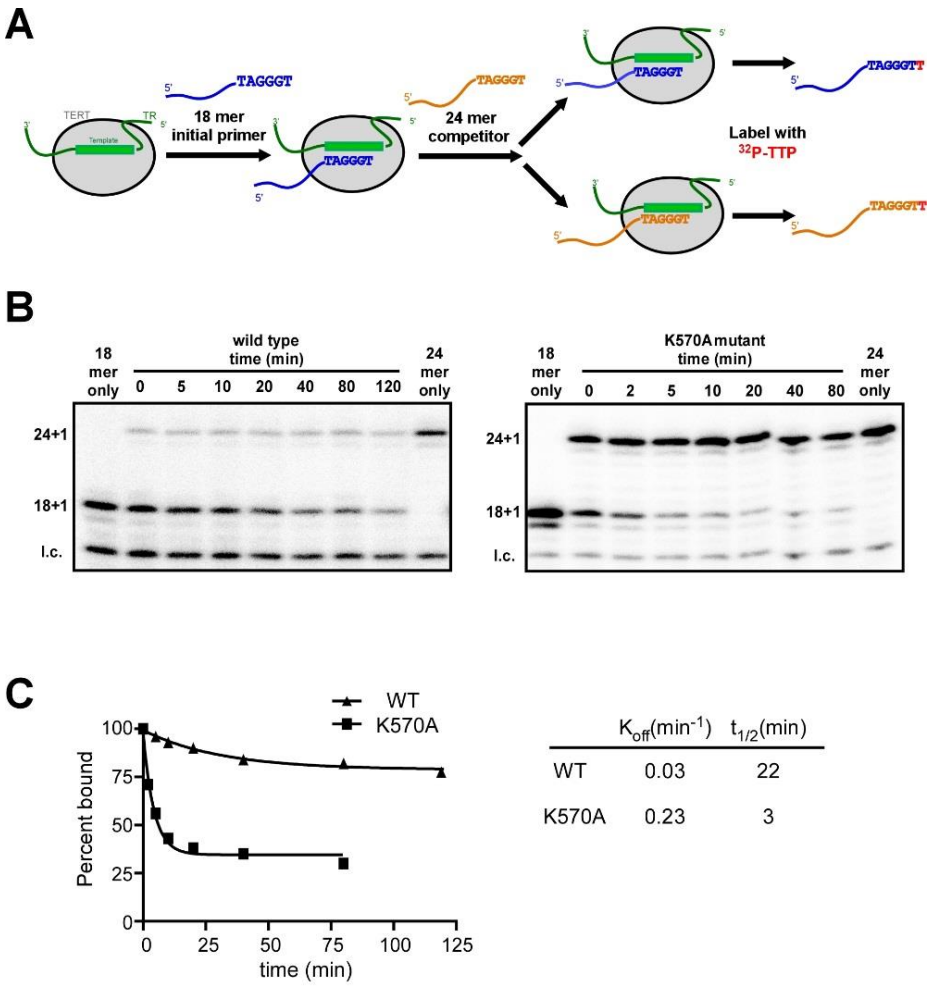

Figure 4.10. Dissociation rates of K570A mutants and wild type. (A) Schematic of the process for measuring K_{off}. Wild type or K570A mutant telomerases were *in vivo* reconstituted and then immuno-purified. The initial DNA primer $(TAGGGT)_3$ was incubated with an enzyme on beads for 10 min at 30 °C. Following the addition of the competitor primer $(TAGGGT)_4$, aliquots were removed at 2, 5, 10, 15, 20, 40, or 80 mins and 1 µL 0.165 µM α-^{32}P-dTTP was added for isotopic labeling for 10 min at 30 °C. (B) Representative gels for K_{off} measurements for wild type telomerase and K570A mutant. A ^{32}P-end-labeled 18-mer was used as a recovery control (r.c.). (C) Bands depicted in panel B were quantitated by PhosphorImager analysis. Plots derived from the normalized intensity of the 18+1 initial product over the total intensity of products (18+1 and 24+1) for the specified time points and normalize to start point. The rate constants were determined by fitting the data to the equation $y=Aexp^{(-kt)}$, using the Prism software package to determine the K_{off} and $t_{1/2}$.

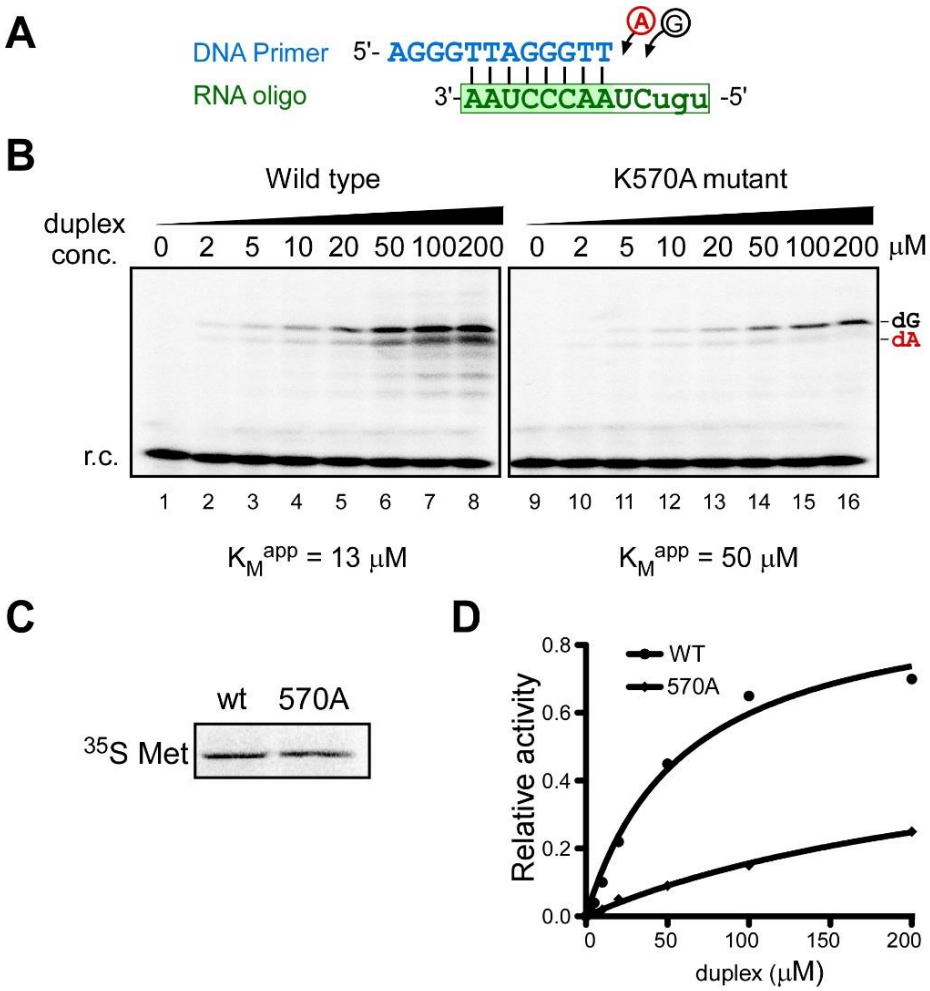

Figure 4.11. K_M comparison for DNA/RNA duplex of wild type and K570A mutant enzyme. (A) *In vitro* reconstituted template-free (TF) telomerase were analyzed with titration of DNA/RNA hybrid substrates to determine the apparent K_M. The nucleotides added (black) to the DNA in the hybrid are shown, with the first incorporation a ^{32}P-dATP (circled). (B) Representative gels for K_M^{app} measurements. A ^{32}P end-labeled DNA recovery control (r.c.) was added prior to product purification and precipitation. (C) The [^{35}S] methionine labeled TERTs analyzed by SDS–PAGE for quantitation are shown. (D) Plots derived from the normalized intensity of the +1 and +2 products for the specified DNA/RNA duplex concentration. The Michaelis–Menten equation, $Y=Vmax*X/(K_M+X)$, was used to fit the nonlinear curve to determine the K_M^{app}.

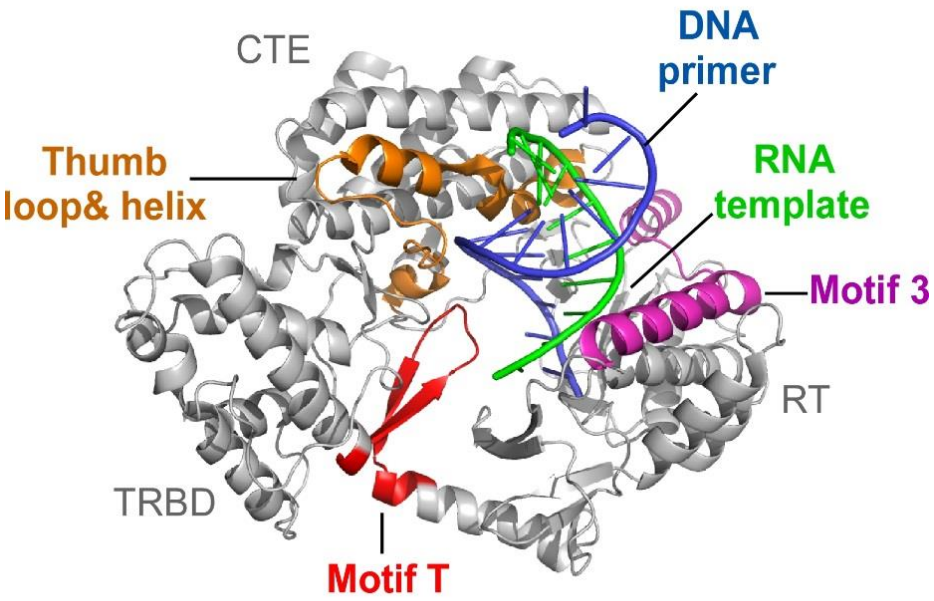

Figure 4.12. Motifs proximal to the TERT active-site cavity. TERT active-site motifs are colored within the overall ribbon diagram of *Tribolium* TERT crystallized in complex with a model DNA–RNA duplex (PBD accession code 3KYL). The product DNA strand is in blue, and RNA template strand is in green. Red: motif T; Purple: motif 3; Orange: thumb loop and thumb helix.

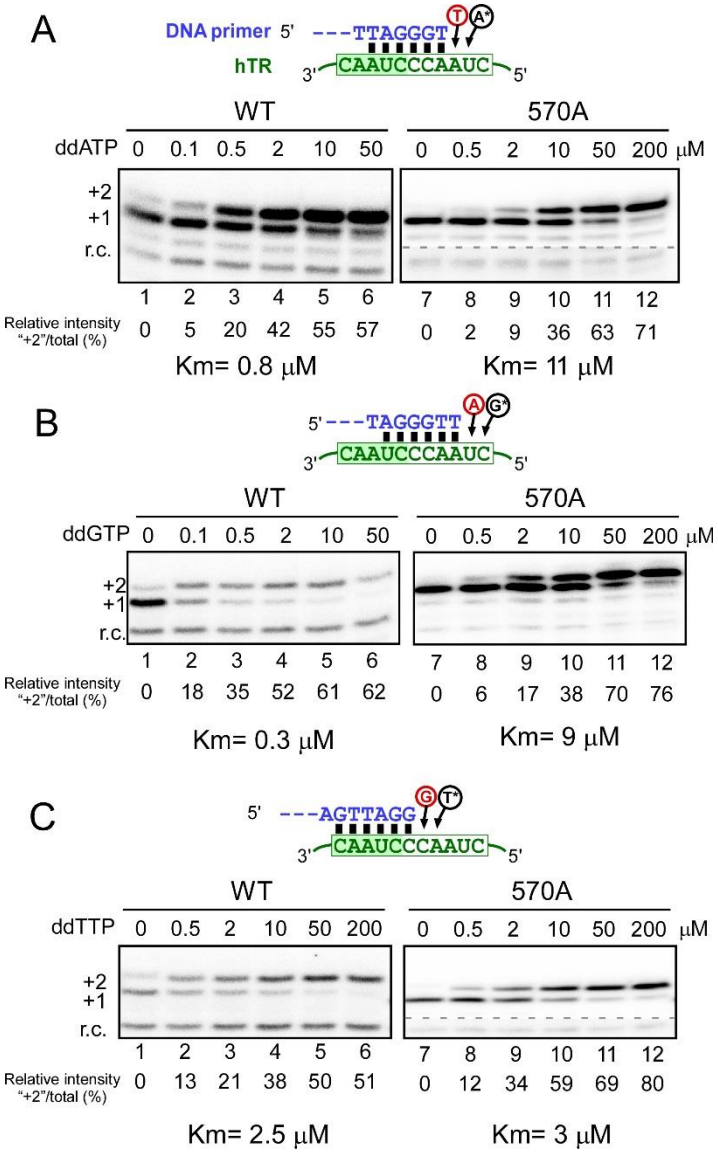

Figure 4.13. Defect of K570A mutant on K_M^{app} for ddNTP incorporation. *In vivo* reconstituted wild type telomerases and K570A mutant were immune-purified and analyzed with various denoted DNA substrates and labeled with ^{32}P-dNTP to determine the apparent K_M for ddNTP. Numbers on the left (+1, +2) of the gel indicate the number of nucleotides added to the primer. A ^{32}P end-labeled DNA recovery control (r.c.) was added before product purification and precipitation. At the bottom of the gel is the quantification of the intensity of the +2 products over the total intensity of products for the specified nucleotide concentration. The Michaelis–Menten equation, $Y=V_{max}*X/(K_M+X)$, was used to fit the nonlinear curve to determine the K_M^{app}.

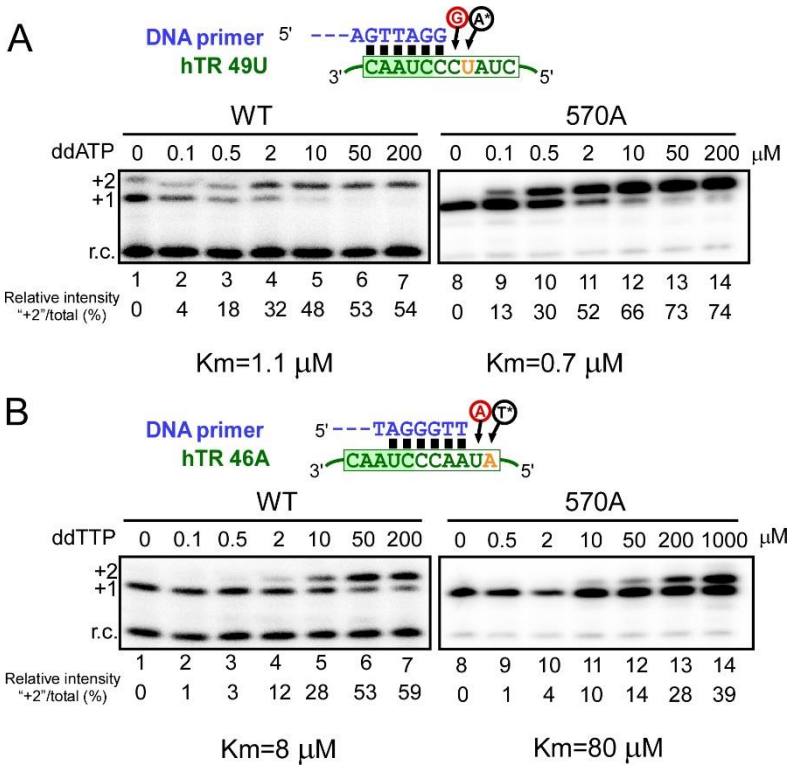

Figure 4.14. Defect of K570A mutant on K_M^{app} for ddNTP incorporation at specific position. *In vivo* reconstituted wild type telomerases and K570A mutant with different hTR mutant were immune-purified and analyzed with various denoted DNA substrates and labeled with ^{32}P-dNTP to determine the apparent K_M for ddNTP. Numbers on the left (+1, +2) of the gel indicate the number of nucleotides added to the primer. A ^{32}P end-labeled DNA recovery control (r.c.) was added before product purification and precipitation. At the bottom of the gel is the quantification of the intensity of the +2 products over the total intensity of products for the specified nucleotide concentration. The Michaelis–Menten equation, $Y=V_{max}*X/(K_M+X)$, was used to fit the nonlinear curve to determine the K_M^{app}.

CHAPTER 5

EXPLORATION OF THE MOLECULAR MECHANISM OF TELOMERASE INHIBITOR BIBR1532

5.1 Abstract

Telomerase is a ribonucleoprotein with reverse transcriptase activity that has long been identified as a potential target for cancer therapy. The non-nucleoside, synthetic compound BIBR1532 is a potent and selective telomerase inhibitor capable of inducing senescence in human cancer cells. Although BIBR1532 has been extensively applied in both *in vivo* and *in vitro* studies, the molecular basis of inhibition is unclear. To characterize the function of the telomerase inhibitor BIBR 1532, we use the *in vitro* reconstituted telomerase from RRL (rabbit reticulocyte lysate) in direct primer extension assays. We confirmed the ability of BIBR 1532 to inhibit telomerase activity in a concentration dependent manner. Additionally, we found BIBR 1532 to specifically repress human telomerase catalytic activity, but not telomerases from other species. The apparent K_M for nucleotide incorporation is not affected in the presence of the inhibitor. This study provides crucial information to understand the molecular mechanism of BIBR 1532 inhibition of telomerase catalytic function. Further investigation is required to uncover the exact and detailed role of the inhibitor for each step of the catalytic cycle of human telomerase.

5.2 Introduction

Telomerase is a highly specialized reverse transcriptase that adds DNA repeats to the ends of chromosomes to offset the loss of telomeric DNA during each DNA replication cycle (Greider & Blackburn, 1987). The core components of telomerase include the catalytic telomerase reverse transcriptase (TERT) and telomerase RNA

(TR). Since the discovery of telomerase, progress has been made in the identification of the core components of representative organisms of various evolutionary groups across eukaryotes (Greider & Blackburn, 1989; Shippen-Lentz & Blackburn, 1990). A variety of accessory proteins, while dispensable for enzyme activity *in vitro*, play important roles in regulation, biogenesis, and localization *in vivo* (Egan & Collins, 2010; Podlevsky et al, 2008).

Recently we have reviewed telomerase as a promising target in oncogenesis and summarize recent advances in potential telomerase inhibitors for antitumor therapy (Chen & Zhang, 2016). Telomerase, and specifically its catalytic subunit TERT, is over-expressed in 85–90% of cancers and has become a widely accepted tumor marker and a compelling target for anticancer therapeutics (Ruden & Puri, 2013). Telomere maintenance by telomerase is a key requisite for human cancer cells to gain unlimited proliferation potential and is regarded as an essential alteration in the physiology of the tumor cell to acquire malignant growth (Hanahan & Weinberg, 2011). Constitutive overexpression of the telomerase in various pre-senescent and normal cells conveyed an unlimited growth potential onto these cells, further confirming the role of telomerase in the immortalization process (Bodnar et al, 1998). In contrast, inhibition of telomerase results in telomere-shortening, subsequent growth arrest, and senescence in cancer cells (Xi et al, 2015).

In the growing list of promising telomerase inhibitors, BIBR1532 (2-[(E)-3-naphtalen-2-yl-but-2-enoylamino]-benzoic acid) is one of the most potent non-peptidic, non-nucleosidic small molecule inhibitor of the telomerase catalytic subunit (hTERT) (Figure 5.1A). The anticancer value of BIBR 1532 has been evaluated in numerous studies, suggesting the strong ability to suppress tumor cell growth in

several types of cancers (Bashash et al, 2012; Bashash et al, 2017; Brassat et al, 2011; Liu et al, 2017). There is also evidence showing that BIBR1532 may find potential application as an adjunctive agent in cancer chemotherapy. For instance, BIBR1532 in combination with carboplatin demonstrates the synergistic effect in eliminating ovarian cancer spheroid-forming cells by inhibition of telomerase activity (Meng et al, 2012). Despite extensive use of BIBR1532 in biochemical, as well as *in vivo* studies, its precise mechanism of inhibition of telomerase remains unclear. The co-crystal structure of BIBR1532 bound to a conserved hydrophobic pocket in *Tribolium castaneum* catalytic subunit of telomerase (tcTERT) provides useful information to explore the molecular function of BIBR 1532 inhibiting the telomerase activity (Bryan et al, 2015). In this project, we showed BIBR 1532 to specifically inhibit human telomerase activity during catalytic action in a concentration dependent manner. The preliminary data are useful to further study the inhibition mechanism of this promising telomerase inhibitor.

5.3 Material and Methods

In vitro reconstitution of telomerase from representative species.

Human TERT, purple sea urchin TERT, filamentous fungi (*Neurospora*) TERT, medaka fish TERT, and ciliate (*Tetrahymena*) TERT proteins were expressed in rabbit reticulocyte lysate (RRL) from the pNFLAG-TERT plasmid DNA using the TnT T7 Quick Coupled transcription/translation kit (Promega) following manufacturer's instructions. The hTR pseudoknot (residues 32–195) and CR4/5 (residues 239–328) fragments, the *Spu*TR (residues 63–154), *Ncr*TR (residues 457–1501/Δ463–1288/insGGAC) pseudoknots, P4.2 (residues 288–446) and three-way junction (residues 1813–1877) fragments, and medaka TR fragments PK (1-150) and

CR4/5 (170-220) were *in vitro* transcribed, gel purified, and assembled together with the TERT proteins in RRL for 30 min at 30°C at a final concentration of 1.0 μM. *Tetrahymena thermophila* telomerase was reconstituted as previously described (Hong et al, 2013).

Telomerase direct primer-extension assay.

Two microliters *in vitro* reconstituted telomerase enzyme was assayed in a 10 μL reaction containing 1x telomerase reaction buffer, 1 μM DNA primer, specified dNTPs and 0.165 μM of the α-^{32}P-dGTP in the presence of denoted concentrations of BIBR 1532 (ApexBio). Reactions were incubated at 30°C for 60 min and terminated by phenol/chloroform extraction, followed by ethanol precipitation. The DNA products were resolved on a 10% (wt/vol) polyacrylamide/8 M urea denaturing gel, dried, exposed to a phosphor storage screen and imaged on a Bio-Rad FX-Pro phosphorimager.

K_M measurement using template free (TF) telomerase.

Two microliters of RRL reconstituted TF telomerase enzyme was assayed in a 10 μL reaction containing 1X telomerase reaction buffer, 40 μM pre-annealed DNA/RNA duplex, 0.165 μM of the α-^{32}P-dATP with or without BIBR 1532 (5 μM). For K_M^{app} measurements, the activity assays were performed with nucleotide concentrations ranging from 0 to 1 mM. Reactions were incubated at 30°C for 60 min and terminated by phenol/chloroform extraction, followed by ethanol precipitation. The DNA products were resolved on a 15% (wt/vol) polyacrylamide/8 M urea denaturing gel, dried, exposed to a phosphor storage screen and imaged on a Bio-Rad FX-Pro phosphorimager. The intensities of specific products were normalized to the total product intensity and plotted against the nucleotide concentrations with the

Michaelis-Menten equation, $Y=V_{max}*X/(K_M+X)$, used to fit the nonlinear curve to determine the K_M^{app} (Prism 5, Graphpad Software).

5.4 Results

BIBR1532 is an inhibitor of recombinant Telomerase

BIBR1532 has been identified as a potent and selective inhibitor of human telomerase instead of other RTs or polymerases (Damm et al, 2001). To obtain a better understanding of the mechanism of action exerted by this compound, we use *in vitro* reconstituted hTERT from RRL assembled with hTR and telomerase direct primer extension assay to quantify the effect of BIBR 1532 on telomerase activity. The native enzyme synthesized long extension products in the conventional assay similar to the vector, 1% DMSO which did not affect the activity (Figure 5.1B). The telomerase inhibitor, BIBR1532, inhibits the accumulation of telomeric DNA in a dose-dependent manner, which is consistent with previous results from TRAP assays as well as direct assays. Noticeably, at low concentrations of the inhibitor, the synthesis of long extension products appears to be more affected than the synthesis of shorter products. It suggests that the BIBR 1532 may impede the repeat addition processivity during the extension of the telomeric DNA substrate by human telomerase.

BIBR1532 inhibits telomerase catalytic activity but not enzyme assembly

To determine whether BIBR1532 would directly interfere with telomerase catalytic activity, 2 μM of inhibitor was added at various stages of enzyme reconstitution: before hTERT expression in RRL, following hTERT expression but prior to the addition of *in vitro* transcribed hTR and just before the primer direct

extension assay to assembled telomerase (Figure 5.2A). The BIBR 1532 had a similar influence on the telomeric DNA synthesis for each reaction. The earlier treatments with inhibitor, before hTERT expression or reconstitution failed to repress telomerase function (Figure 5.2B). Meanwhile, it also means the longer incubation with telomerase is dispensable for the inhibitory function of BIBR 1532. The result indicates the inhibitor does not further inhibit telomerase activity with pre-incubation, thus it is only functional during the telomerase catalytic cycle.

BIBR 1532 does not affect apparent K_M for the first nucleotide incorporation in human telomerase.

Previously, we discovered that the human telomerase template is uniquely embedded with a single-nucleotide pause signal that arrests DNA synthesis at the template boundary (Brown et al, 2014). And the pause signal mediates high K_M for nucleotide incorporation. To investigate the effect of telomerase inhibitor BIBR 1532 on nucleotide incorporation, we measured the apparent K_M (K_M^{app}) value of nucleotide incorporation with or without BIBR 1532 (5 μM) using DNA/RNA hybrid substrates and template-free (TF) human telomerase that lacks the template sequence in the integral hTR component (Qi et al, 2012). Human TF telomerase was reconstituted by assembling *in vitro* expressed human TERT protein in rabbit reticulocyte lysate with the two essential hTR fragments, CR4/5 and pseudoknot lacking the template region. The K_M^{app} for incorporating first nucleotide after template translocation is very similar in the presence or absence of BIBR 1532, even though the total activity decreased after treatment (Figure 5.3). It suggests that the BIBR 1532 did not act as a competitive inhibitor for nucleotide addition, which is consistent

with previous results reporting BIBR 1532 as a non-competitive inhibitor of telomerase activity (Pascolo et al, 2002).

BIBR 1532 specifically inhibits human telomerase activity but not in other species.

BIBR 1532 has been previously shown to inhibit telomerase but does not affect conventional reverse transcriptase or DNA polymerase activity (Damm et al, 2001). It has also been shown to bind a conserved hydrophobic pocket (FVYL motif) on the outer surface of the thumb domain in *Tribolium* co-crystal structure. For comprehensive studies on the species-specific telomerase inhibition of BIBR 1532, we incubate the inhibitor with *in vitro* reconstituted telomerase from representative organisms covering ciliates, fungi, invertebrates and vertebrates. Interestingly, BIBR 1532 demonstrated inhibition of only human telomerase instead of other species.

5.5 Discussion

A number of genetic validation experiments indicated telomere maintenance by telomerase is an important process of human cancers (Arndt & MacKenzie, 2016). The pharmacological studies showed cancer cells treated with the non-nucleosidic small telomerase inhibitor BIBR1532 leads to progressive telomere shortening, cell proliferation arrest and senescence (Barma et al, 2003; El-Daly et al, 2005). Understanding the mechanism of telomerase inhibition by small-molecule inhibitors such as BIBR1532 will assist to identify and develop useful telomerase inhibitors as potential therapeutics. Structural data show that BIBR1532 binds to a hydrophobic pocket on the outer surface of the thumb domain in *Tribolium castaneum* (Bryan et al, 2015). The key residues in the structural organization of the FVYL motif are conserved across species, and the pocket is solvent-accessible for substrate binding. However, according to the results of telomerase functional assays in the presence of

BIBR 1532, it failed to show significant inhibition of telomerase activity in other species except human. Further studies as well as functional assay are required for the solid conclusion for the binding site of the inhibitor with TERT protein. Since BIBR 1532 has been shown to neither inhibit other polymerases nor reverse transcriptase, this suggests the high specificity of these small molecules to be a potent human telomerase inhibitor (Damm et al, 2001). More detailed understanding of the molecular basis of BIBR1532 inhibition will require the crystal structure analysis of the human telomerase-inhibitor complex.

BIBR 1532 anticancer value has been evaluated in numerous preclinical studies, it suggested capability of this inhibitor to suppress tumor cell growth in several types of cancers (Bashash et al, 2012; Liu et al, 2017). There is also evidence showing the potential application of BIBR1532 as an adjunctive agent in cancer chemotherapy (Ward & Autexier, 2005). Previous pharmacology studies demonstrated that BIBR 1532 inhibits telomerase activity, which result in sensitizing drug-resistant cell lines to several DNA damaging agents, and preventing the additional activation of telomerase in response to these drugs (Bashash et al, 2017; Meng et al, 2012). However, the prevalently inhibitory mechanism of BIBR 1532 ranging from the biogenesis of the enzyme to its catalytic activity remains unclear. To dissect the question, it is added at each stage of the reconstitution process *in vitro*: protein expression, enzyme reconstitution as well as immediately before the functional assay. There are no significant differences in repression of enzymatic activities regardless of the various stages of addition. It indicates the compound only play the role in the inhibition telomerase catalytic function instead protein expression or RNP assembly. More studies are required to answer whether high-dose BIBR1532

could repress the biogenesis of the telomerase as well as binding of protein partners of the telomerase resulting in telomere dysfunction *in vivo*.

To further investigate how BIBR 1532 repress human telomerase catalytic function, we measure the apparent K_M of the first nucleotide incorporation after template translocation, which is the rate limiting step for template translocation. In the presence of 5 μM BIBR 1532, the total activity is decreased, but the apparent K_M for nucleotide incorporation is close to the negative control group. This is consistent with the conclusion of an earlier study that BIBR 1532 inhibits telomerase function in a non-competitive manner (Pascolo et al, 2002). Moreover, the inhibitor leads to an overall reduction in the number of added TTAGGG repeats. To sum up, BIBR1532 does not block the basic catalytic steps involved in template copying, but specifically suppress elongation of the DNA substrate following primer extension to the 5'-end of the template.

All results are supporting the hypothesis that the binding site of the drug and the binding site of the deoxyribonucleotides is in close proximity or overlap, creating a steric reciprocal interference for the binding efficiency (Pascolo et al, 2002). BIBR1532 is involved in template translocation of the enzyme-substrate complex or dissociation between the DNA substrate and the enzyme upon completion of template copying, unique to telomerase. That could be the reason of the compound's specificity. During the catalytic cycle of the telomerase including the nucleotide addition and template translocation, BIBR 1532 could either act as non-competitor for the nucleotide incorporation or suppress the template translocation for regenerating hTR template. However, more information is required to uncover the effect of inhibitor on each step of human telomerase catalytic.

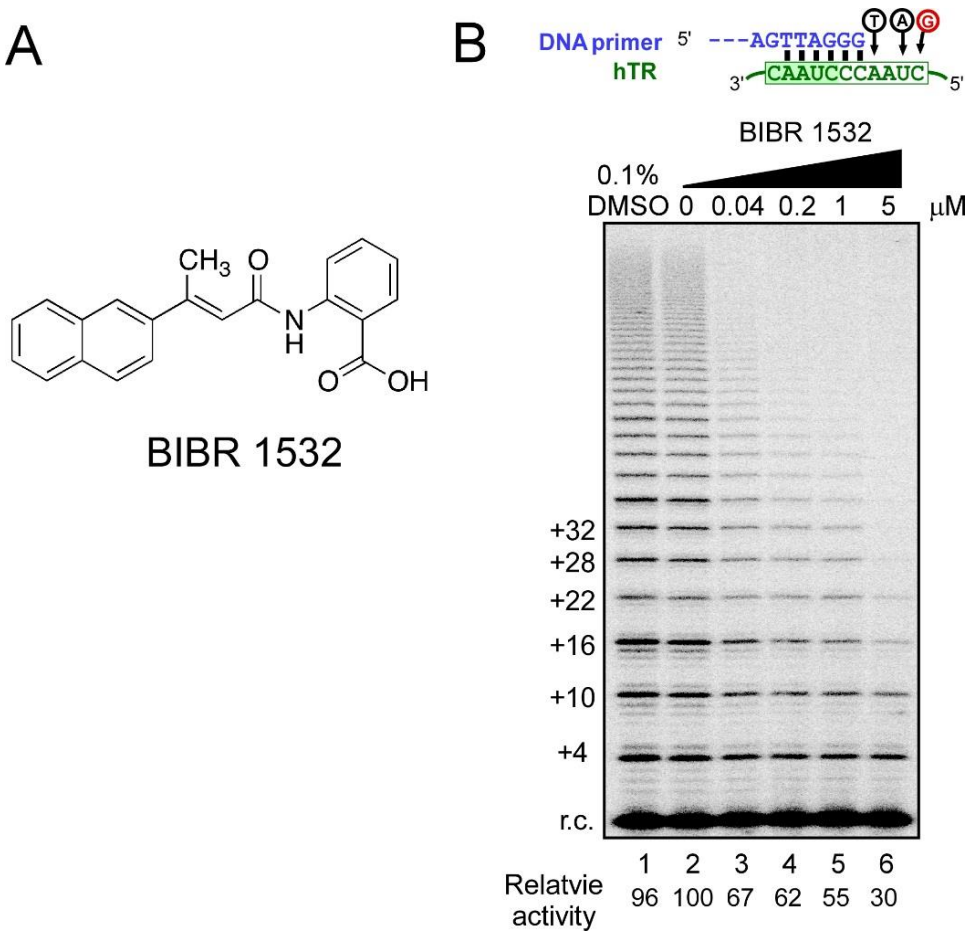

Figure 5.1. BIBR1532 inhibits the recombinant telomerase activity. (A) Chemical structure of the BIBR 1532. (B). Telomerase was reconstituted *in vitro* in RRL and incubated with $(TTAGGG)_3$, dATP, dTTP, and ^{32}-P-dGTP with various concentrations of BIBR1532. Telomerase products were separated on a sequencing gel. The inhibitor was dissolved in dimethyl sulfoxide (DMSO) and diluted with water before adding to the reaction mix prior to the addition of telomerase. The gel shows a control with or without dimethyl sulfoxide and reactions in the presence of different concentrations of inhibitor. A radiolabeled DNA recovery control (r.c.) was added prior to product purification and precipitation. Numbers on the left (+4, +10, +16, etc.) of the gel indicate the number of nucleotides added to the primer in each major band. Quantitation of telomerase activity in relation to control are shown below the gel.

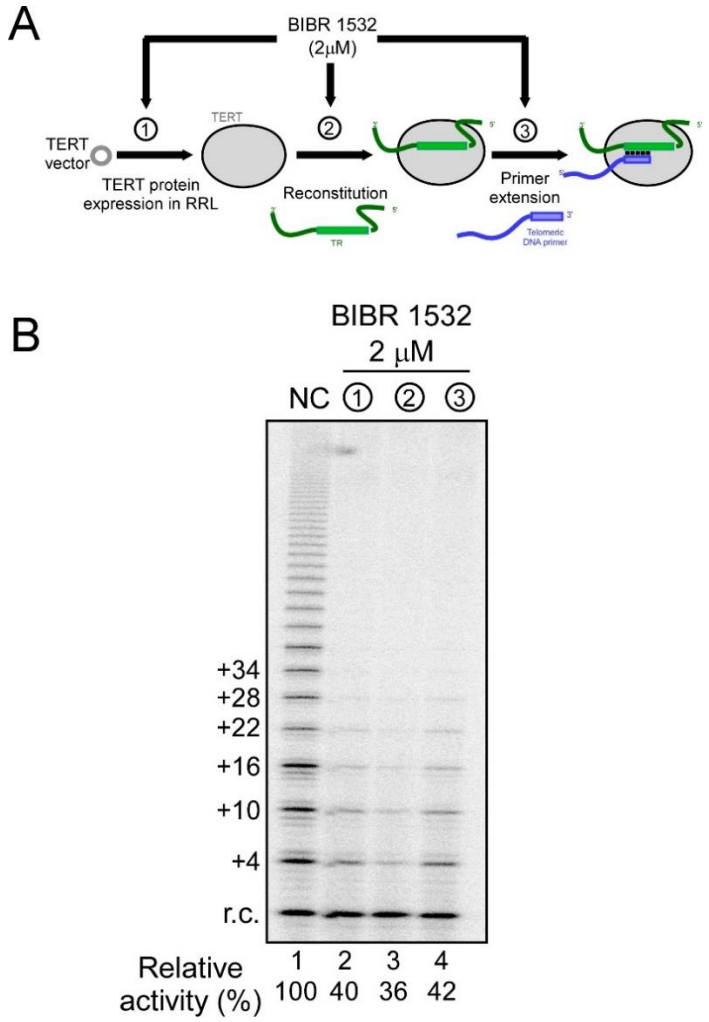

Figure 5.2. BIBR1532 inhibits recombinant telomerase activity not reconstitution process. (A) Schematic of the stages in which BIBR1532 was introduced during the human telomerase *in vitro* reconstitution: Human TERT protein was expressed in RRL using pNFLAG-hTERT vector ①; *In vitro* assembly of telomerase with the two essential hTR fragments, CR4/5 and the pseudoknot (PK) ②; The telomeric DNA primer is the substrate used for the telomerase activity assay ③. Telomerase inhibitor BIBR 1532 was added to each step respectively. (B). Telomerase was reconstituted *in vitro* by RRL and incubated with $(TTAGGG)_3$, dATP, dTTP and ^{32}-P-dGTP in the absence or presence of 2μM of BIBR1532 added at each step. A radiolabeled DNA recovery control (r.c.) was added before product purification and precipitation. Numbers on the left (+4, +10, +16, etc.) of the gel indicate the number of nucleotides added to the primer in each major band. Quantitation of telomerase activity in relation to control are shown below the gel.

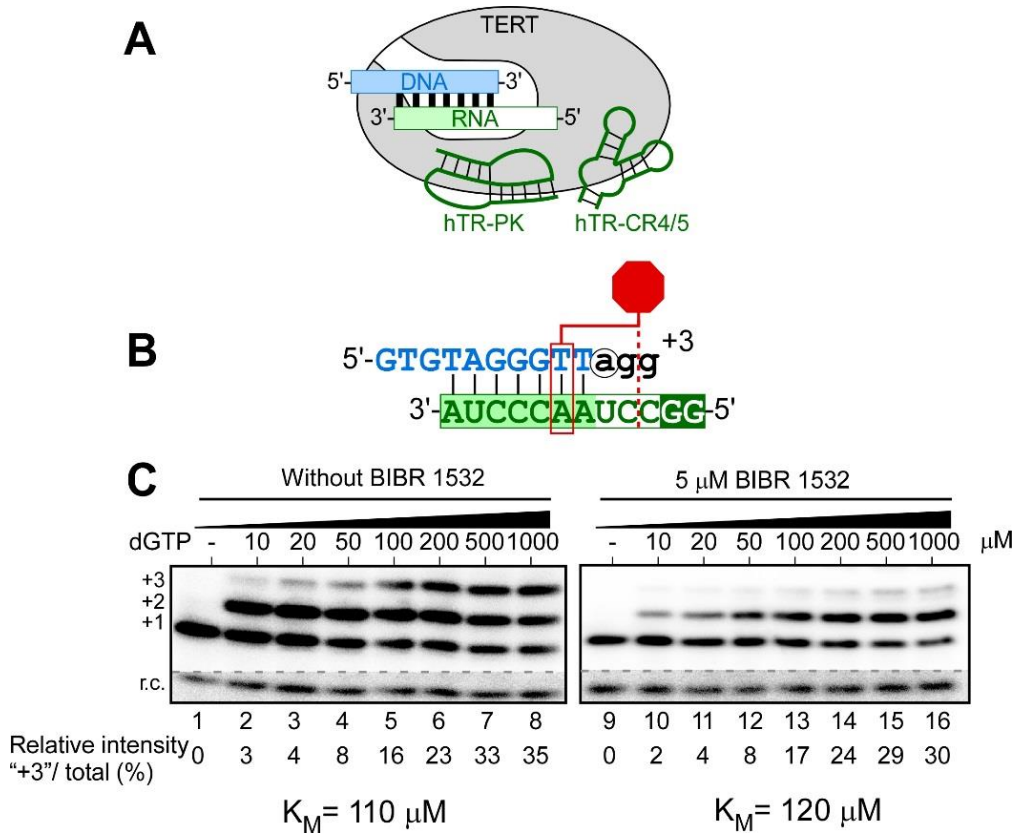

Figure 5.3. BIBR 1532 does not affect nucleotide incorporation kinetics. (A) *In vitro* assembly of template-free (TF) telomerase. TF telomerase was reconstituted by assembling *in vitro* expressed human TERT protein with the two essential hTR fragments, CR4/5 and the pseudoknot (PK) that had the template region excised. (B) The pre-annealed DNA primer and RNA template are the substrate used for the TF telomerase activity assay. The nucleotides added (black) to the DNA in the hybrid are shown, with the first incorporation a ^{32}P-dATP (circled) to determine the apparent K_M for the 1st nucleotide incorporation with or without telomerase inhibitor BIBR 1532 (5 μM). (C) Representative gels for K_M^{app} measurements. Numbers on the left (+1, +2, +3.) of the gel indicate the number of nucleotides added to the primer. A ^{32}P end-labeled DNA recovery control (r.c.) was added before product purification and precipitation. At the bottom of the gel is the quantification of the intensity of the +3 products over the total intensity of products for the specified nucleotide concentration. The Michaelis–Menten equation, $Y=V_{max}*X/(K_M+X)$, was used to fit the nonlinear curve to determine the K_M^{app}.

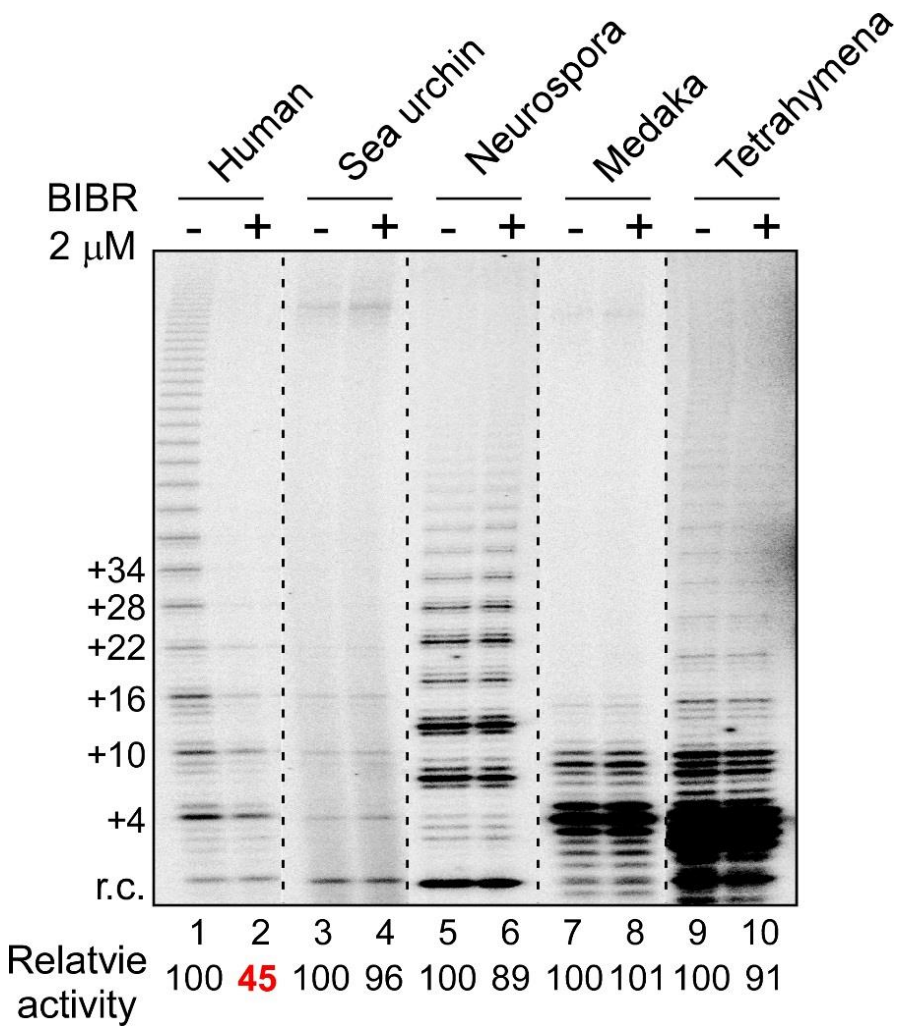

Figure 5.4. BIBR 1532 specifically inhibits human telomerase activity but not other species. *In vitro* reconstituted telomerases of human, purple sea urchin, *N. crassa*, *Tetrahymena* and medaka were analyzed with specific DNA substrates, dATP, dTTP and labeled with ^{32}P-dGTP in the presence (+) or absence (−) of 2 μM BIBR 1532 as denoted above the gel. Numbers on the left (+4, +10, +16 etc.) of the gel indicate the number of nucleotides added to the substrate primer. A ^{32}P end-labeled 18-mer oligonucleotide was used as a recovery control (r.c.). At the bottom of the gel is the quantification of the relative total intensity normalized by recovery control.

CHAPTER 6

EXPLORATION OF HTERT DOMAIN AND HTR TEMPLATE REGIOIN FOR TELOMEASE ACTIVITY AND PROCESSIVITY

6.1 Abstract

Telomerase is a ribonucleoprotein (RNP) enzyme requiring the catalytic subunit telomerase reverse transcriptase (TERT) protein and the integral telomerase RNA (TR) component. The featured ability of TERT to precisely utilize the short template region within TR for telomeric DNA synthesis is different from all known DNA polymerases or reverse transcriptase. The template sequence of the TR not only determines the sequence of the substrate, but also play an important role in determining telomerase enzymatic function, including repeat addition processivity and rate. Previously we have discovered the embedding the pause signal in human TR sequence to arrest nucleotide incorporation when reaching the end of the template. This self-regulating system is crucial for the fidelity of telomeric DNA synthesis. To determine the detailed mechanism for sequence-dependent pausing of telomerase enzymatic activity, we investigate on the motif E of hTERT, which close to the active site of the telomerase. Meanwhile, we also tried to elucidate the role of the hTR template region for its role in the template translocation process. In sum, we use the mutagenesis of the hTERT and hTR subunits to explore motif E residues and hTR nucleotide sequence for their role in the telomerase enzymatic function.

6.2 Introduction

Telomerase is a ribonucleoprotein complex, including a catalytic protein subunit, and an integral RNA subunit. The telomerase reverse transcriptase (TERT) contains the polymerase activity to utilize a short region within the telomerase RNA

(TR) as the template for the telomeric DNA synthesis. In addition to servings as a template for DNA synthesis, the hTR assists in the realignment of substrate at the end of each round product synthesis. The base-pairing interaction with the alignment region allows proper positioning of the telomeric DNA for the next round of polymerization. Previous studies have been shown the hTR temple sequence play an important role for the telomerase enzymatic function, including repeat addition rate (Drosopoulos et al, 2005; Drosopoulos & Prasad, 2010). The sequences in the RNA provide the pausing signal together with template boundary elements defined the boundary for high-fidelity synthesis of telomeric DNA repeats (Brown et al, 2014).

The catalytic subunit of human telomerase, hTERT, contains conserved motifs common to retroviral reverse transcriptase and telomerase. The initial identification of the TERT protein was facilitated from the homology model to the traditional reverse transcriptase (Lingner et al, 1997). The sequence analysis of hTERT revealed the presence of conserved motifs important for enzymatic function. The hTERT RT motif consist of two subdomains, which resemble the finger and palm subdomains of the reverse transcriptase (Wyatt et al, 2010). These domains are connected by the conserved motif E, which include the primer grip region (Gillis et al, 2008). The treading molecular model indicates the loop of the motif E may direct interaction with DNA/RNA duplex in the active site. Previously we have discovered that telomerase recognizes a dT:rA base-pair in the DNA/RNA duplex as the pausing signal to terminate telomerase nucleotide addition activity (Brown et al, 2014). To further determine the detailed mechanism for sequence-dependent pausing on telomerase enzymatic activity, we did the alanine screen test the function of the residues of the motif E for the telomerase activity as well as a repeat addition processivity.

6.3 Material and Methods

Plasmid construction and mutagenesis.

Specific mutations in the human TERT genes were introduced into the pNFLAG-hTERT by site directed mutagenesis using overlapping PCR strategy (Ge & Rudolph, 1997). Intended mutations were confirmed by sequencing.

In vitro reconstitution of human telomerase.

Human TERT protein was expressed in rabbit reticulocyte lysate (RRL) from the pNFLAG-hTERT plasmid DNA using the TnT T7 Quick Coupled transcription/translation kit (Promega) following manufacturer's instructions (Xie et al, 2010). The hTR pseudoknot (residues 32–195) and CR4/5 (residues 239–328) fragments were *in vitro* transcribed, gel purified, and assembled together with the TERT protein in RRL for 30 min at 30°C at a final concentration of 1.0 μM (Brown et al, 2014; Qi et al, 2012). For template free human telomerase, the hTR pseudoknot (residues 64–184) and CR4/5 (residues 239–328) fragments were *in vitro* transcribed, gel purified, and assembled together with the TERT protein in RRL for 30 min at 30°C at a final concentration of 1.0 μM (Brown et al, 2014; Qi et al, 2012).

Telomerase direct primer-extension assay.

One microliters *in vitro* reconstituted telomerase enzyme was assayed in a 10 μL reaction containing 1x telomerase reaction buffer, 1 μM DNA primer, denoted dNTP, and 0.165 μM of denoted α-^{32}P-dGGP. Reactions were incubated at 30°C for 60 min and terminated by phenol/chloroform extraction, followed by ethanol precipitation. The DNA products were resolved on a 10% (wt/vol) polyacrylamide/8 M urea denaturing gel, dried, exposed to a phosphorstorage screen and imaged on a Bio-Rad FX-Pro phosphorimager. For template free telomerase, 1μL of RRL

reconstituted enzyme was assayed in a 10 μL reaction containing 1X telomerase reaction buffer, specified dNTPs and 0.165 μM of the denoted α-^{32}P-dNTP. Reactions were incubated at 30°C for 60 min and terminated by phenol/chloroform extraction, followed by ethanol precipitation. The DNA products were resolved on a 15% (wt/vol) polyacrylamide/8 M urea denaturing gel, dried, exposed to a phosphor rstorage screen and imaged on a Bio-Rad FX-Pro phosphorimager. The quantification is same as described above.

6.4 Results

Some residue mutants of motif E displays defects in telomerase enzymatic function.

Motif E located in the RT domain of the TERT, which includes a conserved loop region for primer grip in many species. (Figure 6.1) The structure model predicts the loop may interact with the DNA/RNA duplex directly at the 3' end close to the active site of the enzyme (Gillis et al, 2008). To experimentally explore the function of each residue of motif E, comprehensive alanine as well as tyrosine screening mutagenesis were performed. Coding sequence mutations were generated by overlap PCR. The mutants of motif E were expressed reconstituted in RRL with *in vitro* transcribed two hTR fragments for the activity assay. Certain residues in motif E appear to be essential for telomerase enzymatic functions. The mutants F928Y, F928A, W930A, G932Y, D936A, D936Y, R938A, V942Y, D945Y, I954A, G963A, A966Y, G967A abolished the telomerase activity, which behave like the catalytically inactive hTERT mutant K868N. (Figure 6.2) Some other mutants including G932Y, G932A, L933Y, Y946A, Y949A, T952Y, I954Y, S957Y, L958A, L958Y, G967Y significantly decreased telomerase repeat addition processivity, which show similar patterns like the motif T mutant K570A. (Figure 6.2)

We have identified an embedding pausing previously (see chapter 2). To test if the residues from motif E contribute to the arrest of the nucleotide addition, we investigated mutants function in template free system. The template free telomerase mutants were assayed with DNA/RNA duplex. (Figure 6.3) In presence of ^{32}P-dATP and dGTP, the avian myeloblastosis virus (AMV) RT extended the DNA primers to the RNA template. DNA primer was extended by one or two nucleotides by the wild type enzyme with or without the presence of dGTP, because of the pausing signal. (Figure 6.3) The mutant S948Y shows the +3 band in the presence of dGTP, which indicates reaching the end of the template. However, compare with AMV RT, the intensity of the +3 band is relatively weaker than +2 bands. The last nucleotide incorporation could because of the higher total activity instead of the deficiency of the pausing signal. (Figure 6.3) Further test or structural information required to elucidate the mechanism of how human telomerase arrest nucleotide addition at the end of the template region.

Human telomerase RNA template sequence plays an important role for enzymatic function.

Human telomerase utilizes the short RNA template within the hTR for telomease DNA repeats synthesis. *In vitro* telomerase activity assay, the product observed as six nucleotide ladder patterns, each band of the ladder representing telomerase stalling or dissociation of product. To test the sequence of hTR template affect telomerase function, a series of mutants were created and tested. (Figure 6.4) The mechanistic model for human telomerase repeat synthesis, including extension of the DNA substrate to the end of the template sequence followed by template translocation and repositioning of the 3’ end product with the 3’ end of the template

region of hTR. The alignment region which contains partial repeats of the template sequence played an important role for the repeat addition processivity. The previous study has shown the alignment regions contribute to the repeat addition processivity (Drosopoulos et al, 2005). In our test, the mutants 48U49U and 47A significant reduced repeat addition processivity compared with 48U49U54U55U and 47A53A mutants. This indicates the base-pair at the alignment regions after template translocation is crucial for the telomerase repeat addition processivity. (Figure 6.5) Some of the mutants including 48C54C and 48C49C54C55C increased the higher weigh molecular product accumulation comparison with the wild type enzyme. (Figure 6.6) The 48C54C mutant has been tested previously showed a higher repeat addition rate (Drosopoulos et al, 2005). This mutant showed relative higher processivity with ^{32}P-dGTP or ^{32}P-dTTP labeling. The mutant 48C49C54C55C shows near inactive for ^{32}P-dTTP labeling because of unable to incorporate dTTP according to the template sequence. (Figure 6.6) Interestingly, the 47C48C53C54C mutant, which shows less processive than wild type with ^{32}P-dGTP labeling but more processive with ^{32}P-dTTP labeling. One explanation could be the concentration of cold dGTP affect the enzymatic function. The total concentration of dGTP is much higher with ^{32}P-dTTP labeling. The other mutants 46U52U and 46U51U52U both showed deficiency for the repeat addition processivity. (Figure 6.6) In chapter 3, we have shown the Δpause mutant is much more processive than the wild type enzyme and it lack the stimulation by higher concentrations of dGTP. Compare with the Δpause mutant, the mutants 48U54U and 49U55U, which only convert one of the T-A base-pair to A-U base-pair, both showed accumulation of higher molecular weight product. (Figure 6.7) Importantly, the processivity of both 48U54U and 49U55U

mutants can be stimulated by the higher concentration of the dGTP. Since the existing of the pause signal within the mutants, it further to demonstrate that the incorporation of the first nucleotide after the pause signal is essential for the catalytic cycle of human telomerase. (Figure 6.7)

6.5 Discussion

Even though with increasing knowledge of the telomerase enzyme, there are still many questions about the unique mechanism of human telomerase remain unclear. This project aims to characterizing the role of the hTERT and TR residues by mutational analysis. The catalytic domain of hTERT contains evolutionarily conserved RT motifs crucial for telomerase function. (Figure 6.1) The RT domain of the hTERT can be organized into two subdomains that resemble the 'fingers' and 'palm' in the conventional reverse transcriptase (Gillis et al, 2008). The motif E contains a conserved primer grip region connect the subdomains. According to the molecular model, the motif E loop may directly interact with the DNA/RNA duplex. Previously we have identified telomerase has the ability of recognizing a single base-pair (bp) signal in the DNA primer/RNA template duplex to terminate nucleotide addition in template free telomerase system (Brown et al, 2014). (Chapter 2) The sequence-dependent pause signal could be recognized by TERT protein residues close to the DNA/RNA duplex near the active site. The amino acid residues in hTERT near the DNA/RNA duplex are possibly making physical contact with the dT-rA base pair. The comprehensive mutagenesis studies by alanine and tyrosine screening of the motif E failed to find a residue responsible for the pause signal by allowing TF telomerase incorporate nucleotide after the pause site. (Figure 6.3) However, some of the residues have played an important role for the repeat addition processivity of

human telomerase. (Figure 6.3) Further studies could be focused on exploring the mechanism of those residues for human telomerase enzymatic functions.

In addition to providing the template for telomeric DNA repeat synthesis, hTR contains motifs necessary for the reconstitution and catalytic function (Podlevsky & Chen, 2012). The mutations on the hTR template, both the alignment and templating region, have been shown directly influenced overall repeat addition rate and processivity (Drosopoulos et al, 2005). It has been demonstrated the complementarity of TR templating and alignment region is required for the processive enzymatic function (Chen & Greider, 2003; Gavory et al, 2002). Our date consistent with this conclusion: the mutants 48U49U as well as 47A show obvious deficiency for the repeat addition processivity compares with 48U49U54U55U and 47A53A. (Figure 6.5) Previously, we have shown that the pause signal responsible for the low processivity and rate of human telomerase. (Chapter 3) The mutants 48U54U and 49U55U, which are only mutated one rA residue in the hTR template and the pause signal is not completely depleted, showed accumulation of the higher molecular weight product comparison with the wild type enzyme. (Figure 6.7) More importantly, a contrast to the Δpause mutant that independent of dGTP stimulation of repeat addition activity, higher concentration of dGTP increased the higher molecular weight product by 48U54U and 49U55U mutants. (Figure 6.7) This indicates the first nucleotide incorporation after the pause signal still limited catalytic cycle of the mutant. Taken together, these results provided more information for the protein and RNA subunits of their role in human telomerase.

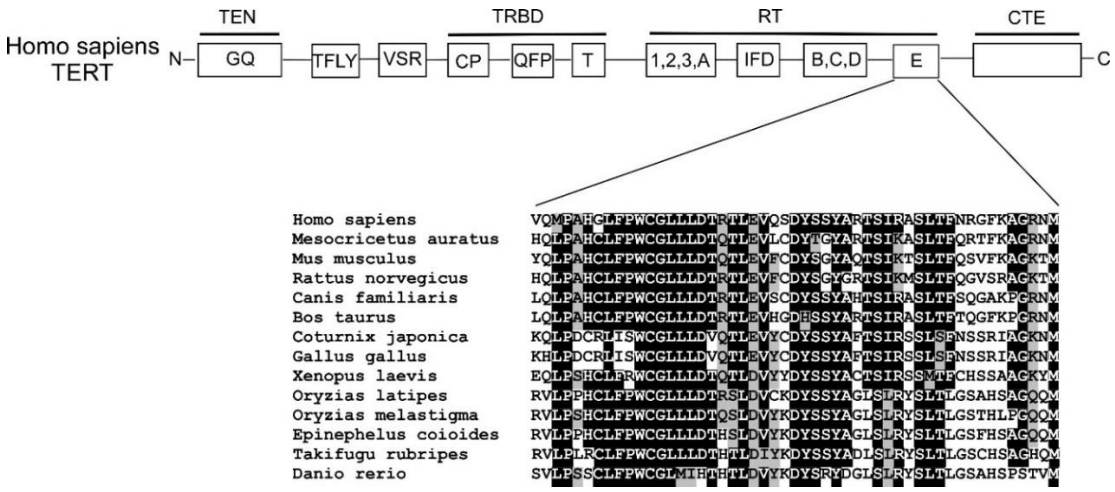

Figure 6.1. Schematic of domain and motif organization of human TERT protein. Sequence alignment of TERT motif E from vertebrates, invertebrates, fungi, plants and ciliates. Darker shading indicates greater identity conservation with the human sequence (<30% light, 30–60% medium and >60% dark).

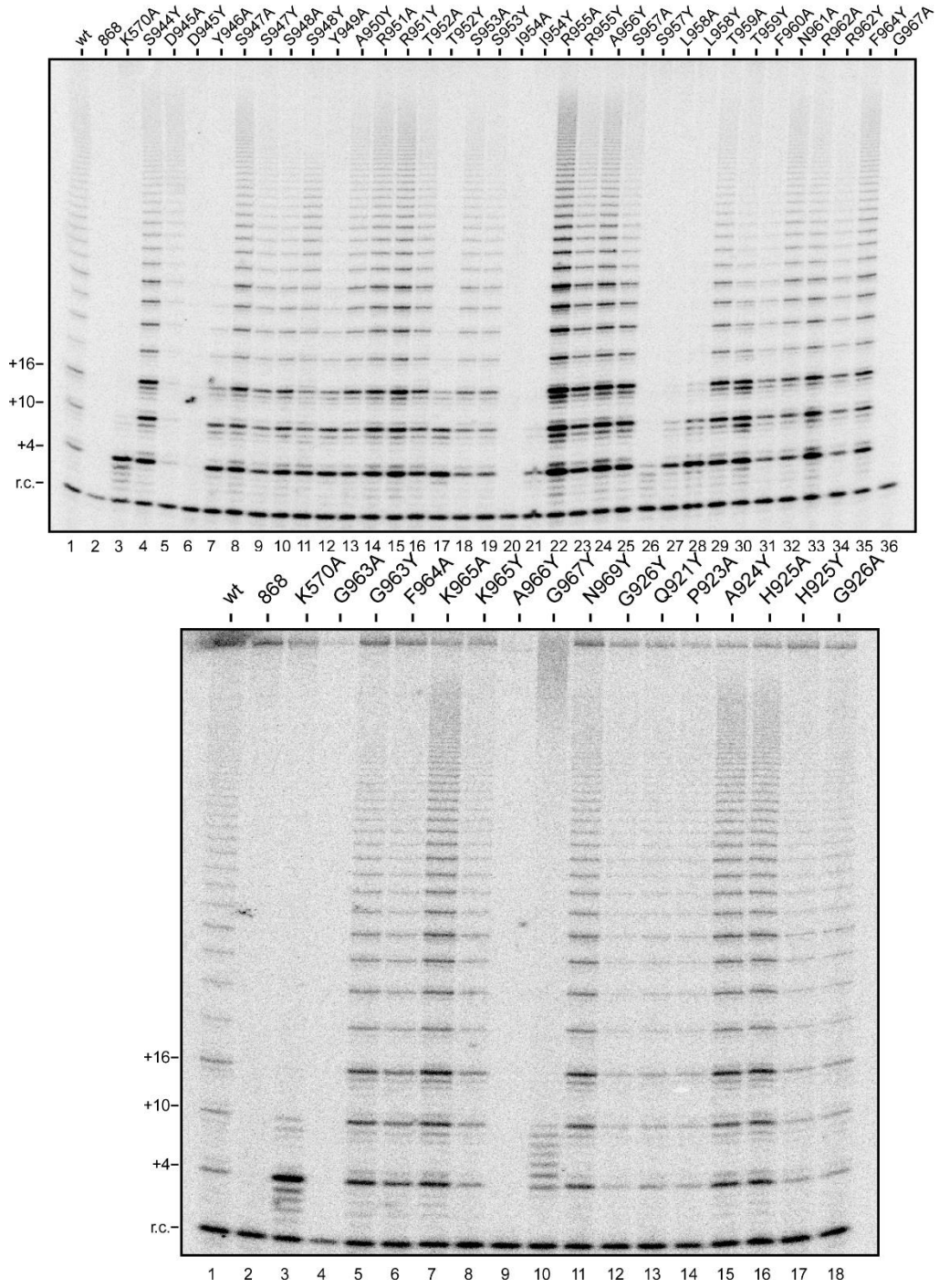
wt
868
K570A
S944Y
D945A
D945Y
Y946A
S947A
S947Y
S948A
S948Y
Y949A
A950Y
R951A
R951Y
T952A
T952Y
S953A
S953Y
I954A
I954Y
R955A
R955Y
A956Y
S957A
S957Y
L958A
L958Y
T959A
T959Y
F960A
N961A
R962A
R962Y
F964Y
G967A
+16
+10
+4
r.c.
1 2 3 4 5 6 7 8 9 10 11 12 13 14 15 16 17 18 19 20 21 22 23 24 25 26 27 28 29 30 31 32 33 34 35 36
wt
868
K570A
G963A
G963Y
F964A
K965A
K965Y
A966Y
G967Y
N969Y
G926Y
Q921Y
P923A
A924Y
H925A
H925Y
G926A
+16
+10
+4
r.c.
1 2 3 4 5 6 7 8 9 10 11 12 13 14 15 16 17 18

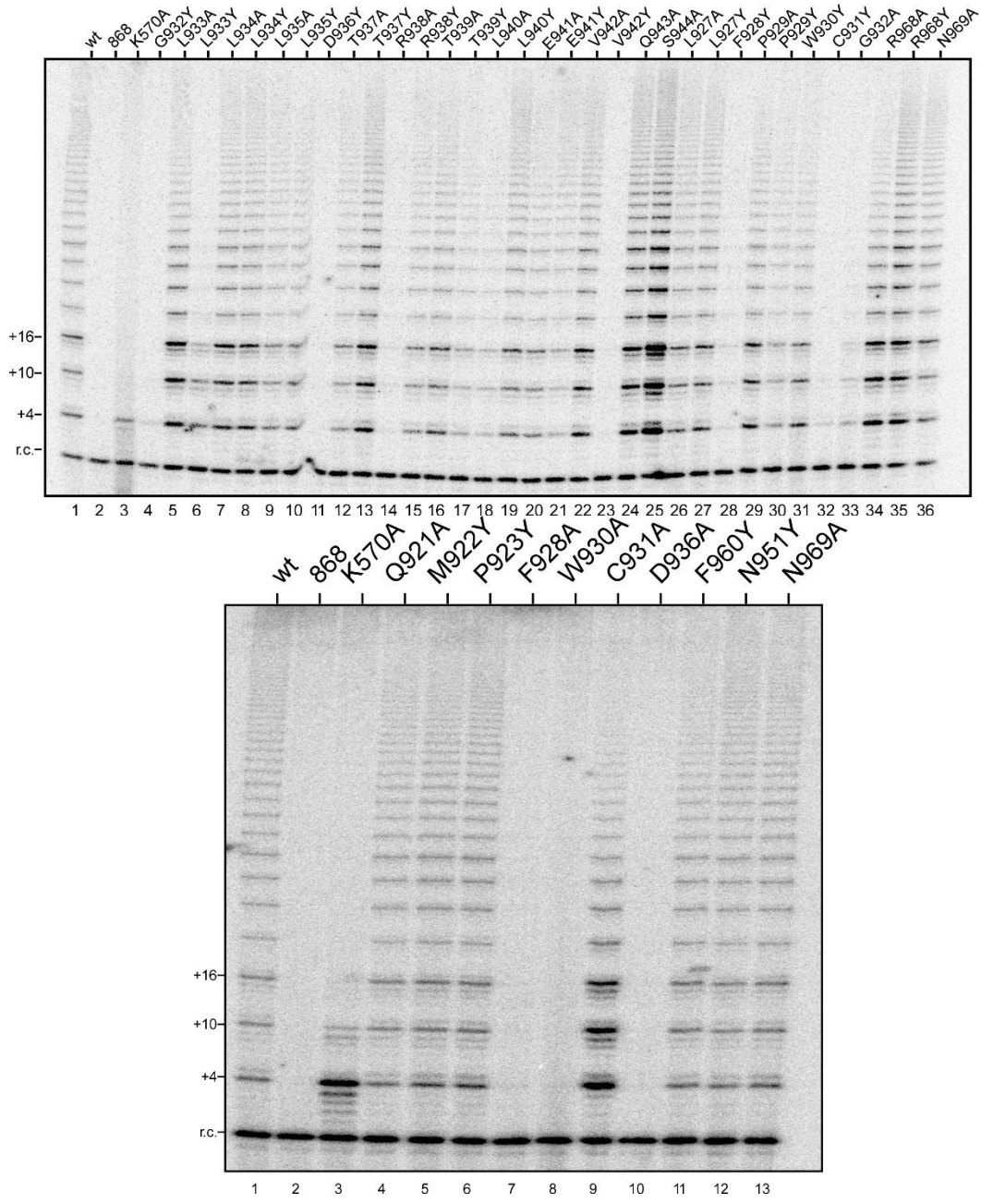
wt
868
K570A
G932Y
L933A
L933Y
L934A
L934Y
L935A
L935Y
D936Y
T937A
T937Y
R938A
R938Y
T939A
T939Y
L940A
L940Y
E941A
E941Y
V942A
V942Y
Q943A
S944A
L927A
L927Y
F928Y
P929A
P929Y
W930Y
C931Y
G932A
R968A
R968Y
N969A
+16
+10
+4
r.c.
1 2 3 4 5 6 7 8 9 10 11 12 13 14 15 16 17 18 19 20 21 22 23 24 25 26 27 28 29 30 31 32 33 34 35 36
wt
868
K570A
Q921A
M922Y
P923Y
F928A
W930A
C931A
D936A
F960Y
N951Y
N969A
+16
+10
+4
r.c.
1 2 3 4 5 6 7 8 9 10 11 12 13

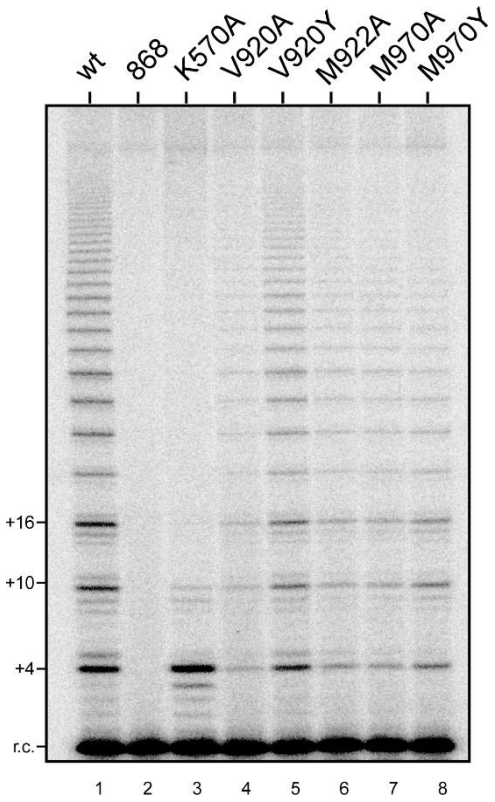

Figure 6.2. Alanine substitution screening of motif E. Activity assays of the motif E mutants. Human telomerases with alanine substitutions in motif E were reconstituted *in vitro* and assayed for activity. $(TTAGGG)_3$ is used as DNA substrate and ^{32}P-dGTP for labeling with unlabeled other nucleotides. Wild type human telomerase as well as catalytical inactive mutant enzyme used as control for each panel. Numbers on the left (+4, +10, +16.) of the gel indicate the number of nucleotides added to the primer in each major band. r.c.: recovery control, a ^{32}P-end-labeled 18-nt DNA oligonucleotide.

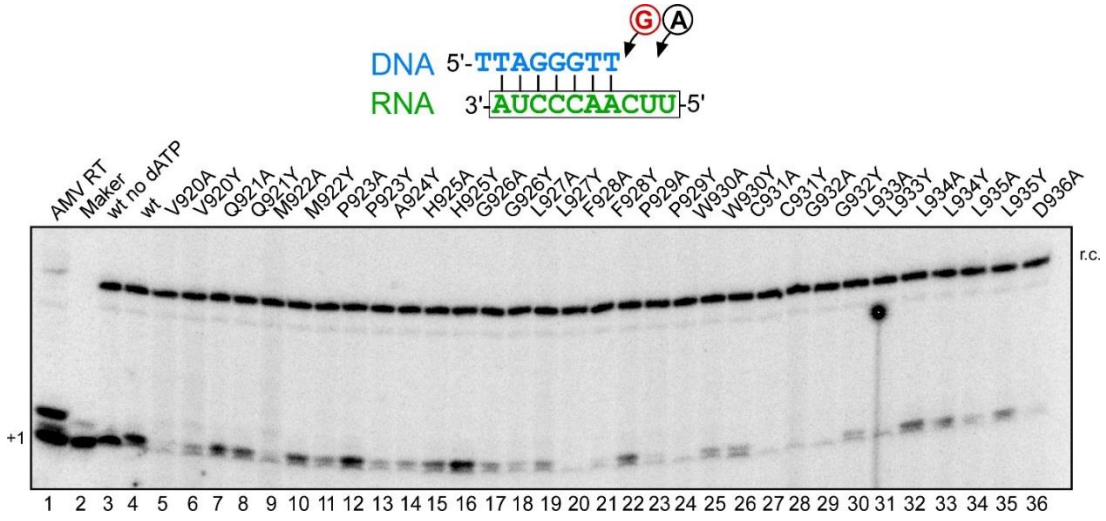

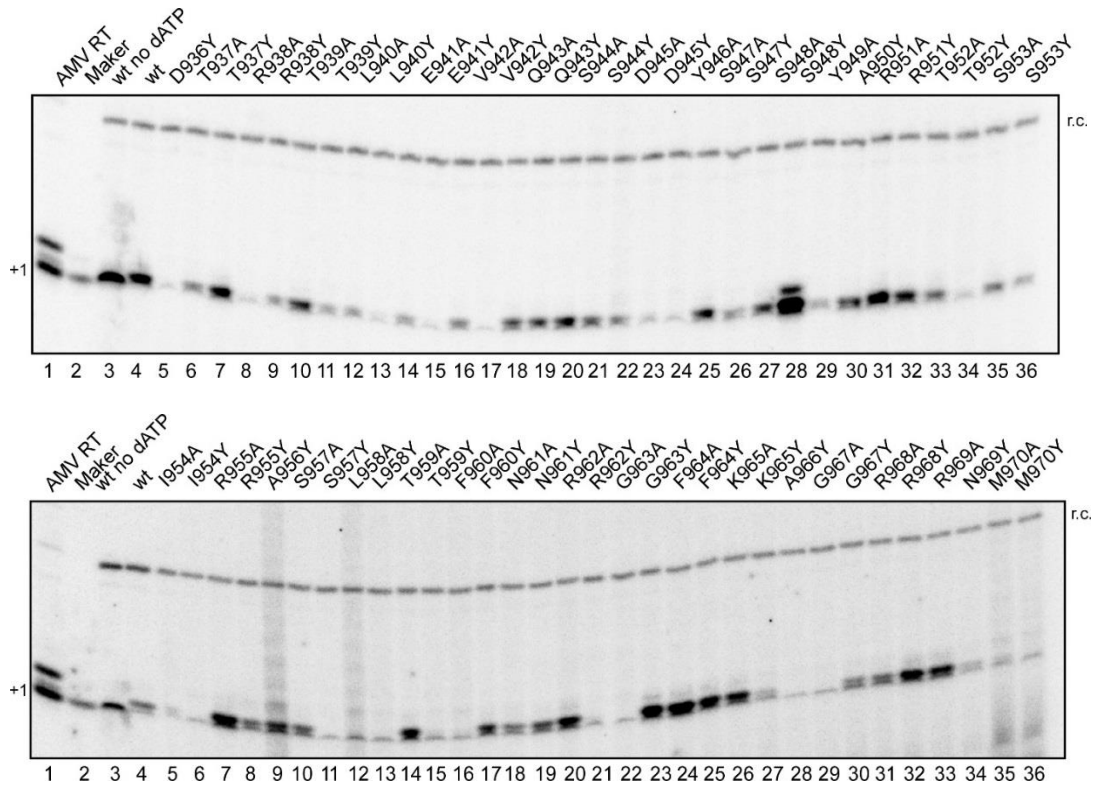
AMV RT
Maker
wt no dATP
wt
D936Y
T937A
T937Y
R938A
R938Y
T939A
T939Y
L940A
L940Y
E941A
E941Y
V942A
V942Y
Q943A
Q943Y
S944A
S944Y
D945A
D945Y
Y946A
S947A
S947Y
S948A
S948Y
Y949A
A950Y
R951A
R951Y
T952A
T952Y
S953A
S953Y
r.c.
+1
1 2 3 4 5 6 7 8 9 10 11 12 13 14 15 16 17 18 19 20 21 22 23 24 25 26 27 28 29 30 31 32 33 34 35 36
AMV RT
Maker
wt no dATP
wt
I954A
I954Y
R955A
R955Y
A956Y
S957A
S957Y
L958A
L958Y
T959A
T959Y
F960A
F960Y
N961A
N961Y
R962A
R962Y
G963A
G963Y
F964A
F964Y
K965A
K965Y
A966Y
G967A
G967Y
R968A
R968Y
R969A
N969Y
M970A
M970Y
r.c.
+1
1 2 3 4 5 6 7 8 9 10 11 12 13 14 15 16 17 18 19 20 21 22 23 24 25 26 27 28 29 30 31 32 33 34 35 36

Figure 6.3. Alanine substitution screening of motif E with TF telomerase. Human TF telomerases with alanine substitutions in motif E were reconstituted *in vitro* and assayed for activity. Wild type human telomerase as well as AMV RT used as control for each panel. DNA/RNA duplex is used as substrate and ^{32}P-dATP for labeling with unlabeled dGTP. Numbers on the left (+1) of the gel indicate the number of nucleotides added to the primer in each major band. r.c.: recovery control, a ^{32}P-end-labeled 18-nt DNA oligonucleotide. The DNA primers TTAGGGTT extended by one α-^{32}P-dATP with terminal deoxynucleotidyl transferase (TdT) were included as size markers.

Figure 6.4. Schematic representation of human telomerase template region and its mutants. Sequences of the hTR mutants (bottom). Changes from wild type telomerase sequence are underlined. Predicted product is shown on the right of the bottom. * stand for the non-processive product.

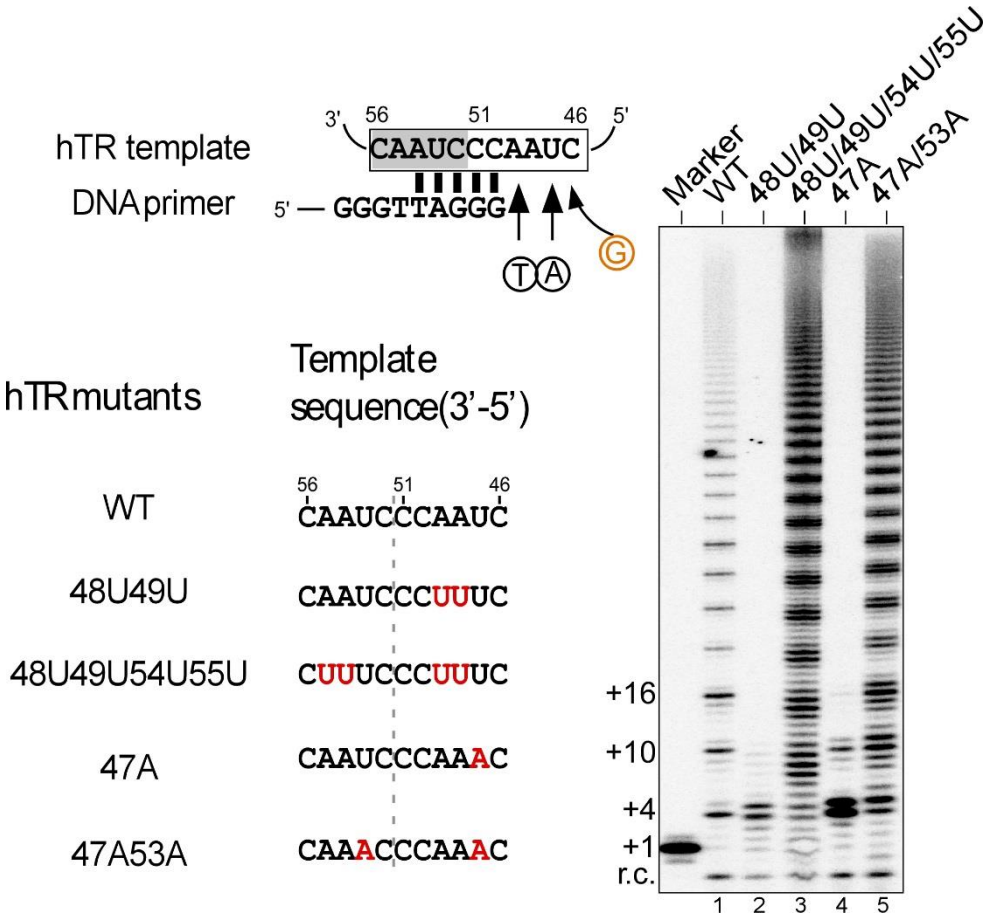

Figure 6.5. Primer extension by human telomerase template mutants. Sequences of hTR mutant templates used in this assay. Direct primer extension assays of telomerase template mutants. (Left) Wild-type and mutant telomerases were reconstituted *in vitro* were assayed in the presence of 0.165 μM ^{32}P-dGTP, 100 μM dATP and dTTP. Numbers to the left of the gel denote the number of nucleotide added to the telomeric primer. An ^{32}P end-labeled DNA recovery control (r.c.) was added before product purification and precipitation. The DNA primers $(TTAGGG)_3$ extended by one α-^{32}P-dTTP with terminal deoxynucleotidyl transferase (TdT) were included as size markers. (Right)

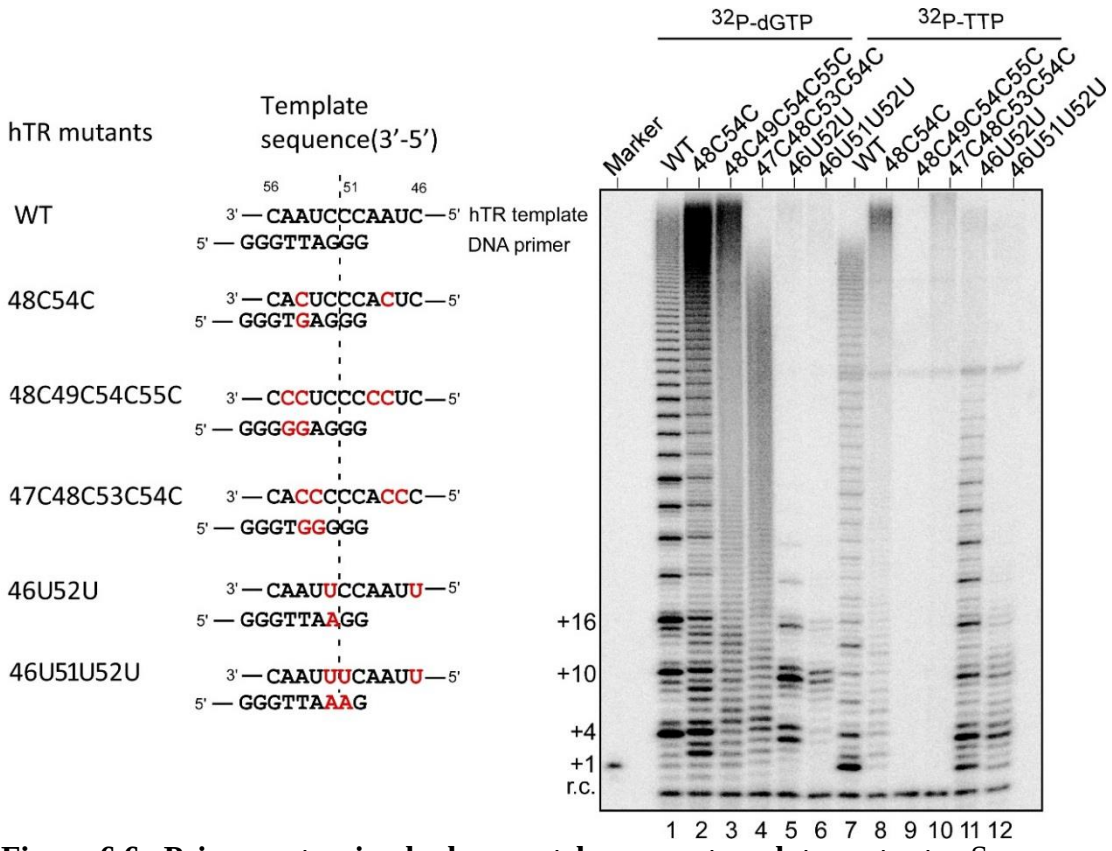

Figure 6.6. Primer extension by human telomerase template mutants. Sequences of hTR mutant templates and the DNA primers used in this assay. Direct primer extension assays of telomerase template mutants. (Left) Wild-type and mutant telomerases were reconstituted *in vitro* were assayed in the presence of 0.165 μM ^{32}P-dGTP, 100 μM dATP and dTTP or 0.165 μM ^{32}P-dTTP, 100 μM dATP and dGTP. Numbers to the left of the gel denote the number of nucleotide added to the telomeric primer. An ^{32}P end-labeled DNA recovery control (r.c.) was added before product purification and precipitation. The DNA primers $(TTAGGG)_3$ extended by one α-^{32}P-dTTP with terminal deoxynucleotidyl transferase (TdT) were included as size markers. (Right)

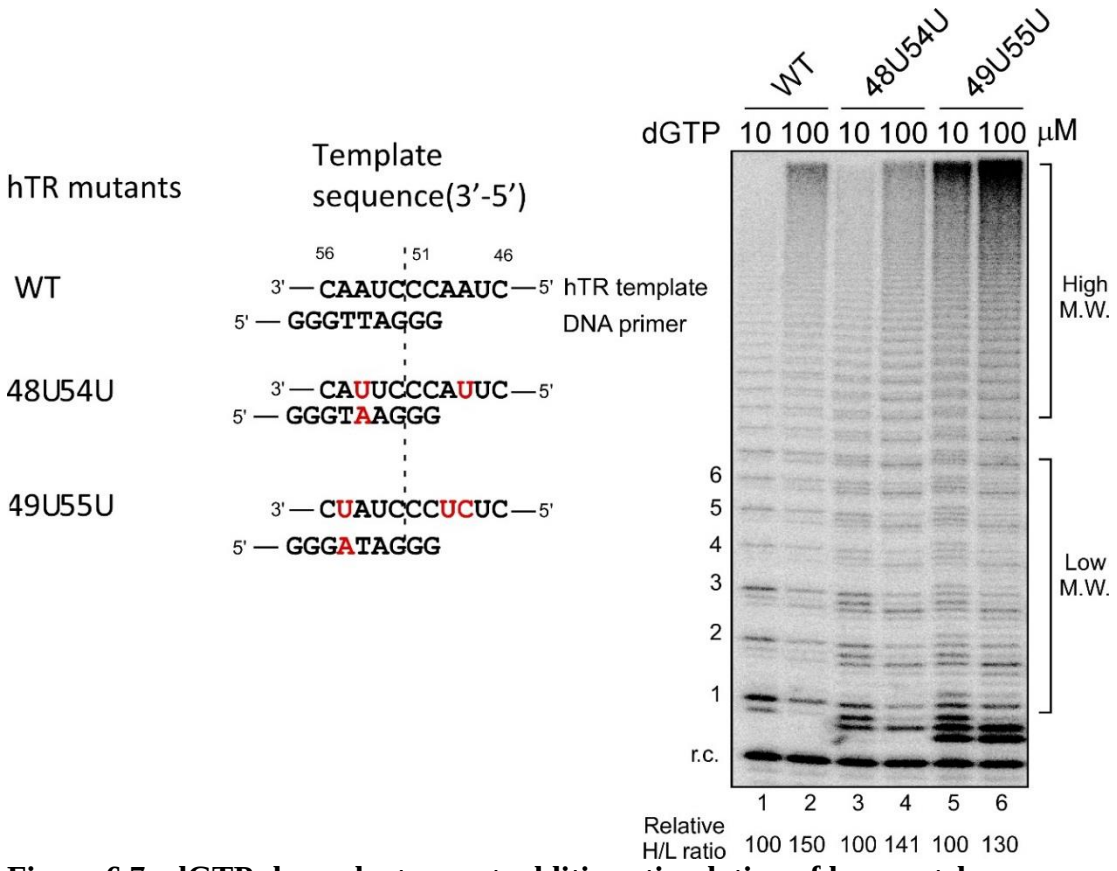

Figure 6.7. dGTP-dependent repeat addition stimulation of human telomerase. Sequences of hTR mutant templates and the DNA primers used in this assay. Direct primer extension assays of telomerase template mutants. (Left) Wild-type and mutant telomerases were reconstituted *in vitro* were assayed in the presence of 0.165 μM ^{32}P-dATP, 100 μM dTTP and 10 or 100 μM dGTP. Numbers to the left of the gel denote the number of repeat added to the telomeric primer. An ^{32}P end-labeled DNA recovery control (r.c.) was added before product purification and precipitation. Ratio as a percent for the intensity of high over low M.W. DNA products generated relative to the reaction with the low nucleotide concentrations. (Right)

REFERENCES

Akiyama BM, Parks JW, Stone MD (2015) The telomerase essential N-terminal domain promotes DNA synthesis by stabilizing short RNA-DNA hybrids. *Nucleic Acids Research* 43: 1-13

Alder JK, Chen JJ-L, Lancaster L, Danoff S, Su S-c, Cogan JD, Vulto I, Xie M, Qi X, Tuder RM, Phillips Ja, Lansdorp PM, Loyd JE, Armanios MY (2008) Short telomeres are a risk factor for idiopathic pulmonary fibrosis. *Proceedings of the National Academy of Sciences of the United States of America* 105: 13051-13056

Alder JK, Cogan JD, Brown AF, Anderson CJ, Lawson WE, Lansdorp PM, Phillips Ja, Loyd JE, Chen JJ-L, Armanios M (2011) Ancestral mutation in telomerase causes defects in repeat addition processivity and manifests as familial pulmonary fibrosis. *PLoS genetics* 7: e1001352

Armanios MY (2009) Syndromes of Telomere Shortening. *Annual Review of Genomics and Human Genetics* 10: 45-61

Armanios MY, Chen JJ-L, Chang Y-PC, Brodsky Ra, Hawkins A, Griffin Ca, Eshleman JR, Cohen AR, Chakravarti A, Hamosh A, Greider CW (2005) Haploinsufficiency of telomerase reverse transcriptase leads to anticipation in autosomal dominant dyskeratosis congenita. *Proceedings of the National Academy of Sciences of the United States of America* 102: 15960-15964

Armanios MY, Chen JJ-L, Cogan JD, Alder JK, Ingersoll RG, Markin C, Lawson WE, Xie MY, Vulto I, Phillips JA, Lansdorp PM, Greider CW, Loyd JE (2007) Telomerase mutations in families with idiopathic pulmonary fibrosis. *New England Journal of Medicine* 356: 1317-1326

Arndt GM, MacKenzie KL (2016) New prospects for targeting telomerase beyond the telomere. *Nature Reviews Cancer* 16: 508-524

Arnoult N, Karlseder J (2015) Complex interactions between the DNA-damage response and mammalian telomeres. *Nature Structural & Molecular Biology* 22: 859-866

Autexier C, Lue NF (2006) The structure and function of telomerase reverse transcriptase. *Annual Review of Biochemistry* 75: 493-517

Barma DK, Elayadi A, Falck JR, Corey DR (2003) Inhibition of telomerase by BIBR 1532 and related analogues. *Bioorganic & Medicinal Chemistry Letters* 13: 1333-1336

Bashash D, Ghaffari SH, Zaker F, Hezave K, Kazerani M, Ghavamzadeh A, Alimoghaddam K, Mosavi SA, Gharehbaghian A, Vossough P (2012) Direct short-term cytotoxic effects of BIBR 1532 on acute promyelocytic leukemia cells through

induction of p21 coupled with downregulation of c-Myc and hTERT transcription. *Cancer Investigation* 30: 57-64

Bashash D, Zareii M, Safaroghli-Azar A, Omrani MD, Ghaffari SH (2017) Inhibition of telomerase using BIBR1532 enhances doxorubicin-induced apoptosis in pre-B acute lymphoblastic leukemia cells. *Hematology* 22: 330-340

Berman AJ, Akiyama BM, Stone MD, Cech TR (2011) The RNA accordion model for template positioning by telomerase RNA during telomeric DNA synthesis. *Nature Structural & Molecular Biology* 18: 1371-5

Blackburn EH, Collins K (2011) Telomerase: An RNP Enzyme Synthesizes DNA. *Cold Spring Harbor perspectives in biology* 3: a003558

Blackburn EH, Gall JG (1978) A tandemly repeated sequence at the termini of the extrachromosomal ribosomal RNA genes in Tetrahymena. *Journal of Molecular Biology* 120: 33-53

Bley CJ, Qi X, Rand DP, Borges CR, Nelson RW, Chen JJ-L (2011) RNA-protein binding interface in the telomerase ribonucleoprotein. *Proceedings of the National Academy of Sciences of the United States of America* 108: 20333-20338

Bodnar AG, Ouellette M, Frolkis M, Holt SE, Chiu CP, Morin GB, Harley CB, Shay JW, Lichtsteiner S, Wright WE (1998) Extension of life-span by introduction of telomerase into normal human cells. *Science* 279: 349-352

Bosoy D, Lue NF (2001) Functional analysis of conserved residues in the putative "finger" domain of telomerase reverse transcriptase. *Journal of Biological Chemistry* 276: 46305-46312

Bradshaw PC, Samuels DC (2005) A computational model of mitochondrial deoxynucleotide metabolism and DNA replication. *American Journal of Physiology Cell Physiology* 288: C989-1002

Brassat U, Balabanov S, Bali D, Dierlamm J, Braig M, Hartmann U, Sirma H, Gunes C, Wege H, Fehse B, Gontarewicz A, Dikomey E, Borgmann K, Brumrnendorf TH (2011) Functional p53 is required for effective execution of telomerase inhibition in BCR-ABL-positive CML cells. *Experimental Hematology* 39: 66-76

Brown AF, Podlevsky JD, Qi XD, Chen YN, Xie MY, Chen JJ-L (2014) A self-regulating template in human telomerase. *Proceedings of the National Academy of Sciences of the United States of America* 111: 11311-11316

Brown Y, Abraham M, Pearl S, Kabaha MM, Elboher E, Tzfati Y (2007) A critical three-way junction is conserved in budding yeast and vertebrate telomerase RNAs. *Nucleic Acids Research* 35: 6280-6289

Bryan C, Rice C, Hoffman H, Harkisheimer M, Sweeney M, Skordalakes E (2015) Structural Basis of Telomerase Inhibition by the Highly Specific BIBR1532. *Structure* 23: 1934-1942

Bryan TM, Goodrich KJ, Cech TR (2000) Telomerase RNA bound by protein motifs specific to telomerase reverse transcriptase. *Molecular Cell* 6: 493-499

Chen JJ-L, Blasco Ma, Greider CW (2000) Secondary structure of vertebrate telomerase RNA. *Cell* 100: 503-514

Chen JJ-L, Greider CW (2003a) Determinants in mammalian telomerase RNA that mediate enzyme processivity and cross-species incompatibility. *The EMBO Journal* 22: 304-314

Chen JJ-L, Greider CW (2003b) Template boundary definition in mammalian telomerase. *Genes & Development*: 2747-2752

Chen JJ-L, Greider CW (2004) An emerging consensus for telomerase RNA structure. *Proceedings of the National Academy of Sciences of the United States of America* 101: 14683-14684

Chen JJ-L, Greider CW (2005) Functional analysis of the pseudoknot structure in human telomerase RNA. *Proceedings of the National Academy of Sciences of the United States of America* 102: 8080-8085; discussion 8077-8089

Chen JJ-L, Opperman KK, Greider CW (2002) A critical stem-loop structure in the CR4-CR5 domain of mammalian telomerase RNA. *Nucleic Acids Research* 30: 592-597

Chen YN, Zhang YM (2016) Functional and mechanistic analysis of telomerase: An antitumor drug target. *Pharmacology & Therapeutics* 163: 24-47

Cheng X, Roberts RJ (2001) AdoMet-dependent methylation, DNA methyltransferases and base flipping. *Nucleic Acids Research* 29: 3784-3795

Collins K (2006) The biogenesis and regulation of telomerase holoenzymes. *Nature Reviews Molecular Cell Biology* 7: 484-494

Collins K, Greider CW (1995) Utilization of ribonucleotides and RNA primers by Tetrahymena telomerase. *The EMBO Journal* 14: 5422-5432

Counter CM, Meyerson M, Eaton EN, Weinberg RA (1997) The catalytic subunit of yeast telomerase. *Proceedings of the National Academy of Sciences of the United States of America* 94: 9202-9207

Cristofari G, Adolf E, Reichenbach P, Sikora K, Terns RM, Terns MP, Lingner J (2007) Human telomerase RNA accumulation in Cajal bodies facilitates telomerase recruitment to telomeres and telomere elongation. *Molecular Cell* 27: 882-889

Damm K, Hemmann U, Garin-Chesa P, Hauel N, Kauffmann I, Priepke H, Niestroj C, Daiber C, Enenkel B, Guilliard B, Lauritsch I, Müller E, Pascolo E, Sauter G, Pantic M, Martens UM, Wenz C, Lingner J, Kraut N, Rettig WJ, Schnapp a (2001) A highly selective telomerase inhibitor limiting human cancer cell proliferation. *The EMBO Journal* 20: 6958-6968

de Lange T (2009) How telomeres solve the end-protection problem. *Science* 326: 948-952

Dokal I (2003) Dyskeratosis congenita: its link to telomerase and aplastic anaemia. *Blood Reviews* 17: 217-225

Drosopoulos WC, DiRenzo R, Prasad VR (2005) Human telomerase RNA template sequence is a determinant of telomere repeat extension rate. *Journal of Biological Chemistry* 280: 32801-32810

Drosopoulos WC, Prasad VR (2010) The telomerase-specific T motif is a restrictive determinant of repetitive reverse transcription by human telomerase. *Molecular and Cellular Biology* 30: 447-459

Du H-Y, Pumbo E, Ivanovich J, An P, Maziarz RT, Reiss UM, Chirnomas D, Shimamura A, Vlachos A, Lipton JM, Goyal RK, Goldman F, Wilson DB, Mason PJ, Bessler M (2009) TERC and TERT gene mutations in patients with bone marrow failure and the significance of telomere length measurements. *Blood* 113: 309-316

Eckert B, Collins K (2012) Roles of the telomerase reverse transcriptase N-terminal domain in the assembly and activity of Tetrahymena telomerase holoenzyme. *Journal of Biological Chemistry* 287: 12805-12814

Egan ED, Collins KL (2010) Specificity and stoichiometry of subunit interactions in the human telomerase holoenzyme assembled in vivo. *Molecular and Cellular Biology* 30: 2775-2786

El-Daly H, Kull M, Zimmermann S, Pantic M, Waller CF, Martens UM (2005) Selective cytotoxicity and telomere damage in leukemia cells using the telomerase inhibitor BIBR1532. *Blood* 105: 1742-1749

Finger SN, Bryan TM (2008) Multiple DNA-binding sites in Tetrahymena telomerase. *Nucleic Acids Research* 36: 1260-1272

Fogarty PF, Yamaguchi H, Wiestner A, Baerlocher GM, Sloand E, Zeng WS, Read EJ, Lansdorp PM, Young NS (2003) Late presentation of dyskeratosis congenita as apparently acquired aplastic anaemia due to mutations in telomerase RNA. *The Lancet* 362: 1628-1630

Förstemann K, Lingner J (2005) Telomerase limits the extent of base pairing between template RNA and telomeric DNA. *The EMBO Journal* 6: 361-366

Förstemann K, Zaug AJ, Cech TR, Lingner J (2003) Yeast telomerase is specialized for C/A-rich RNA templates. *Nucleic Acids Research* 31: 1646-1655

Fu D, Collins K (2003) Distinct biogenesis pathways for human telomerase RNA and H/ACA small nucleolar RNAs. *Molecular Cell* 11: 1361-1372

Garforth SJ, Parniak MA, Prasad VR (2008) Utilization of a deoxynucleoside diphosphate substrate by HIV reverse transcriptase. *PLoS ONE* 3: e2074

Gavory G, Farrow M, Balasubramanian S (2002) Minimum length requirement of the alignment domain of human telomerase RNA to sustain catalytic activity in vitro. *Nucleic Acids Research* 30: 4470-4480

Ge LM, Rudolph P (1997) Simultaneous introduction of multiple mutations using overlap extension PCR. *Biotechniques* 22: 28-30

Gilley D, Blackburn EH (1996) Specific RNA residue interactions required for enzymatic functions of Tetrahymena telomerase. *Molecular and Cellular Biology* 16: 66-75

Gilley D, Lee MS, Blackburn EH (1995) Altering specific telomerase RNA template residues affects active site function. *Genes & Development* 9: 2214-2226

Gillis AJ, Schuller AP, Skordalakes E (2008) Structure of the Tribolium castaneum telomerase catalytic subunit TERT. *Nature* 455: 633-637

Girard JP, Caizergues-Ferrer M, Lapeyre B (1993) The SpGAR1 gene of Schizosaccharomyces pombe encodes the functional homologue of the snoRNP protein GAR1 of Saccharomyces cerevisiae. *Nucleic Acids Research* 21: 2149-2155

Gramatges MM, Qi XD, Sasa GS, Chen JJ-L, Bertuch AA (2013) A homozygous telomerase T-motif variant resulting in markedly reduced repeat addition processivity in siblings with Hoyeraal Hreidarsson syndrome. *Blood* 121: 3586-3593

Greider CW (1991) Telomerase Is Processive. *Molecular and Cellular Biology* 11: 4572-4580

Greider CW (2016) Regulating telomere length from the inside out: the replication fork model. *Genes & Development* 30: 1483-1491

Greider CW, Blackburn EH (1985) Identification of a specific telomere terminal transferase activity in Tetrahymena extracts. *Cell* 43: 405-413

Greider CW, Blackburn EH (1987) The telomere terminal transferase of Tetrahymena is a ribonucleoprotein enzyme with two kinds of primer specificity. *Cell* 51: 887-898

Greider CW, Blackburn EH (1989) A telomeric sequence in the RNA of Tetrahymena telomerase required for telomere repeat synthesis. *Nature* 337: 331-337

Hamma T, Reichow SL, Varani G, Ferré-D'Amaré AR (2005) The Cbf5-Nop10 complex is a molecular bracket that organizes box H/ACA RNPs. *Nature Structural & Molecular Biology* 12: 1101-1107

Hammond PW, Cech TR (1997) dGTP-dependent processivity and possible template switching of euplotes telomerase. *Nucleic Acids Research* 25: 3698-3704

Hammond PW, Cech TR (1998) Euplotes telomerase: evidence for limited base-pairing during primer elongation and dGTP as an effector of translocation. *Biochemistry* 37: 5162-5172

Hanahan D, Weinberg RA (2011) Hallmarks of Cancer: The Next Generation. *Cell* 144: 646-674

Hardy CD, Schultz CS, Collins K (2001) Requirements for the dGTP-dependent repeat addition processivity of recombinant Tetrahymena telomerase. *Journal of Biological Chemistry* 276: 4863-4871

Harkisheimer M, Mason M, Shuvaeva E, Skordalakes E (2013) A Motif in the Vertebrate Telomerase N-Terminal Linker of TERT Contributes to RNA Binding and Telomerase Activity and Processivity. *Structure* 21: 1870-1878

Harley CB (2002) Telomerase is not an oncogene. *Oncogene* 21: 494-502

Harrington L, Zhou W, McPhail T, Oulton R, Yeung DS, Mar V, Bass MB, Robinson MO (1997) Human telomerase contains evolutionarily conserved catalytic and structural subunits. *Genes & Development* 11: 3109-3115

Hayflick L, Moorhead PS (1961) The serial cultivation of human diploid cell strains. *Experimental Cell Research* 25: 585-621

Hiyama E, Hiyama K (2007) Telomere and telomerase in stem cells. *British Journal of Cancer* 96: 1020-1024

Hockemeyer D, Collins K (2015) Control of telomerase action at human telomeres. *Nature Structural & Molecular Biology* 22: 848-852

Hong K, Upton H, Miracco EJ, Jiang JS, Zhou ZH, Feigon J, Collins K (2013) Tetrahymena Telomerase Holoenzyme Assembly, Activation, and Inhibition by Domains of the p50 Central Hub. *Molecular and Cellular Biology* 33: 3962-3971

Hossain S, Singh S, Lue NF (2002) Functional analysis of the C-terminal extension of telomerase reverse transcriptase. A putative "thumb" domain. *Journal of Biological Chemistry* 277: 36174-36180

Huang J, Brown AF, Wu J, Xue J, Bley CJ, Rand DP, Wu LJ, Zhang RG, Chen JJ-L, Lei M (2014) Structural basis for protein-RNA recognition in telomerase. *Nature Structural & Molecular Biology* 21: 507-512

Huard S, Moriarty TJ, Autexier C (2003) The C terminus of the human telomerase reverse transcriptase is a determinant of enzyme processivity. *Nucleic Acids Research* 31: 4059-4070

Huffman KE, Levene SD, Tesmer VM, Shay JW, Wright WE (2000) Telomere shortening is proportional to the size of the G-rich telomeric 3'-overhang. *Journal of Biological Chemistry* 275: 19719-19722

Hwang H, Opresko P, Myong S (2014) Single-molecule real-time detection of telomerase extension activity. *Scientific Reports* 4: 6391

Jacobs Sa, Podell ER, Cech TR (2006) Crystal structure of the essential N-terminal domain of telomerase reverse transcriptase. *Nature Structural & Molecular Biology* 13: 218-225

Jády BE, Bertrand E, Kiss T (2004) Human telomerase RNA and box H/ACA scaRNAs share a common Cajal body-specific localization signal. *The Journal of Cell Biology* 164: 647-652

Jansson LI, Akiyama BM, Ooms A, Lu C, Rubin SM, Stone MD (2015) Structural basis of template-boundary definition in Tetrahymena telomerase. *Nature Structural & Molecular Biology* 22: 883-888

Jiang J, Chan H, Cash DD, Miracco EJ, Ogorzalek Loo RR, Upton HE, Cascio D, O'Brien Johnson R, Collins K, Loo JA, Zhou ZH, Feigon J (2015) Structure of Tetrahymena telomerase reveals previously unknown subunits, functions, and interactions. *Science* 350: aab4070

Kim NW, Piatyszek MA, Prowse KR, Harley CB, West MD, Ho PL, Coviello GM, Wright WE, Weinrich SL, Shay JW (1994) Specific association of human telomerase activity with immortal cells and cancer. *Science* 266: 2011-2015

Kiss T, Fayet-Lebaron E, Jády BE (2010) Box H/ACA small ribonucleoproteins. *Molecular Cell* 37: 597-606

Kornberg A (1957) Pathways of Enzymatic Synthesis of Nucleotides and Polynucleotides. In *The Chemical Basis of Heredity*, McElroy WD, Glass B (eds), pp 579-608.

Kornberg A (1969) Active center of DNA polymerase. *Science* 163: 1410-1418

Lai CK, Mitchell JR, Collins K (2001) RNA Binding Domain of Telomerase Reverse Transcriptase. *Society* 21: 990-1000

Latrick CM, Cech TR (2010) POT1-TPP1 enhances telomerase processivity by slowing primer dissociation and aiding translocation. *The EMBO Journal* 29: 924-933

Lattmann S, Stadler MB, Vaughn JP, Akman SA, Nagamine Y (2011) The DEAH-box RNA helicase RHAU binds an intramolecular RNA G-quadruplex in TERC and associates with telomerase holoenzyme. *Nucleic Acids Research*: 1-15

Lee MS, Blackburn EH (1993) Sequence-specific DNA primer effects on telomerase polymerization activity. *Molecular and Cellular Biology* 13: 6586-6599

Lin J, Ly H, Hussain A, Abraham M, Pearl S, Tzfati Y, Parslow TG, Blackburn EH (2004) A universal telomerase RNA core structure includes structured motifs required for binding the telomerase reverse transcriptase protein. *Proceedings of the National Academy of Sciences of the United States of America* 101: 14713-14718

Lingner J, Cooper JP, Cech TR (1995) Telomerase and DNA end replication: no longer a lagging strand problem? *Science* 269: 1533-1534

Lingner J, Hughes TR, Shevchenko A, Mann M, Lundblad V, Cech TR (1997) Reverse transcriptase motifs in the catalytic subunit of telomerase. *Science* 276: 561-567

Liu WR, Yin YS, Wang J, Shi BW, Zhang LM, Qian D, Li CG, Zhang H, Wang SG, Zhu JF, Gao LW, Zhang Q, Jia B, Hao LG, Wang CL, Zhang B (2017) Kras mutations increase telomerase activity and targeting telomerase is a promising therapeutic strategy for Kras-mutant NSCLC. *Oncotarget* 8: 179-190

Lue NF (2004) Adding to the ends: what makes telomerase processive and how important is it? *Bioessays* 26: 955-962

Lue NF, Bosoy D, Moriarty TJ, Autexier C, Altman B, Leng SY (2005) Telomerase can act as a template- and RNA-independent terminal transferase. *Proceedings of the National Academy of Sciences of the United States of America* 102: 9778-9783

Lue NF, Li Z (2007) Modeling and structure function analysis of the putative anchor site of yeast telomerase. *Nucleic Acids Research* 35: 5213-5222

Lue NF, Lin Y-c, Mian IS (2003) A conserved telomerase motif within the catalytic domain of telomerase reverse transcriptase is specifically required for repeat addition processivity. *Molecular and Cellular Biology* 23: 8440-8449

Ly H, Blackburn EH, Parslow TG (2003) Comprehensive structure-function analysis of the core domain of human telomerase RNA. *Molecular and Cellular Biology* 23: 6849-6856

Ly H, Calado RT, Allard P, Baerlocher GM, Lansdorp PM, Young NS, Parslow TG (2005) Functional characterization of telomerase RNA variants found in patients with hematologic disorders. *Leukemia and Lymphoma* 105: 2332-2339

Maine IP, Chen SF, Windle B (1999) Effect of dGTP concentration on human and CHO telomerase. *Biochemistry* 38: 15325-15332

Maiorano D, Brimage LJ, Leroy D, Kearsey SE (1999) Functional conservation and cell cycle localization of the Nhp2 core component of H + ACA snoRNPs in fission and budding yeasts. *Experimental Cell Research* 252: 165-174

Makarov VL, Hirose Y, Langmore JP (1997) Long G tails at both ends of human chromosomes suggest a C strand degradation mechanism for telomere shortening. *Cell* 88: 657-666

Marcand S, Gilson E, Shore D (1997) A protein-counting mechanism for telomere length regulation in yeast. *Science* 275: 986-990

Marrone A, Stevens D, Vulliamy T, Dokal I, Mason PJ (2004) Heterozygous telomerase RNA mutations found in dyskeratosis congenita and aplastic anemia reduce telomerase activity via haploinsufficiency. *Analysis* 104: 3936-3942

McClintock B (1941) The Stability of Broken Ends of Chromosomes in Zea Mays. *Genetics* 26: 234-282

Meng E, Taylor B, Ray A, Shevde LA, Rocconi RP (2012) Targeted inhibition of telomerase activity combined with chemotherapy demonstrates synergy in eliminating ovarian cancer spheroid-forming cells. *Gynecologic Oncology* 124: 598-605

Meyne J, Ratliff RL, Moyzis RK (1989) Conservation of the human telomere sequence (TTAGGG)n among vertebrates. *Proceedings of the National Academy of Sciences of the United States of America* 86: 7049-7053

Miller MC, Liu JK, Collins K (2000) Template definition by Tetrahymena telomerase reverse transcriptase. *The EMBO Journal* 19: 4412-4422

Miracco EJ, Jiang JS, Cash DD, Feigon J (2014) Progress in structural studies of telomerase. *Current Opinion in Structural Biology* 24: 115-124

Mitchell JR, Cheng J, Collins K (1999) A box H/ACA small nucleolar RNA-like domain at the human telomerase RNA 3' end. *Molecular and Cellular Biology* 19: 567-576

Mitchell JR, Collins KL (2000) Human telomerase activation requires two independent interactions between telomerase RNA and telomerase reverse transcriptase. *Molecular Cell* 6: 361-371

Mitchell M, Gillis A, Futahashi M, Fujiwara H, Skordalakes E (2010) Structural basis for telomerase catalytic subunit TERT binding to RNA template and telomeric DNA. *Nature Structural & Molecular Biology* 17: 513-518

Moriarty TJ, Huard S, Dupuis S, Autexier C (2002) Functional multimerization of human telomerase requires an RNA interaction domain in the N terminus of the catalytic subunit. *Molecular and Cellular Biology* 22: 1253-1265

Moriarty TJ, Marie-Egyptienne DT, Autexier C (2004) Functional Organization of Repeat Addition Processivity and DNA Synthesis Determinants in the Human Telomerase Multimer. *Molecular and Cellular Biology* 24: 3720-3733

Moriarty TJ, Ward RJ, Taboski MAS, Autexier C (2005) An anchor site-type defect in human telomerase that disrupts telomere length maintenance and cellular immortalization. *Molecular Biology of the Cell* 16: 3152-3161

Moyzis RK, Buckingham JM, Cram LS, Dani M, Deaven LL, Jones MD, Meyne J, Ratliff RL, Wu JR (1988) A highly conserved repetitive DNA sequence, (TTAGGG)n, present at the telomeres of human chromosomes. *Proceedings of the National Academy of Sciences of the United States of America* 85: 6622-6626

Muller H (1938) The Remaking of Chromosomes. *Collecting Net-Woods Hole* 13:181-198

Nakamura TM, Morin GB, Chapman KB, Weinrich SL, Andrews WH, Lingner J, Harley CB, Cech TR (1997) Telomerase Catalytic Subunit Homologs from Fission Yeast and Human. *Science* 277: 955-959

Nakayama J, Tahara H, Tahara E, Saito M, Ito K, Nakamura H, Nakanishi T, Ide T, Ishikawa F (1998) Telomerase activation by hTRT in human normal fibroblasts and hepatocellular carcinomas. *Nature Genetics* 18: 65-68

Ohki R, Tsurimoto T, Ishikawa F (2001) In vitro reconstitution of the end replication problem. *Molecular and Cellular Biology* 21: 5753-5766

Olovnikov AM (1973) A theory of marginotomy. The incomplete copying of template margin in enzymic synthesis of polynucleotides and biological significance of the phenomenon. *Journal of Theoretical Biology* 41: 181-190

Palm W, de Lange T (2008) How shelterin protects mammalian telomeres. *Annual Review of Genetics* 42: 301-334

Parks JW, Kappel K, Das R, Stone MD (2017) Single-molecule FRET-Rosetta reveals RNA structural rearrangements during human telomerase catalysis. *RNA* 23: 175-188

Parks JW, Stone MD (2014) Coordinated DNA dynamics during the human telomerase catalytic cycle. *Nature Communications* 5:4146

Pascolo E, Wenz C, Lingner J, Hauel N, Priepke H, Kauffmann I, Garin-Chesa P, Rettig WJ, Damm K, Schnapp A (2002) Mechanism of human telomerase inhibition by BIBR1532, a synthetic, non-nucleosidic drug candidate. *Journal of Biological Chemistry* 277: 15566-15572

Peng Y, Mian IS, Lue NF (2001) Analysis of telomerase processivity: mechanistic similarity to HIV-1 reverse transcriptase and role in telomere maintenance. *Molecular Cell* 7: 1201-1211

Podlevsky JD, Bley CJ, Omana RV, Qi X, Chen JJ-L (2008) The telomerase database. *Nucleic Acids Research* 36: D339-343

Podlevsky JD, Chen JJ-L (2012) It all comes together at the ends: telomerase structure, function, and biogenesis. *Mutation Research* 730: 3-11

Podlevsky JD, Chen JJ-L (2016) Evolutionary perspectives of telomerase RNA structure and function. *Rna Biology* 13: 720-732

Podlevsky JD, Li Y, Chen JJ-L (2016) The functional requirement of two structural domains within telomerase RNA emerged early in eukaryotes. *Nucleic Acids Research* 44: 9891-9901

Pogacić V, Dragon F, Filipowicz W (2000) Human H/ACA small nucleolar RNPs and telomerase share evolutionarily conserved proteins NHP2 and NOP10. *Molecular and Cellular Biology* 20: 9028-9040

Qi X, Li Y, Honda S, Hoffmann S, Marz M, Mosig A, Podlevsky JD, Stadler PF, Selker EU, Chen JJ-L (2013) The common ancestral core of vertebrate and fungal telomerase RNAs. *Nucleic Acids Research* 41: 450-462

Qi X, Xie M, Brown AF, Bley CJ, Podlevsky JD, Chen JJ-L (2012) RNA/DNA hybrid binding affinity determines telomerase template-translocation efficiency. *The EMBO Journal* 31: 150-161

Qiao F, Cech TR (2008) Triple-helix structure in telomerase RNA contributes to catalysis. *Nature Structural & Molecular Biology* 15: 634-640

Robart AR, Collins KL (2010) Investigation of human telomerase holoenzyme assembly, activity, and processivity using disease-linked subunit variants. *Journal of Biological Chemistry* 285: 4375-4386

Romi E, Baran N, Gantman M, Shmoish M, Min B, Collins K, Manor H (2007) High-resolution physical and functional mapping of the template adjacent DNA binding site in catalytically active telomerase. *Proceedings of the National Academy of Sciences of the United States of America* 104: 8791-8796

Rouda S, Skordalakes E (2007) Structure of the RNA-binding domain of telomerase: implications for RNA recognition and binding. *Structure* 15: 1403-1412

Ruden M, Puri N (2013) Novel anticancer therapeutics targeting telomerase. *Cancer Treatment Reviews* 39: 444-456

Sarek G, Marzec P, Margalef P, Boulton SJ (2015) Molecular basis of telomere dysfunction in human genetic diseases. *Nature Structural & Molecular Biology* 22: 867-874

Schmidt JC, Cech TR (2015) Human telomerase: biogenesis, trafficking, recruitment, and activation. *Genes & Development* 29: 1095-1105

Sealey DC, Zheng L, Taboski MA, Cruickshank J, Ikura M, Harrington LA (2010) The N-terminus of hTERT contains a DNA-binding domain and is required for telomerase activity and cellular immortalization. *Nucleic Acids Research* 38: 2019-2035

Sekaran VG, Soares J, Jarstfer MB (2010) Structures of telomerase subunits provide functional insights. *Biochimica et Biophysica Acta* 1804: 1190-1201

Seto AG, Umansky K, Tzfati Y, Zaug AJ, Blackburn EH, Cech TR (2003) A template-proximal RNA paired element contributes to Saccharomyces cerevisiae telomerase activity. *RNA* 9: 1323-1332

Sexton AN, Collins K (2011) The 5' guanosine tracts of human telomerase RNA are recognized by the G-quadruplex binding domain of the RNA helicase DHX36 and function to increase RNA accumulation. *Molecular and Cellular Biology* 31: 736-743

Sfeir a, de Lange T (2012) Removal of Shelterin Reveals the Telomere End-Protection Problem. *Science* 336: 593-597

Sfeir AJ, Chai W, Shay JW, Wright WE (2005) Telomere-end processing the terminal nucleotides of human chromosomes. *Molecular Cell* 18: 131-138

Shawi M, Autexier C (2008) Telomerase, senescence and ageing. *Mechanisms of Ageing and Development* 129: 3-10

Shay JW, Keith WN (2008) Targeting telomerase for cancer therapeutics. *British Journal of Cancer* 98: 677-683

Shefer K, Brown Y, Gorkovoy V, Nussbaum T, Ulyanov NB, Tzfati Y (2007) A triple helix within a pseudoknot is a conserved and essential element of telomerase RNA. *Molecular and Cellular Biology* 27: 2130-2143

Shippen-Lentz DE, Blackburn EH (1990) Functional evidence for an RNA template in telomerase. *Science* 247: 546-552

Steitz TA (1999) DNA polymerases: Structural diversity and common mechanisms. *Journal of Biological Chemistry* 274: 17395-17398

Stohr BA, Xu L, Blackburn EH (2010) The terminal telomeric DNA sequence determines the mechanism of dysfunctional telomere fusion. *Molecular Cell* 39: 307-314

Sun D, Lopez-Guajardo CC, Quada J, Hurley LH, Von Hoff DD (1999) Regulation of catalytic activity and processivity of human telomerase. *Biochemistry* 38: 4037-4044

Tesmer VM, Ford LP, Holt SE, Frank BC, Yi X, Aisner DL, Ouellette M, Shay JW, Wright WE (1999) Two inactive fragments of the integral RNA cooperate to assemble active telomerase with the human protein catalytic subunit (hTERT) in vitro. *Molecular and Cellular Biology* 19: 6207-6216

Theimer Ca, Blois Ca, Feigon J (2005) Structure of the human telomerase RNA pseudoknot reveals conserved tertiary interactions essential for function. *Molecular Cell* 17: 671-682

Theimer Ca, Feigon J (2006) Structure and function of telomerase RNA. *Current Opinion in Structural Biology* 16: 307-318

Theimer Ca, Finger LD, Trantirek L, Feigon J (2003) Mutations linked to dyskeratosis congenita cause changes in the structural equilibrium in telomerase RNA. *Proceedings of the National Academy of Sciences of the United States of America* 100: 449-454

Theimer Ca, Jády BE, Chim N, Richard P, Breece KE, Kiss T, Feigon J (2007) Structural and functional characterization of human telomerase RNA processing and cajal body localization signals. *Molecular Cell* 27: 869-881

Tomlinson CG, Moye AL, Holien JK, Parker MW, Cohen SB, Bryan TM (2015) Two-step mechanism involving active-site conformational changes regulates human telomerase DNA binding. *Biochemical Journal* 465: 347-357

Tsakiri KD, Cronkhite JT, Kuan PJ, Xing C, Raghu G, Weissler JC, Rosenblatt RL, Shay JW, Garcia CK (2007) Adult-onset pulmonary fibrosis caused by mutations in telomerase. *Proceedings of the National Academy of Sciences of the United States of America* 104: 7552-7557

Tzfati Y, Fulton TB, Roy J, Blackburn EH (2000) Template boundary in a yeast telomerase specified by RNA structure. *Science* 288: 863-867.

Venteicher AS, Artandi SE (2009) A Human Telomerase Holoenzyme Protein Required for Cajal Body Localization and Telomere Synthesis. *Science* 323

Vulliamy ST (2002) Aplastic anaemia and telomerase RNA mutations Time to do the right things right : Nigerian health care For personal use . Only reproduce with permission from The Lancet Publishing Group . *The Lancet* 360: 2002-2002

Vulliamy TJ, Marrone A, Knight SW, Walne A, Mason PJ, Dokal I (2006) Mutations in dyskeratosis congenita: their impact on telomere length and the diversity of clinical presentation. *Blood* 107: 2680-2685

Wallweber G, Gryaznov S, Pongracz K, Pruzan R (2003) Interaction of human telomerase with its primer substrate. *Biochemistry* 42: 589-600

Wang F, Podell ER, Zaug AJ, Yang Y, Baciu P, Cech TR, Lei M (2007) The POT1-TPP1 telomere complex is a telomerase processivity factor. *Nature* 445: 506-510

Ward RJ, Autexier C (2005) Pharmacological telomerase inhibition can sensitize drug-resistant and drug-sensitive cells to chemotherapeutic treatment. *Molecular Pharmacology* 68: 779-786

Watson JD (1972) Origin of concatemeric T7 DNA. *Nature: New biology* 239: 197-201

Weinrich SL, Pruzan R, Ma L, Ouellette M, Tesmer VM, Holt SE, Bodnar AG, Lichtsteiner S, Kim NW, Trager JB, Taylor RD, Carlos R, Andrews WH, Wright WE, Shay JW, Harley CB, Morin GB (1997) Reconstitution of human telomerase with the template RNA component hTR and the catalytic protein subunit hTRT. *Nature Genetics* 17: 498-502

Wellinger RJ, Zakian VA (2012) Everything You Ever Wanted to Know About Saccharomyces cerevisiae Telomeres: Beginning to End. *Genetics* 191: 1073-1105

Wu RA, Tam J, Collins K (2017a) DNA-binding determinants and cellular thresholds for human telomerase repeat addition processivity. *The EMBO Journal* 36: 1908-1927

Wu RA, Upton HE, Vogan JM, Collins K (2017b) Telomerase Mechanism of Telomere Synthesis. *Annual Review of Biochemistry* 86: 439-460

Wyatt HDM, Lobb Da, Beattie TL (2007) Characterization of physical and functional anchor site interactions in human telomerase. *Molecular and Cellular Biology* 27: 3226-3240

Wyatt HDM, West SC, Beattie TL (2010) InTERTpreting telomerase structure and function. *Nucleic Acids Research* 38: 5609-5622

Xi LH, Schmidt JC, Zaug AJ, Ascarrunz DR, Cech TR (2015) A novel two-step genome editing strategy with CRISPR-Cas9 provides new insights into telomerase action and TERT gene expression. *Genome Biology* 16:231

Xie MY, Mosig A, Qi X, Li Y, Stadler PF, Chen JJ-L (2008) Structure and function of the smallest vertebrate telomerase RNA from teleost fish. *Journal of Biological Chemistry* 283: 2049-2059

Xie MY, Podlevsky JD, Qi XD, Bley CJ, Chen JJ-L (2010) A novel motif in telomerase reverse transcriptase regulates telomere repeat addition rate and processivity. *Nucleic Acids Research* 38: 1982-1996

Xin ZT, Beauchamp AD, Calado RT, Bradford JW, Regal JA, Shenoy A, Liang YY, Lansdorp PM, Young NS, Ly H (2007) Functional characterization of natural telomerase mutations found in patients with hematologic disorders. *Blood* 109: 524-532

Yamaguchi H, Baerlocher GM, Lansdorp PM, Chanock SJ, Nunez O, Sloand E, Young NS (2003) Mutations of the human telomerase RNA gene (TERC) in aplastic anemia and myelodysplastic syndrome. *Blood* 102: 916-918

Yang G, Franklin M, Li J, Lin TC, Konigsberg W (2002) Correlation of the kinetics of finger domain mutants in RB69 DNA polymerase with its structure. *Biochemistry* 41: 2526-2534

Yang W, Lee YS (2015) A DNA-hairpin model for repeat-addition processivity in telomere synthesis. *Nature Structural & Molecular Biology* 22: 844-847

Zappulla DC, Goodrich KJ, Cech TR (2005) A miniature yeast telomerase RNA functions in vivo and reconstitutes activity in vitro. *Nature Structural & Molecular Biology* 12: 1072-1077

Zaug AJ, Crary SM, Jesse Fioravanti M, Campbell K, Cech TR (2013) Many disease-associated variants of hTERT retain high telomerase enzymatic activity. *Nucleic Acids Research* 41: 8969-8978

Zaug AJ, Podell ER, Cech TR (2008) Mutation in TERT separates processivity from anchor-site function. *Nature Structural & Molecular Biology* 15: 870-872

Zhang Q, Kim N-K, Feigon J (2011) Telomerase and Retrotransposons: Reverse Transcriptases That Shaped Genomes Special Feature Sackler Colloquium: Architecture of human telomerase RNA. *Proceedings of the National Academy of Sciences of the United States of America* 2011: 1-8

Zhang Q, Kim N-K, Peterson RD, Wang Z, Feigon J (2010) Structurally conserved five nucleotide bulge determines the overall topology of the core domain of human telomerase RNA. *Proceedings of the National Academy of Sciences of the United States of America* 107: 18761-18768

APPENDIX A

CO-AUTHOR APPROVAL

I verify that the following co-authors have approved of my use of our publication in my dissertation.

Julian Chen (Arizona State University)

Xiaodong Qi (Arizona State University)

Andrew Brown (Arizona State University)

Joshua Podlevsky (Arizona State University)

Mingyi Xie (Arizona State University)

Dhenugen Logeswaran (Arizona State University)